THESIS APPROVAL

GRADUATE SCHOOL, KASETSART UNIVERSITY

Doctor of Philosophy (Chemistry)
DEGREE

Physical Chemistry
FIELD

Chemistry
DEPARTMENT

TITLE: Investigation on Electronic Structures and Properties of Fluorene-Thiophene Conducting Polymers: Theoretical Studies

NAME: Miss Potjaman Poolmee

THIS THESIS HAS BEEN ACCEPTED BY

Supa Hannongbua. **THESIS ADVISOR**
(Associate Professor Supa Hannongbua, Dr.rer.nat.)

COMMITTEE MEMBER
(Professor Peter Wolschann, Dr.rer.nat.)

COMMITTEE MEMBER
(Miss Pensri Bunsawansong, Ph.D.)

COMMITTEE MEMBER
(Miss Pinsuda Viravathana, Ph.D.)

COMMITTEE MEMBER
(Assistant Professor Charanai Panichjakul, Ph.D.)

Surapol Patharakorn **DEPARTMENT HEAD**
(Mr. Surapol Patharakorn, Ph.D.)

APPROVED BY THE GRADUATE SCHOOL ON 23 / 11 / 2005

Vinai Artkongharn. **DEAN**
(Associate Professor Vinai Artkongharn, M.A.)

THESIS

INVESTIGATION ON ELECTRONIC STRUCTURES AND PROPERTIES OF FLUORENE-THIOPHENE CONDUCTING POLYMERS: THEORETICAL STUDIES

POTJAMAN POOLMEE

A Thesis Submitted in Partial Fulfillment of
the Requirements for the Degree of
Doctor of Philosophy (Chemistry)
Graduate School, Kasetsart University
2005

ISBN 974-9846-87-7

Potjaman Poolmee 2005: Investigation on Electronic Structures and Properties of Fluorene-Thiophene Conducting Polymers: Theoretical Studies. Doctor of Philosophy (Chemistry), Major Field: Physical Chemistry, Department of Chemistry, Thesis Advisor: Associate Professor Supa Hannongbua, Dr.rer.nat. 170 pages.
ISBN 974-9846-87-7

In this work, quantum-chemical calculations were applied to investigate the structural, energetic and electronic properties of the fluorene-thiophene class: poly[2,7-(fluorene)-co-*alt*-2,5-(thiophene)] (P1), poly[2,7-(fluorene)-co-*alt*-2,5-(3-methylthiophene)] (P2), poly[2,7-(9,9-dihexylfluorene)-co-*alt*-2,5-(decylthiophene)] (P3), poly[2,7-(9,9-dihexylfluorene)-co-*alt*-2,5-(3,4-decylthiophene)] (P4), poly[2,7-(9,9-dihexylfluorene)-co-*alt*-2,5-(*S,S*-dioxidethiophene)] (P5) and poly[2,7-(9,9-dihexylfluorene)-co-*alt*-2,5-(3,4-ethylenedioxythiophene)] (P6). A conformational study of those polymers calculated at B3LYP/6-31G* level demonstrated that these molecules show non-planar structures and provide a reliable structural results as compared to experimental data. The energy gaps of the corresponding polymers were obtained by extrapolating HOMO-LUMO energy gap and the lowest excitation energy of oligomers to infinite chain length. The obtained results of P3 and P4 calculated by TDDFT/B3LYP/6-31G*//B3LYP/6-31G* method are 2.47 and 3.07 eV, which are in consistent agreement with the experimental data. On the contrary, HOMO-LUMO energy gap calculated at B3LYP/6-31G* level is suitable to estimate the energy gap of P5 (2.24 eV) and P6 (2.56 eV). The results indicate that thiophene derivative units which were copolymerized to be fluorene-thiophene copolymers decrease the energy gap of polyfluorene. These reduce the torsional angle between fluorene and thiophene units, therefore, the conjugation can be enhanced. Moreover, the excited states of the fluorene-thiophene compounds of which polymers are useful as a light-emitting diode were studied by SAC-CI method. The effect of torsional angle between fluorene and thiophene units on the excited states was examined for 2-(fluoren-2-yl)thiophene (FT) and 2-(fluoren-2-yl)-3-methylthiophene (FMT) in detail. The first three excited states were found to change their excitation characters along the torsional angle. The accurate absorption spectra were simulated by taking thermal average for the conformers of some torsional angles from 0° to 90° in good agreement with the observed spectra. The equilibrium structures at S_1 state were nearly planar for both FT and FMT, and the calculated emission energies were in agreement with the experiment. The effect of applying the electric fields on the electronic spectra was also examined. The absorption spectra of dimer and trimer of FT were also calculated at the equilibrium structure. The oscillator strength of S_1 states of dimer and trimer was large and the red shift occurred due to the elongation of the π-conjugation.

Potjaman Poolmee
Student's signature

Supa Hannongbua.
Thesis Advisor's signature

21 / 11 / 05

ACKNOWLEDGEMENTS

I wish to express my deep gratitude to a number of persons who giving me guidance, help and support to reach my goal of this thesis. First of all, most of credits in this thesis should justifiably go to my advisor, Associate Professor Dr. Supa Hannongbua, for her valuable guidance, continuous support, kindness and encouragement throughout the course of my graduate.

I would like to thank my committees, Professor Dr. Peter Wolschann, Dr. Pensri Bunsawansong, Dr. Pinsuda Viravathana and Assistant Professor Dr. Charanai Panichjakul for their helpful comments and suggestions.

Furthermore, special thanks are due to Professor Dr. Hiroshi Nakatsuji who offers me a grant for Creative Scientific Research from the Ministry of Education, Science and Culture, and Sport of Japan. Associate Professor Dr. Ehara Mashahiro is also appreciated for his help guidance and valuable suggestions when I did the research at Kyoto University.

Kasetsart University and the Graduate School are grateful acknowledged for some financial supports for my Ph.D. study and for partial support via Grant-in-Aid for thesis. The Cooperative Research Network of Nanoscience and Nanotechnology under the Commission of Higher Education is also grateful acknowledged for financial support for presentation at the international conference.

The Postgraduate Education and Research Programs in Petroleum and Petrochemical Technology (ADB-MUA), and Laboratory for Computational and Applied Chemistry (LCAC) and Center of Nanotechnology, Kasetsart University are grateful acknowledged for research facilities. In addition, Kasetsart University Research and Development Institute (KURDI) is also acknowledged for some financial support.

My colleagues at Laboratory for Computational and Applied Chemistry (LCAC) at Kasetsart University are sincere thanked for their helpful assistance and supporting during my study.

Finally, I would like to express my most profound gratitude to my parents and my brother, who sustained and encouraged me throughout my educations.

Potjaman Poolmee
October, 2005

TABLE OF CONTENTS

Page

LIST OF TABLES

LIST OF TABLES (cont'd)

Appendix Table

LIST OF FIGURES

LIST OF FIGURES (cont'd)

LIST OF FIGURES (cont'd)

Appendix Figure **Page**

ABBREVIATIONS

η_{EL} = Electroluminescence quantum efficiency
η_{PL} = Photoluminescence quantum efficiency
ΔE = Excitation energy
f = Oscillator strength
$< r >$ = Dipole moment
AM1 = Semiempirical Austin Model 1
BT = Benzothiadiazole
B3LYP = Becke ’s three parameter hybrid functional using the LYP Correlation functional
CASPT2 = Second-order perturbation theory
CASSCF = Complete active space self-consistent field
CC = Couple Cluster
CCSD = Singles and doubles couple cluster
CIS = Singles configuration interaction
CISD = Singles and doubles configuration interaction
CISDT = Singles, doubles and triples configuration interaction
CISDTQ = Singles, doubles, triples and quadruples configuration Interaction
CSF = Configurational state Functions
CV = Cyclic voltammetry
DFT = Density functional theory
DMABN = 4,-*N*,*N*-dimethylaminobenzonitrile
E_g = Energy gap
EA = Electron affinity
EDOT = Ethylenedioxythiophene
EHT = Extended Hückel theory
EL = Electroluminescence
EEL = Electron energy loss
FET = 2-(9,9-diethylfluoren-2-yl)-4-ethylthiophene
FEET = 2-(9,9-diethylfluoren-2-yl)-3,4-ethylthiophene

FTSO2 = 2-(9,9-diethylfluoren-2-yl)-*S,S*-dioxidethiophene

FTSOO = 2-(9,9-diethylfluoren-2-yl)-3,4-ethylenedioxythiophene

FT = 2-(fluoren-2-yl)thiophene

FMT = 2-(fluoren-2-yl)-3-methylthiophene

HF = Hartree Fock theory

HOMO = Highest occupied molecular orbital

INDO/s = Intermediate neglect of differential overlap

IP = Ionization potential

LEPs = Light-emitting polymers

LEDs = Light-emitting diodes

LUMO = Lowest unoccupied molecular orbital

MRCI = Multireference configuration interaction

MO = Molecular orbital

OLED = Organic light emitting diode

PA = Polyacetylene

PBF = Poly(2,7-borafluorene)

PC = Polycarbozole

PDHF = Poly(dihexylfluorene)

PEDOT = Poly(3,4-ethylenedioxythiophene)

PF = Polyfluorene

PFs = Polyfluorene derivatives

PFET = Poly[2,7-(9,9-diethylfluorene)-co-*alt*-2,5-(4-ethylthiophene)]

PFEET = Poly[2,7-(9,9-diethylfluorene)-co-*alt*-2,5-(3,4-ethylthiophene)]

PFTT = Poly(9,9-dioctylfluorene-*alt*-thieno[3,2- b]thiophene)

PFTSO2 = Poly[2,7-(9,9-diethylfluorene)-co-*alt*-2,5-(*S,S*-dioxidethiophene)]

PFTSOO = Poly[2,7-(9,9-diethylfluorene)-co-*alt*-2,5-(3,4-ethylenedioxythiophene)]

P3HT = Poly(3-hexylthiophene)

PL = Photoluminescence

PLEDs = Polymer light-emitting diodes

PPP = Poly(para-phenylene)

PPV = Poly(para-phenylenevinylene)

PT(s) = Polythiophene(s)

RPA = Random-phase approximation

RCIS = Restricted configuration interaction

RHF = Restricted Hartree-Fock

S_0 = Ground state

S_1 = First excited state

S_2 = Second excited state

S_3 = Third excited state

SAC = Symmetry adapted cluster

SAC-CI = Symmetry adapted cluster-configuration interaction

SAC-CI SD-R = Symmetry adapted cluster configuration interaction single-double-R

TDA = Tanm-Dancoff approximation

TGA = Thermogravimetric analysis

TD-DFT = Time-dependent density functional theory

TV = Thienylene vinylene

UAM1 = Spin-unrestricted Austin Model1

UZINDO = Spin-unrestricted Zerner ’s Intermediate Neglect Differential Overlap

VUV = Vacuum ultraviolet spectroscopy

ZINDO = Zerner ’s Intermediate Neglect Differential Overlap

INVESTIGATION ON ELECTRONIC STRUCTURES AND PROPERTIES OF FLUORENE-THIOPHENE CONDUCTING POLYMERS: THEORETICAL STUDIES

INTRODUCTION

Conjugated polymers have been attractive attention as a novel class of organic semiconductors. Since polyacetylene can be made as a conductive material which is similar to a metal. Polyacetylene, known as a black powder, was prepared as a silvery film in 1974. In 1977, however, Heeger, MacDiarmid, Shirakawa and co-workers discovered that oxidation with chlorine, bromine or iodine vapour made polyacetylene films 109 times more conductive than they were originally (Chiang *et al*., 1977). Treatment with halogen was called “doping” by analogy with the doping of semiconductors. A key property of a conductive polymer is the presence of conjugated double bonds along the backbone of the polymer. In conjugation, the bonds between carbon atoms are alternately single and double. Every bond contains a localized “sigma” (σ) bond which forms a strong chemical bond. In addition, they also contains a less strongly localized “pi” (π) bond which is weaker.

Today conductive plastics are being developed for many used, such as in corrosion inhibitors, compact capacitors, antistatic coating, electromagnetic shielding of computers. A second generation of electrical polymers has also appeared in, e.g., film transistors (Meng *et al*., 2003 and Kudo 2005), light-emitting diodes (Zhang *et al*., 2000; Liu *et al*., 2002; Wu *et al*., 2004; Ortega *et al*., 2005) and solar cells (Yohannes *et al*., 2004).

Compared to inorganic materials, conjugated polymers have the advantages of easy control of semiconducting properties through chemical modification, and ease of processing over large areas, leading to major potential cost saving in device manufacture. Since these advantages are unsuitable for silicon technology. In the past decade, great efforts have been devoted to the design and synthesis of light-emitting polymers (LEPs) for applications in light-emitting diodes (LEDs) in which three primary colors (blue, red and green) are essential for full color displays. However, white light emission is recently emerging to be a major area of research activity in the coming years (Gong *et al.*, 2004; Vardeny *et al.*, 2005; Tsou *et al.*, 2005; Moiorano *el at.*, 2005; Wei *et al.*, 2005). The organic materials will be the main target for developing white light emissive conducting polymer because of a difficult problem to generate white light using inorganic semiconductors. LEDs, transistors and solar cells based on conjugated materials are now being actively developed for commercial applications by a number of companies. A number of conjugated backbone structures, as shown in Fig. 1, have been shown to be of importance in realizing various emissive colors.

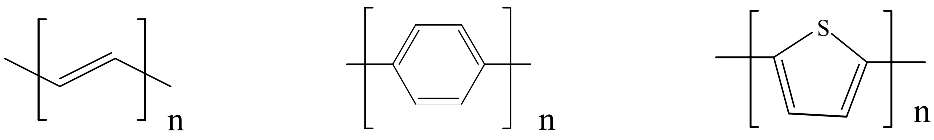

Polyacetylene (PA) Poly (para-phenylene) (PPP) Polythiophene (PT)

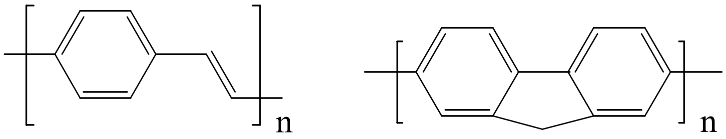

Poly(para-phenylenevinylene) (PPV) Polyfluorene (PF)

Figure 1 Conjugated backbone structures of conducting polymers

Polyfluorene and its derivatives (PFs) are one of the most widely investigated LEPs due to their high efficient blue emission in both photoluminescence (PL) and electroluminescence (EL). However, the drawbacks of PFs, such as aggregation and/or excimers formation in the solid state, insufficient stability, and high energy barrier for hole injection, limit their application in polymers LEDs. In an attempt of tuning the physical properties of PFs by molecular structure modification, one has to face the problem that the only available possibility of remote functionalization is at the C_9 position, and any other position of the fluorene unit is very difficult for performing functional chemical reactions. It was found that copolymerization of fluorene with various aryls allows for tuning of electronic properties and enhanced thermal stability. Various fluorene-based copolymers have been synthesized, aiming at achieving color tuning over the visible spectrum and tuning of the frontier levels energetic position in order to minimize (possibly eliminate) the anodic and cathodic injection barriers of LED structure.

It was found that thiophene unit has grabbed attention because it can be copolymerized into the fluorene unit. Therefore, the advantages of thiophene which can be found include; good stability both in neutral and doped state, wide electronic and optical tuning. By attaching different functional groups, controlling regioregularity and steric interaction on polythiophenes (PTs), light emission ranging can be tuned from blue to near-infrared spectra. One of the most important considerations in developing conjugated polymers for polymer light-emitting diodes (PLEDs) is the photoluminescence quantum efficiency (η_{PL}) of the polymers, which associate with the electroluminescence quantum efficiency (η_{EL}) by a theoretical relation of $\eta_{EL} \leq \frac{1}{4}\, \eta_{PL}$. Unfortunately, PTs exhibit very low PL quantum efficiency, typically 1-3%, in the solid film, and poor electroluminescence (EL). This observation is consistent with the finding for the substituted polythiophenes, in which the fluorescence quantum yields of disubstituted polythiophenes (0.01-0.04) are usually much lower than those of the monosubstituted polythiophenes (0.18-0.27) (Andersson *et al.,* 1999). The low PL quantum efficiency and poor EL limit their application as the active materials in PLEDs. The enhanced PL efficiency in the solid state of thiophene oligomer results from the fluorene units or the lower number of the thiophene rings in the main conjugated backbone as reported by Liu *et al*. (2000).

Copolymerization between fluorene moiety and thiophene moiety to be fluorene-based copolymers is the way to improve the drawbacks of those polymers. The structures of fluorene-based copolymers are shown in Fig. 2.

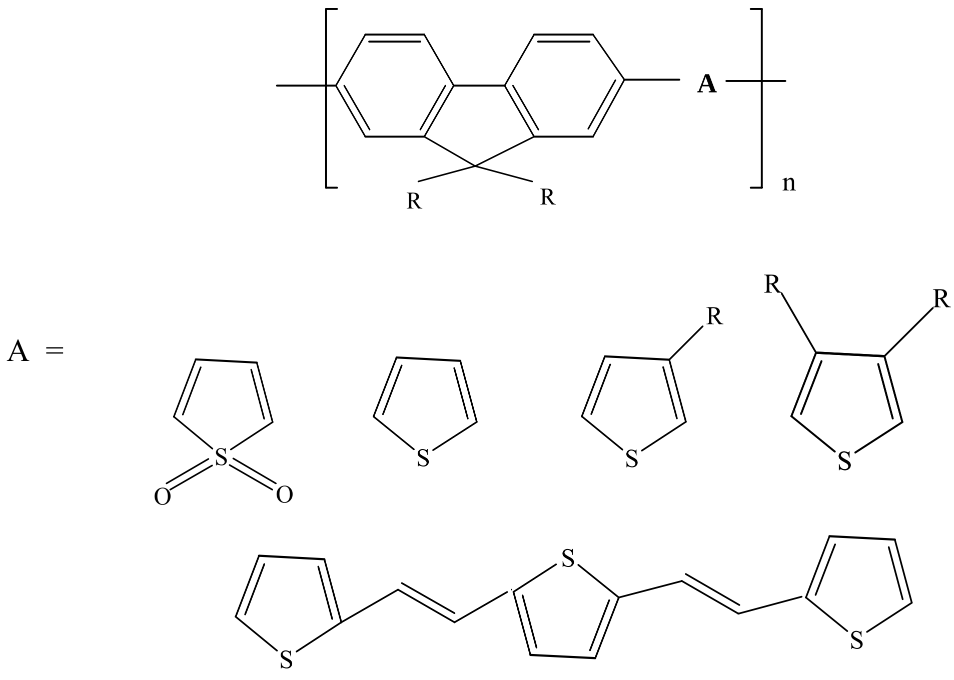

Figure 2 Fluorene-based copolymers

A series of alkyl chain end–capped oligofluorene-thiophenes have been prepared with high yields using Suzuki or Stille coupling reactions (Meng *et al.*, 2003). Thermogravimetric analysis (TGA) reveals that these oligomers are thermally stable, with the onset of decomposition temperatures at 400°C under nitrogen atmosphere. In contrast, oligothiophene decomposes at 320°C under the similar conditions. The chromic polyfluorene derivatives, which exhibit an excellent thermal stability, were also synthesized by Blondin *et al.* (Blondin *et al.*, 2000). Chen *et al.* (2004) proposed a new way to design fluorene-based alternating copolymer family with fine color control for obtaining a good degree color tuning by varying the substitution patterns on the incorporating thienylene vinylene units. The fluorene-based copolymers provided the different color luminescent materials which showing emission in the blue, orange and red. The synthesis of a family of thiophene containing conjugated polymers with high PL quantum efficiencies and different HOMO and LUMO energy levels which enhance the anodic and cathodic injection barriers of LED structure was described (Pei *et al*., 2001). It was obviously improved in comparison with those of poly(3-hexylthiophene) (Theander *et al*., 1999).

The electronic properties of copolymer can be modified by functionalisation on the thiophene unit (Charas *et al.,* 2000). The *S*,*S*-dioxide functionalisation of the thiophene ring leads to a stabilization of the frontier levels that makes the polymer interesting, especially for improving electron injection from stable cathode. The functionalisation also reduces the optical energy gap to 2.2 eV. The optical energy gap values also exhibit a systematic decrease with the extension of the thiophene-moiety. The incorporation of the electron-rich thiophene moiety into the backbone leads to higher HOMO and lower LUMO in the copolymers (Lim *et al*., 2003). Many groups reported the fabrication and characterization of light-emitting diodes from various fluorene-based conjugated polymers. (Bouillud *et al*., 2000; Levesque *et al*., 2001; Stephan *et al*., 2002; You *et al*., 2005).

Experimental researches have not only dedicated to explore novel conjugated polymer but also investigated the theoretical studies simultaneously (Feng *et al*., 2004). Obviously, a theoretical investigation on the energy gaps is one of the main studies which is very useful in guiding the experimental synthesis (Yang *et al*., 2004). To evaluate the energy gap, there are two different theoretical approaches. One is the polymer approach in which the periodic structures are assumed for infinite polymers. Another one is the oligomer extrapolation technique that is popular in this field. In this approach, a sequence of increasing longer oligomer is calculated, and extrapolation to infinite chain length is followed. A distinct advantage of this approach is that it can provide the convergence behavior of the structural and electronic properties of oligomers.

It was found that *ab initio* and density functional theory can be used to estimate the HOMO-LUMO energy gap, which sometimes agrees fairly well with the experimental energy gap in many cases (Oliveira *et al*., 2000). It may perhaps due to the error cancellation. Time-dependent density functional theory (TDDFT) is a recently developed tool for calculating excitation energies. Ma *et al.* (2002) employed TDDFT to calculate energy gaps and effective conjugation lengths of a conjugated polymer. They obtained energy gaps of the polymer by extrapolating vertical excitation energies of the trimer through pentamer to infinite chain length. TDDFT was also applied to calculate vertical excitation energies of linear polyene oligomer; butadiene to decapentaene (Hua *et al*., 2001). Suramitr *et al.* (2005) investigated the electronic properties of alkoxy derivatives of poly(para-phenylenevinylene) by TDDFT. In addition, this method is also used to study electroluminescent polymers (Yu *et al*., 2003).

Many experimental and theoretical works have been devoted to the structures and electronic properties of conjugated polymers on the ground state. In addition, optimization ground-state geometries can be performed for the absorption energies (Belletete *et al*., 2000 and Briere *et al*., 2004). On the other hand, theoretical investigation on the excited states is limited, in particular, changes in molecular structure upon excitation. In the case of conjugated polymer for using as light-emitting diode, optimization of the excited state is essential for the computation of emission energies, which are largely concerned for conjugated polymer in LED applications. Theoretical methods which are performed for investigating absorption and emission process are time-dependent densitiy functional theory (TDDFT), configuration interaction (CIS) and semiempirical ZINDO.

The SAC (symmetry adapted cluster)/SAC-CI (configuration interaction) method (Nakatsuji *et al*., 1978 and 1979) has been established as a reliable and useful method for investigating a wide variety of molecular spectroscopy through many successful applications (Wan *et al*., 2001 and 2004; Poolmee *et al*., 2005). It was found that a remarkable merit of the SAC-CI method lies in its wide applicability to different electronic states and in its rather constant accuracy. Using the SAC method, a closed-shell state of molecule was calculated. In case of the SAC-CI method, the different electronic states of the molecule which are produced by excitations, ionizations, and electron attachments from the close-shell state were calculated. Recently, the SAC-CI method has been emerged in the Gaussian03 (Frisch *et al.*, 2004) to be a useful method for studying molecular excited states. This method has clarified the details of the excited states of various kinds of molecules, like π-conjugated compounds and transition metal complexes.

In this study, the objectives are following;

1. To investigate the structures of both ground and excited states of fluorene-thiophene copolymers
2. To calculate the energy gap of fluorene-thiophene copolymers
3. To investigate the optical properties of FT and FMT
4. To give an accurate characterization of the excited states of FT and FMT
5. To give an accurate spectra (absorption and emission) of FT and FMT

From our basic knowledge of these polymers, therefore, a new conjugated polymer which is being interested in nanoelectronic-device materials can be designed.

LITERATURE REVIEW

First attempts to synthesize soluble, processable poly(2,7-fluorene) via an attachment of solubilizing substituents in 9-position of the fluorene core were published in 1989 by Yoshino and co-workers. 9,9-dihexylfluorene was coupled to be poly(9,9-dihexylfluorene) which has a low molecular weight by oxidation with $FeCl_3$. However, this oxidative coupling is not strictly regioselective, as structural defects are created besides “regular” 2,7-linkages. So that the enormous progress in the availability of efficient and strictly regioselective transition metal-catalyzed aryl-aryl couplings has paved the way for the synthesis of high molecular weight, structurally well-defined PF derivatives. Especially reductive aryl-aryl couplings of dihaloaryls according to Yamamoto, aryl-aryl cross-couplings of aryldiboronic acids (esters) according to Suzuki, or of distannylaryls and dihaloaryl according to Stille have been successfully applied.

Palladium-catalyzed Suzuki coupling reaction was used for synthesizing a novel series of soluble alternating conjugated copolymers comprised of 9,9-dihexylfluorene and substituted bithiophene or thiophene moieties (Liu *et al.*, 2000). In their study, the structure modifications were controlled for tuning the electronic properties. In the backbone structure of the polymers, the thiophene rings in the bithiophene moieties are β-substituted with decyl chains, the bithiophene moieties are in two different coupling configurations of head-head and tail-tail regioregularities. For the thiophene moieties, they are either mono- or disubstitutes with decyl chains. It was found that all of the polymers demonstrate efficient blue-to-green light emission, good thermal stability, and relatively high glass transition temperatures ($T_g \approx 78°C$). However, their optical and electrochemical properties are independent of the coupling configurations of the substituted bithiophene moieties, whereas the head-to head regularity demonstrates higher glass transition temperature and better environmental stability. Quantum efficiency was also investigated. As for the polymers composed of thiophene moieties, the monosubstitution of a decyl chain on the β-position of thiophene ring produces bluish green emission with high fluorescence quantum efficiency (0.65 in solution). The second attachment of a decyl chain on another *β*-position of thiophene ring pushes the emission to the blue region with reduced fluorescence quantum efficiency (0.39 in solution). Thiophene and bithiophene were also substituted in the backbone of polymer using palladium-catalyzed Suzuki couplings by Ranger *et al.* (1998). These fluorene-based π-conjugated polymers exhibit strong emission in the green region (496 nm). They also show reversible electroactivity upon reduction and oxidation. Many research groups have carried out the synthesis of the polyfluorene derivatives based on thiophene or bithiophene through the Suzuki coupling reaction. This approach to thiophene moieties can also be extended to thieno-acenes (e.g., thieno[3,2-*b*]thiophene) and higher homologues of the linear thiophene-condensed π-system. Lim *et al*. (2003) have synthesized a new PF derivative, poly(9,9-dioctylfluorene-*alt*-thieno[3,2-b]thiophene), PFTT. It shows good thermal stability and displays unique phase transition behavior between the crystalline and liquid-crystalline states. Moreover, PFTT has an electrochemical energy gap of approximately 2.98 eV, which is smaller than that of common polyfluorene homopolymers. In a same reaction, Meng *et al*. (2003) prepared a series of alkyl chain-capped oligofluorene-thiophenes with high yield. Thermal analysis as well as electrochemical measurements of the materials indicated that the new oligomers have high thermal and oxidative stability. In the case of emission, bright emission colors from greenish yellow to orange-red were observed in this new series of oligomers of solid films excited UV light (366 nm). Charas *et al.* (2001) synthesized the novel poly(9,9-bis(2-ethylhexyl)fluorene-*alt*-2,5-thiophene), and the similar poly(9,9-bis(2-ethylhexyl)fluorene-*alt*-2,5-thiophene-*S,S*-dioxide) and poly(9,9-bis(2-ethylhexyl)fluorene-*alt*-1,4-phenylene) luminescent copolymers by the Suzuki coupling reaction. Within this series, an adequate choice of the unit combined with the fluorene monomer, effectively controls the energetic position of the frontier levels of the copolymer. This effect is evidenced by the different optical energy gaps and different emission colours. The decrease of energy gap (E_g), upon substitution of phenylene by thiophene has also been observed in similar copolymers based on 9,9-dioctylfluorene. Furthermore, the results of cyclic voltammetry (CV) studies showed that the *S,S*-dioxide substitution on the thiophene ring increase both the ionization potential (IP) and the electron affinity (EA) in relation to the similar thiophene-based copolymer. Moreover, molecular design and characterization of chromic polyfluorene were also investigated by Blondin *et al.* (2000). Chromic polyfluorene derivatives; poly[2,7-(9,9-dioctylfluorene-*alt*-,2,5-(thiophene)], poly[2,7-(9,9-diocylfluorene)-*alt*-2,5-(3,4-dimethylthiophene)] and poly[2,7-(9,9-dioctylfluorene)-*alt*-2,5-(3,4-ethylenedioxythiophene)] were synthesized by palladium-catalyzed Suzuki coupling reaction. All polyfluorene derivatives have been prepared in good yields (85-90%). Moreover, these polymers exhibit an excellent thermal stability. In 2002, Herguth *et al.* (2002) reported the systematic study of a series of copolymers derived from the copolymerization among 9,9-dihexylfluorene, benzothiadiazole (BT), and a third electron-rich comonomer via palladium-catalyzed Suzuki-coupling reaction. The third electron-rich comonomer was added in order to adjust the charge-injecting and -transporting properties of these polymers. The electron-donating strength of the third comonomer increases in the following trend: 2,5-dimethylbenzene < dioctyloxybenzene < terthiophene. All of these copolymers exhibited strong green emission at around 540 nm which can be attributed to either the charge transfer between an electron-rich segment and an electron-deficient BT-containing segment of the polymers.

The luminescence properties of conjugated polymers are of considerable interest, because of the fundamental information that can be obtained about exciton formation and decay, and the potential applications for conjugated polymer as the emissive material in light-emitting diodes (LEDs). Luminescence in conjugated polymers is believed to be the result of radiative decay of singlet excitons, competing non-radiative processes provide additional means of decay, and therefore reduce the efficiency of luminescence. It is generally assumed that, owing to statistical factors, only a quarter of all excited states of organic materials are a singlet type, from which fluorescence may occur, and in consequence electroluminescence efficiencies (η_{EL}) are related to photoluminescence efficiencies (η_{PL}) by the relationship: $\eta_{EL} \leq 1/4\,\eta_{PL}$. Therefore, luminescence properties should be studied in a deeper understanding of this matter to improve and eventually optimize materials and devices. In 1999, Theander *et al.* (1999) reported the quantum yield, in solution and thin films, for polythiophenes with different substituents. Depending on the different substituents, quantum yields ranged between 0.38 and 0.01 for polymers dissolved in chloroform; for spin-coated films, quantum yields as high as 0.24 were measured. It was found that the increasing the bulkiness of the substituent increases the quantum yield in solution. For spin-coated films an increased ordering can either increase or decrease the quantum yields, depending on the separation of the conjugated backbones. Polythiophenes in which the electronic energy gap are increased by steric hindrance show very low quantum yield, both for film and solution. This low quantum yield originates from a fast nonradiative decay. However, it was found that oligothiophenes display in general appreciably high photoluminescence quantum yields in solution, which increase on increasing the oligomer size (up to 40-50% for the hexamer) but drop by several orders of magnitude in the solid state. From this result, Barbarella *et al.* (2001) showed that the photoluminescence properties of 3,5-dimethyldithieno[3,2-b;2',3'-*d*]-thiophene-4,4-dioxides and of oligomers containing thienyl-*S,S*-dioxide unit as an internal rigid core leads to a dramatic increase of PL in solution and results in oligomers displaying high photoluminescence efficiencies both in solution and in the solid state. Moreover, optical properties and enhancing solid-state emission of poly(thiophene)s can be tuned by molecular control. Li *et al.* (2002) proposed the postfunctionalization approach. This methodology facilitates structural engineering of poly(thiophene) derivatives. Postfunctionalization of poly(3-hexylthiophene) (P3HT) was performed. It was found that in solution, 3,4-disubstituted poly(thiophene)s exhibited a lower fluorescence yield (ϕ_{fl}) than P3HT. In the solid state, bromo, chloro, and formyl groups increase ϕ_{fl}, whearas nitro groups completely quench fluorescence. An extensive enchancement in the solid-state ϕ_{fl}, 12 times greater than that of P3HT, is observed for polymers containing ortho-alkylpenyl or 2-(3-alkyl)thienyl groups. From the previous knowledge that major drawbacks of polyfluorenes, however, are that they could show excimer and/or aggregate formation in thin films or upon thermal annealing. The way to suppress excimer formation and improve efficiency in polyfluorenes like copolymerization with anthracene, end-capping with sterically hindered groups, and by incorporating pendant or bulky dendron groups in the polymer backbone. Tirapattur *et al.* (2002) reported the optical and photophysical properties of fluorene-based polyesters in solution and in the solid state (thin films). The red-shifted emission energies observed in the photoluminescence spectra of the thin films are rationalized in terms of stronger $\pi \rightarrow \pi *$ intermolecular interactions due to the closeness of the molecules (molecular packing) in the solid state. However, these electronic interactions are not strong enough to induce excimer or aggregate formation. The quenching excimer and/or aggregate deactivation channel found in many polymeric systems are less efficient in the present polyesters. As expected, the presence of ester linkage between adjacent oligomers causes an interruptions of the electronic conjugation thus limiting the fluorescence to the blue region. Moreover, the fluorescence efficiencies of thin films, estimated from lifetime measurements of the polyesters in solution and in the solid state, are relatively high (10-25%).

The device fabrication is also the important step for researching in this field. The light-emitting diodes can be fabricated into single and double layer devices. Liu *et al.* (2002) frabricated polyfluorene copolymers comprised of fluorene and thiophene to be light-emitting diode. Single and double layer devices fabricated with the polymers in a conventional configuration appeared to have electron as the majority carrier, and their performance was remarkably improved when poly(3,4-ethylenedioxythiophene) (PEDOT) was selected as the hole-injecting/transporting layer. It was found that double layer device of which the green color emitted demonstrated the best performance. It exhibited luminescence of 356 cd/m^2 at a bias of 8V with an external efficiency of 0.38%. For improving the hole-injecting properties, new organic materials for light emitting devices based on dihexylfluorene (DHF) -co-ethylenedioxythiophene (EDOT) copolymers were synthesized by Stephan *et al.* (2002). These copolymer was fabricated to be ITO|copolymer|Al OLEDs. It was found that even a low EDOT, i.e. 11-15%, within poly(dihexylfluorene) (PDHF) main chain, causes significant and very interesting changes in comparison in the electronic properties in comparison with poly(fluorene)homopolymers. Green light emitting devices with no significant spectral evolution based on this copolymer show improved hole injection compared to the ones using PDHF. Recently, the development of polyfluorene-based RGB materials for light-emitting diodes has been reported by Wu *et al*. (2004). A variety of chromophores can be incorporated into the fluorene polymer backbone. All of these copolymers are highly photoluminescent, and their energy-gap, which defines the emissive wavelength, can be qualitatively correlated to the extent of delocalization in the comonomers. PLEDs devices, using bilayer structures on indium tin oxide substrates and evaporated metal cathodes, have demonstrated unprecedented high efficiencies at high brightness levels and long lifetime performance.

In theoretical points of view, they have also proved to be of importance in this field because of the various limitations of experiments. Therefore, theoretical studies can help to establish relationships between the structure and the electronic properties of conjugated polymers. Many researchers have their attentions to study the relationships between the structure and energy gap. Due to the high level of disorder associated with most of these materials, structural information is hard to come by experimentally. Therefore, the energy structure was then computed employing extended Huckel theory (EHT), Hartree-Fock (HF), and density functional theory (DFT) in preliminary. Salzer *et al*. (1998) proposed the accurate method for calculating energy gaps in conducting polymers. DFT calculations have been used to estimate energy gaps for polyacetylene, polythiophene, polypyrrole, polythiazole, and a thiophene-thiazole copolymer. However, using a slightly modified hybrid functional is necessary. Therefore, they obtained energy gaps within 0.1 eV of experimental solid-state values. Marcos *et al*. (2000) estimated HOMO-LUMO energy gaps for -OMe and -NO_2 α,α'-substituted oligothiophenes up to six monomers using semiempirical, Hartree-Fock and density functional methods. For a direct comparison to the experimental energy gaps, it was found that density functional methods provide good estimates which error bars are ca. 0.2 eV. Moreover, the ΔSCF approach has been found to be an alternative way to estimate energy gaps for molecular systems where Koopmans' theorem may not provide good results, in particular -NO_2 substitution which has charge transfer. However, energy gaps for infinite chains of polymer can be determined by plotting excitation energies against the inverse of the number of monomer units and extrapolating the number of units to infinity. Kwon *et al.* (2000) applied excitation methods: ZINDO, configuration interaction singles (CIS) and time-dependent density functional theory (TDDFT) for calculating excitation energies of polythiophene and the related polymers with a fused benzene ring or a fused pyrazine ring. Geometries of oligomers up to octamers performed by AM1 and up to tetramers performed by B3LYP/6-31G* of those molecules have been optimized. The ZINDO//DFT and TDDFT//DFT give results more consistent with experiment. However, it was also found that DFT HOMO-LUMO energy differences were reasonable in this case. Moreover, they also performed their calculations for investigating the energy gap of polyaniline both in case of neutral and charged forms (doped form) (Kwon *et al.*, 2000). The doped form has been computed with a spin-unrestricted method (UAM1) and the energy gap approximated from an extrapolation of the trimer and octamer. It was found that the calculated energy gap of 1.3 eV (UZINDO//UAM1) is in good agreement with experiment (1.5 eV). The energy gaps of a series of conducting polymer were investigated by Ma *et al.* (2002). Moreover, the chain length dependence of excitation energies of oligomers including polyene, *p*-phenylene, pentafulvene, cyclopentadiene, pyrrole, furan, silole, phosphole, and thiophene, employing the time-dependent density functional theory with B3LYP functional, was studied. Energy gaps and effective conjugation lengths of the corresponding polymers were obtained by extrapolating vertical excitation energies of trimers through pentamers to infinite chain length. It was predicted that polypentafulvene, polycyclopentadiene, polysilole and polyphosphole have smaller energy gaps than polythiophene, and polypentafulvene has the smallest energy gap. Hutchison *et al.* (2002) performed six computational methods which are ZINDO/CIS, ZINDO/RPA, HF/CIS, HF/RPA, TDDFT/TDA, and TDDFT to predict the energy gap of heterocyclic π-electron polymers such as polythiophene, polypyrrole and polyfuran. It shows that among those methods, the semiempirical ZINDO/CIS method applied to DFT-predicted geometries affords the best agreement between computed and experimental energy gaps. Energy gap can be tuned by inserting the donor and acceptor into the main polymer. Therefore, the influence of donor (methoxy and amine groups) and acceptor (cyano group) substituents on the electronic characteristics of poly(fluorene-phenylene) was observed by Zeng *et al.* (2002). The results showed that the use of diamino or dicyano substituent on the phenylene ring allows the energy gaps to decrease significantly. In 2004, Yang *et al*, (2004) compared the performance of various molecular and solid state quantum chemical methods in predicting the energy gaps of conjugated polymers. They found that a combination of semiempirical geometry optimization followed by a hybrid functional theory calculation (B3LYP/PM3) for the energy levels of molecular oligomers provides a reliable and computationally efficient method for predicting energy gaps of a group of diverse conjugated polymers. Moreover, their results show that the gap values depend strongly on the applied quantum chemical level of theory, especially the extent to which the exact exchange is incorporated into the theory. Therefore, the best values are obtained with hybrid functionals. Briere *et al.* (2004) studied the electronic, structural and optical properties of poly(2,7-fluorene) (PF), poly(2,7-carbazole) (PC) and poly(2,7-borafluorene) (PBF). All the calculations were done by using density functional theory (DFT) with a plane wave basis set, pseudopotentials, and local exchange-correlation energy. They found that the energy gaps for carbazole and borafluorene are smaller than biphenyl and fluorene, due to differences in the highest occupied molecular orbital (HOMO) or lowest unoccupied molecular orbital (LUMO) wave functions. However, for the polymers, the experimental energy gap for PC was found to be almost the same as for PPP and PF. Calculations explain this experimental observation which is attributed to a change in the ordering of the last two valence energies between carbozole and its polymer. For theoretical study, they found that the energy gap of PBF, which not been synthesized yet, should be smaller than the minimum energy gaps of the other studied polymers by ~0.5 eV. Therefore, quantum chemical calculations show that they can conduct an experiment for synthesizing an effective polymer.

Consequently, the usefulness of quantum-chemical methods can be shown by investigating the adsorption and luminescence phenomena. Quantum-chemical methods have helped in forging a fundamental understanding of the electronic and optical characteristics of the conjugated materials and in guiding the experimental efforts toward novel compounds with enhanced characteristics. Therefore, accurate calculations of molecular vertical excitation energies and polarizabilities are essential for the modeling of spectroscopic probes, addressing structure-function relations and predicting structures with desired optical properties. Previously, many theoretical investigations have been conducted for the electronic ground state of heterocyclic π-electron oligomers. Comparably few calculations have been investigated for excited-states, and even fewer include changes in molecular structure upon excitation. Heterocyclic π-electron oligomers in the class of fluorene-phenylene and fluorene-thiophene are investigated both in ground and excited states by using quantum-chemical methods by Belletete *et al.* (2000). Moreover, UV-Vis and fluorescence spectroscopics and photophysical properties were also performed. The optimized structures and the characterization of frontier molecular orbitals were obtained by HF/6-31G* *ab initio* calculations. It was shown that all derivatives are non-planar in their ground electronic states. For the excited state, ZINDO/S semiempirical calculations performed on HF/6-31G* optimized geometries were used to investigate the nature and the energy of the first 10 singlet-singlet electronic transitions. For each derivative, excitation to the S_1 state corresponds mainly to the promotion of an electron from the HOMO to the LUMO, and the $S_1 \leftarrow S_0$ electronic transition is strongly favored and polarized along the bond axis of the molecular frame. The energy of the first electronic transition of all derivatives follows the HOMO-LUMO energy gap computed from HF/6-31G* *ab initio* calculations. They concluded that the first absorption energy of each derivative can be assigned to the $S_1 \leftarrow S_0$ electronic transition computed from ZINDO/S calculations. They also interested in fluorene-thiophene oligomers as well as the respective molecules incorporated in polyesters (Belletete *et al.*, 2001). ZINDO/S calculations on the optimized geometries (HF/6-31G*) were used to assigned the first absorption energy which is $S_1 \leftarrow S_0$ electronic transition. This transition corresponds mainly to the promotion of an electron from the HOMO to LUMO and is strongly allowed and polarized along the long axis of the molecular frame. The insertion of alkyl lateral chains at the 3-positon of the thiophene rings caused a torsion of the backbone of the oligomers, which induced a blue shift of the absorption energy. From fluorescence data, it is observed that a more planar conformation is favored in the relaxed excited states. The increase of the oligomer chain or the addition of carbonyl groups at both ends of the molecules induces a red shift of the spectra due to increase in the electronic delocalization along the molecular frame. It was shown by HF/6-31G* *ab initio* calculations that the length of the oligomer chain and/or the presence of carbonyl groups do not significantly influence the ground state molecular conformation. Belletete *et al.* (2004) also performed ZINDO/s to investigate the nature and energy of the first two singlet-singlet electronic transitions of carbazole-based dyads. Whereas restricted Hartree-Fock level (RHF/6-31G*) was carried out for geometry optimization. For all oligomers, the first electronic transition ($\pi \rightarrow \pi^*$) is weakly allowed and polarized along the y-axis (short axis) of the molecule. On the other hand, the $S_2 \leftarrow S_0$ electronic transition of each oligomer possesses a much larger oscillator strength polarized along the x-axis, and is mainly described by the promotion of one electron from the HOMO to the LUMO. It is found that these calculations produce $S_2 \leftarrow S_0$ vertical transition energies in fair agreement with the absorption energies maxima measured in *n*-hexane. For excited state geometry, the optimization (relaxation) of S_1 and S_2 electronic states has been done using the restricted single configuration interaction (RCIS/6-31G*) method. Then electronic transition energies from the relaxed excited states have been obtained form ZINDO/s calculations on the optimized geometries of S_1 and S_2. Recently, Lukes *et al.* (2005) interpreted the spectral of thiophene-fluorene π-conjugated derivatives by using ZINDO/s method. In their calculations, the averaged simulated electron absorption spectra obtained by taking Boltzaman's distribution into account due to the influence of the conformations.

For more accurate data, *ab initio* CI (configuration interaction) calculations are a tool for describing the optical properties of conjugated organic polymers. Therefore, CIS/3-21G* was used to observe the nature of the geometric conformations and electronic transitions in π-conjugated oligo(thiophene)s, and their cyano derivatives (Lagowski *et al.,* 2001). Their investigation indicates that the cyano substituted thiophene polymer has a considerably smaller intrinsic energy gap than its parent polymer. The results indicate that this method produces singlet excitation energies in excellent agreement with experimental values (~0.1-0.5 eV). The lowest (singlet) excited states (S_1) of oligofluorenes were also studied by using the restricted configuration interaction/singles (RCIS/6-31G*) at the restricted Hartree-Fock level (RHF/6-31G*) geometry optimizations by Tirapaturr *et al.* (2003). It was found that these molecules are non-planar in the ground state, whereas, they almost reach planarity in their S_1 excited state. They found that CIS calculations produce singlet excitation energies in good agreement with the 0-0 absorption peaks measured in cyclohexane (differences less than 0.2 eV). In their calculations, the emission energies have been computed by using CIS and the obtained results are very close to those determines from the emission spectra measured in cyclohexane. However, there are many theoretical approaches now available to investigate the excited state properties, such as time-density functional theory (TDDFT), complete active space self-consistent field (CASSCF) and second-order perturbation theory (CASPT2). However, the computational cost and complexity of TDDFT is roughly comparable to single excitation theories based on Hartree-Fock ground state, such as CIS. At the same time, excitation energies to valence excited states are considerably improved, and there is even significant improvement for excitation energies of excited states that, when treated by wave function-based methods, have appreciable double-excitation character. TDDFT is applied to calculate vertical excitation energies of linear polyene oligomers by Hsu *et al.* (2001). Based on comparisons with experimental results and high level *ab initio* calculations in the literatures, significant improvement over singles configuration interaction is observed. Therefore this good performance is very encouraging because TDDFT can be straightforwardly applied to much larger systems, such as carotenoids. Consequently, the theoretical spectra of electroluminescent polymers are studied by Yu *et al.* (2003). TDDFT, followed by a systematic scheme with a symmetry restriction to extrapolate the absorption and emission corresponding to infinite chains avoiding periodic boundary conditions, was used. It was found that the B3LYP is concluded to be the most suitable functional for computation. Besides the singlet excited state and neutral molecule interested, the triplet excited state, cations and dications were also interested. In 2004, the electronic structures of thienylene vinylene oligomers ranging in size from two thienylene rings

(2TV) to 12TV were described by quantum chemical study by Grozema *et al*. (2005). The geometries of the TV oligomers in the ground state, the lowest triplet state, and the singly and doubly oxidized states were oxidized using density functional theory calculations. In the case of electronic spectra, configuration interaction calculations with an INDO/s reference wave function were performed. When compared with the experimental data, they agree well except the triplet-triplet absorption spectra. However, for closed shell systems (ground state and doubly occupied state), the spectra were also calculated by TDDFT. It was found that the (singlet) absorption spectra of doubly oxidized TVs, the results from TDDFT calculations are surprisingly good; particularly for a long chains.

In 2002, Parusel *et al*. (2002) performed an excited state theoretical studies for investigating the excited states of 4,-*N*,*N*-dimethylaminobenzonitrile (DMABN). Theoretical studies are presented for DMABN by using the semiempirical Austin model 1 (AM1) and *ab initio* Hartree-Fock (HF) methodology for optimization of the electronic ground states and AM1/configuration interaction with both single and double excitations (CISD) and HF/configuration interaction with single excitation (CIS) for the lowest excited states. Moreover, the results of AM1/CISD, HF/CIS, complete active space self-consistent field (CASSCF), and second-order perturbation theory (CASPT2), time-dependent density functional theory (TDDFT), density functional theory/single-excitation configuration interaction (DFT/SCI) and multireference configuration interaction (DFT/MRCI) single-point calculations are compared by using both the AM1/CISD- and HF/CIS-optimized geometries for the calculation of adsorption and emission energies. It was found that the results of both the CASPT2 and all DFT-based methods are in qualitatively good agreement with experimentally obtained absorption energies. A comparison of calculated emission energies by using excited-state geometries with data using ground-state optimized geometries shows the necessity to use optimized excited-state geometries for computation of emission energies.

For calculating the electronic spectroscopy, the goal is to obtain accurate transition energies and reliable dipole transition moments in order to assign energies located in the UV-vis spectral domain of energy. The choice of the method will be a compromise taking into account the following factor: (i) the feasibility and computational cost; (ii) the validity of some approximations; (iii) the desired level of accuracy; (iv) the control that can be performed on the analysis of the results. Therefore, the symmetry adapted cluster (SAC)/symmetry adapted cluster configuration interaction (SAC-CI) which is cluster expansion method is one of a reliable tools for investigating the excited state properties recently. Wan *et al.* (2001) investigated the electronic excitation spectrum of thiophene by using SAC/SAC-CI method. To give a satisfactory theoretical interpretation of the vacuum ultraviolet (VUV) spectroscopic study and electron energy loss (EEL) of thiophene, the 70 singlet and four lowest triplet electronic states were computed. Moreover, the similarities and differences in the electronic excitations between thiophene and other five-membered ring compounds were also discussed. They also compared the accuracy and assignment of their results with those of CASPT2 and multireference double configuration interaction methods. In 2004, they (Wan *et al.*) studied the singlet and triplet vertical electronic transitions of styrene. It was found that the present SAC-CI theoretical results, including both the singlet → singlet and singlet → triplet vertical electronic transitions, have well reproduced the profile of the electronic spectra of styrene. Moreover, higher-energy singlet → triplet excited states and Rydberge states were extensively computed. It was found that their results as compared with the previous CASPT2 study are different. Recently, the excited states of the fluorene-thiophene compounds whose polymer are useful as a light-emitting diode were studied by SAC-CI method (Poolmee *et al.*, 2005). The effect of torsional angle between fluorene and thiophene units on the excited states was examined for 2-(fluoren-2-yl)thiophene (FT) and 2-(fluoren-2-yl)-3-methylthiophene (FMT). Consequently, the accurate absorption spectra were simulated by taking thermal average for the conformers of some torsional angles from 0° to 90° and the absorption spectra are good agreement with the observed spectra. In addition, the absorption spectra of dimer and trimer of FT were also calculated at the equilibrium structure.

METHODS OF CALCULATIONS

1. Model Setup

In this study, fluorene-thiophene oligomer and its derivatives were studied. The molecular structures studied are shown in Fig. 3. The geometries of fluorene-thiophene oligomers were constructed by SciPolymer 3.0 program. Then, all calculations were carried out by the GAUSSIAN 03 program running on Linux PC 2.5 GHz.

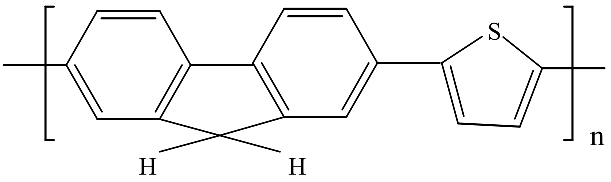

Poly[2,7-(fluorene)-co-*alt*-2,5-(thiophene)] ; **P1**

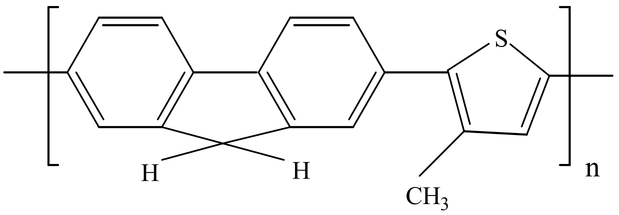

Poly[2,7-(fluorene)-co-*alt*-2,5-(3-methylthiophene)] ; **P2**

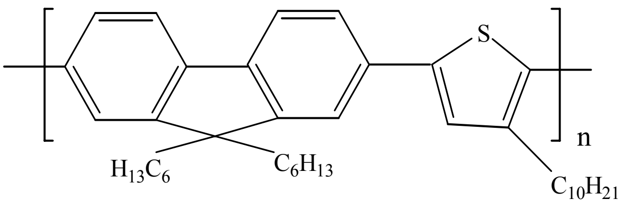

Poly[2,7-(9,9-dihexylfluorene)-co-*alt*-2,5-(decylthiophene)] ; **P3**

Figure 3 Molecular structures of fluorene-thiophene copolymers in this study.

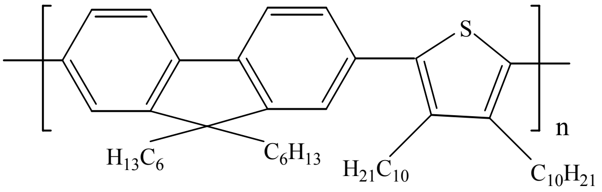

Poly[2,7-(9,9-dihexylfluorene)-co-*alt*-2,5-(3,4-decylthiophene)] ; **P4**

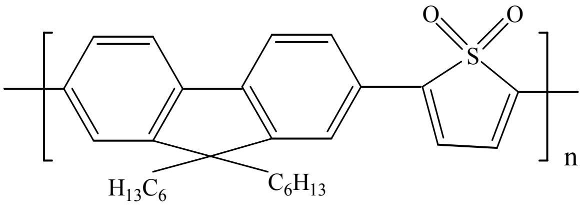

Poly[2,7-(9,9-dihexylfluorene)-co-*alt*-2,5-(*S,S*-dioxidethiophene)] ; **P5**

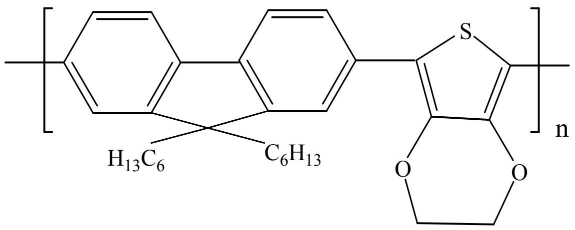

Poly[2,7-(9,9-dihexylfluorene)-co-*alt*-2,5-(3,4-ethylenedioxythiophene)] ; **P6**

Figure 3 (cont'd)

For our models, the hexyl groups at the C_9 position of the fluorene unit of P3-P6 have been replaced by ethyl groups to reduce calculating time. It was found that the presence of alkyl groups at the C_9 position does not significantly affect on the equilibrium geometry of fluorene derivatives (Belletete *et al.*, 2000; Yang *et al.*, 2005). Furthermore, the length and structure of the alkyl substituents do not significantly vary the optical and electronic properties of the PFs in dilute solution, which indicates a negligible influence of the alkyl side-chains on the electronic interaction between adjacent fluorene unit. The length of the side chains located at thiophene unit (decyl group) in the case of P3 and P4 were also reduced to ethyl group as it was found that longer side chain does not obviously affect on the electronic properties of the polymer. It follows that HOMO-LUMO energy gap does not significantly different when the length of the alkyl group increases as illustrated in Table 1. Furthermore, the excitation energy was also shown in Table 2. These calculated results were not only found for P3 but also found similarly in case of P4 in which the two side chains located at thiophene unit. Consequently, the models used in this study are shown in Fig 4.

Table 1 HOMO-LUMO gap (ΔE, eV) of P3 (hexyl groups were replaced by ethyl groups) monomer and dimer when alkyl group (R) at thiophene unit increases. HF/3-21G was carried out.

R	monomer			dimer		
	HOMO	LUMO	ΔE	HOMO	LUMO	ΔE
H	-7.83	2.25	10.08	-7.01	1.41	8.42
CH_3	-7.63	2.28	9.91	-7.34	1.93	9.27
C_2H_5	-7.62	2.28	9.90	-7.34	1.93	9.27
C_3H_7	-7.62	2.28	9.90	-7.40	2.01	9.41
C_4H_9	-7.62	2.28	9.90	-7.40	2.01	9.41
C_5H_{11}	-7.62	2.28	9.90	-7.40	2.01	9.41
C_6H_{13}	-7.62	2.28	9.90	-7.40	2.01	9.41
C_7H_{15}	-7.62	2.28	9.90	-7.40	2.01	9.41
C_8H_{17}	-7.62	2.28	9.90	-7.40	2.01	9.41
C_9H_{19}	-7.62	2.28	9.90	-7.40	2.01	9.41
$C_{10}H_{21}$	-7.62	2.28	9.90	-7.40	2.01	9.41

Table 2 Excitation energy of P3 (hexyl groups were replaced by ethyl groups) monomer and dimer when alkyl group at thiophene unit increases. TDDFT/B3LYP/6-31G*//AM1 was carried out. (The longer side chain was not calculated due to the constant value of the excitation energy)

R	monomer		dimer	
	Excitation energy (eV)	Oscillator strength	Excitation energy (eV)	Oscillator strength
H	3.82	0.81	3.01	2.03
CH_3	3.81	0.82	3.11	1.91
C_2H_5	3.79	0.83	3.16	1.84
C_3H_7	3.80	0.87	3.19	1.78
C_4H_9	3.80	0.88	3.19	1.77
C_5H_{11}	3.80	0.89	3.19	1.76

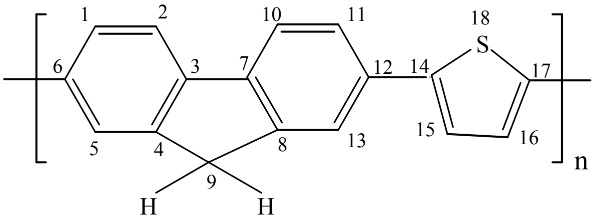

Poly[2,7-(fluorene)-co-*alt*-2,5-(thiophene)] ; **PFT (n=1-3)**

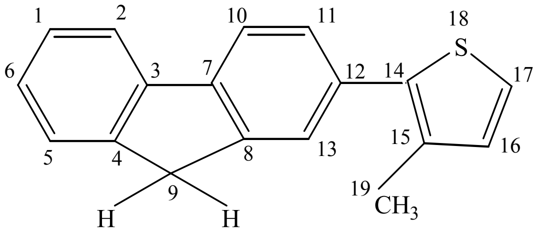

2,7-(fluorene)-co-*alt*-2,5-(3-methylthiophene); **FMT**

Figure 4 Models and atomic numbering of fluorene-thiophene copolymers.

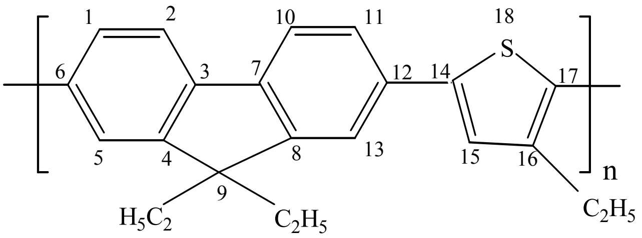

Poly[2,7-(9,9-diethylfluorene)-co-*alt*-2,5-(4-ethylthiophene)] ; **PFET (n=1-5)**

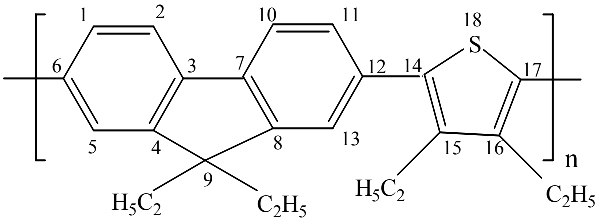

Poly[2,7-(9,9-diethylfluorene)-co-*alt*-2,5-(3,4-ethylthiophene)] ; **PFEET (n=1-5)**

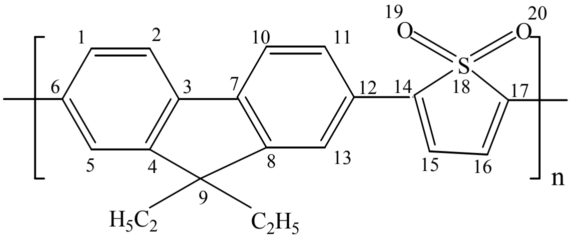

Poly[2,7-(9,9-diethylfluorene)-co-*alt*-2,5-(*S,S*-dioxidethiophene)] ; **PFTSO2 (n=1-5)**

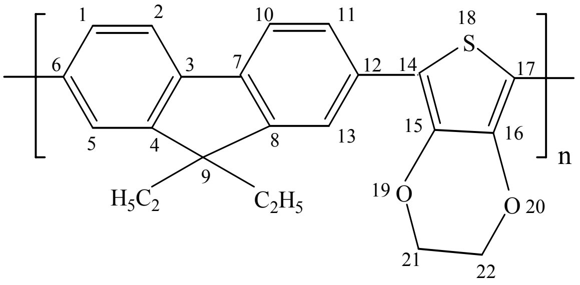

Poly[2,7-(9,9-diethylfluorene)-co-*alt*-2,5-(3,4-ethylenedioxythiophene)] ; **PFTSOO (n=1-5)**

<u>Figure 4</u> (cont'd)

In our calculations, these models were divided into two sets for investigating the electronic properties; PFET, PFEET, PFTSO2 and PFTSOO were investigated for energy gap calculations, whereas PFT and PFMT were selected for optical property investigation

2. Conformational Analysis and Geometrical Optimization

Potential energy curves of FET, FEET, FTSO2 and FTSOO monomers were investigated based on the semiempirical (AM1), *ab initio* (HF/3-21G* and HF/6-31G*), and density functional theory (B3LYP/6-31G*) methods. Conformational analysis was done by changing the torsional angle ($\theta = C_{13}\text{-}C_{12}\text{-}C_{14}\text{-}C_{15}$) by 15° steps between $\theta = 0° - 180°$. To obtain the final torsional angles of the conformers in each minima, calculations of these geometries were performed without constraint on the torsional angle.

In case of FT and FMT monomer, the ground-state potential energy curves along the torsional angle ($\theta = C_{13}\text{-}C_{12}\text{-}C_{14}\text{-}C_{15}$) were calculated by using B3LYP/6-31G* level. Torsional angle was changed by 15°, whereas all other geometrical parameters were fixed. For FT and FMT, the effect of torsional angle on the adsorption spectra was also studied.

3. Electronic Properties

3.1 Energy gap

Extrapolated energy gaps of the polymers were obtained by plotting the HOMO-LUMO energy gap calculated by using AM1, HF/3-21G*, HF/6-31G* and B3LYP/6-31G* methods and the inverse of the number of monomer units (1/n) and extrapolating the number of units to infinity. In the case of excitation energies, they will be calculated by using the semiempirical (ZINDO) and time-dependent density functional theory (TDDFT) methods at the optimized geometries of the ground state using the semiempirical, *ab initio* and density functional theory. Energy gap estimated from excitation energies was also performed in the similar manner for all polymers studied.

3.2 Optical properties

In this part, the excited state electronic structures and optical properties of 2-(fluoren-2-yl)thiophene (FT) and 2-(fluoren-2-yl)-3-methylthiophene (FMT) which are the model unit of fluorene-thiophene polymer for LED were investigated by using SAC-CI method. The SAC-CI SD-*R* calculations were performed for the excitation spectra of FT and FMT monomers at each torsional angle. Double zeta basis set of Huzinaga-Dunning [4s2p/2s] were adopted; the valence excited states relevant for the optical properties were described and the consistent calculations up to trimer were possible with this basis set. In the preliminary calculations, it was found that the three low-lying excited states are important for the first absorption energy in the experimental spectrum. Therefore, we presented the results of these three excited states, although we also calculated higher excited states. In the SAC-CI calculation, 1s orbital of C and 1s, 2s, 2p orbitals of S were taken as the frozen core MOs and their counterparts were excluded from the active space. For monomer, the resultant SAC-CI active space consists of 43 occupied and 125 unoccupied MOs. The excitation spectra of dimer and trimer of FT were also calculated by the SAC-CI method at their ground-state structure optimized by B3LYP/6-31G*. For dimer and trimer, the active spaces were 129 occupied and 247 unoccupied MOs and 193 occupied MOs and 256 unoccupied MOs, respectively.

To reduce the computational requirements, the perturbation selection procedure was adopted (Nakatsuji, 1983). LevelTwo accuracy in SAC-CI Gaussian03 (Frisch *et al.*, 2004) was adopted as follows. The threshold of the linked terms for the ground state was set to $\lambda_g = 5.0 \text{ x } 10^{-6}$. The unlink terms were described as the product of the important linked terms whose SDCI coefficient were larger than 0.005. For excited state, the thresholds of the linked doubles were set to $\lambda_e = 5.0 \text{ x } 10^{-7}$. The thresholds of the CI coefficients for calculating the unlinked operators in the SAC-CI method were 0.05 and 0.0 for the R and S operators, respectively. For dimer and trimer, LevelOne accuracy was adopted.

RESULTS AND DISCUSSION

1. Conformational and Structural Analysis

At the beginning, the conformational analysis has been carried out. The partial optimized torsional angle (θ=C_{13}-C_{12}-C_{14}-C_{15}) for the electronic ground state between fluorene unit and thiophene unit of FET were performed by semiempirical (AM1), *ab initio* (HF/3-21G* and HF/6-31G*) and density functional theory (B3LYP/6-31G*) methods. The relative potential curves of the obtained results for FET are shown in Fig. 5.

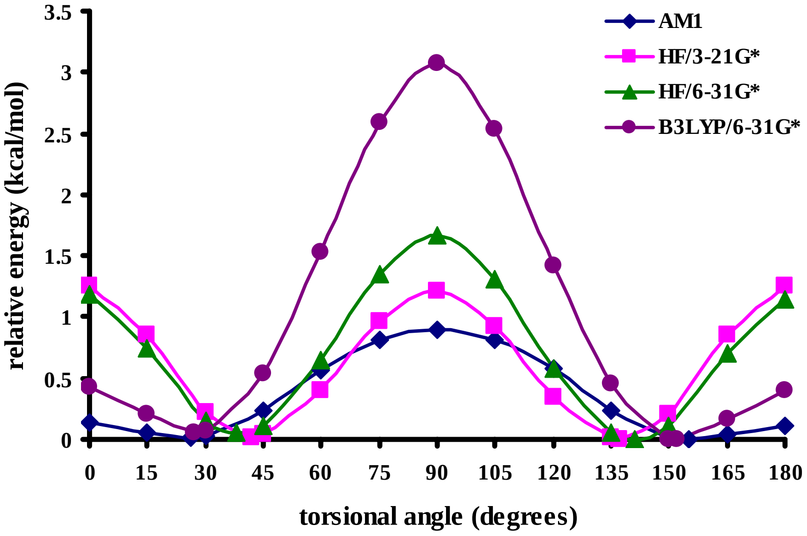

Figure 5 Comparison of potential energy curves of torsional angle (θ = C_{13}-C_{12}-C_{14}-C_{15}) obtained for FET. The curves were calculated by AM1, HF/3-21G*, HF/6-31G* and B3LYP/6-31G* methods.

It was found that the potential energy curves calculated from those methods produced two local minima. HF/3-21G* and HF/6-31G* calculations provided two minima corresponding to θ around 30°-45° and 135°-150°. Similarly, the potential energy curves obtained from AM1 and B3LYP/6-31G* calculations also showed two minima. Even though, the geometry at each local minima calculated from AM1 and

B3LYP/6-31G* methods is more planar than those of *ab initio* results. The two minima were located around 15°-30° and 150°-165°. This can be explained by the effect of delocalization. The π-orbital involved in the intermonomer bond, causing delocalization favor a planar geometry. When the torsional angle increased to 90°, the potential energy curve was dominated by energy increment due to the loss of the π-electron delocalization over the whole molecule, with perpendicular conformation being the most unstable.

The ground state geometries of monomer FET as obtained from AM1, HF/3-21G*, HF/6-31G* and B3LYP/6-31G* calculations are shown in Table 3, and the numbering of the atoms was assigned in Fig. 4. Accordingly, it was found that the geometries obtained from AM1 and B3LYP/6-31G* calculations are not significantly different as compared with those obtained from HF/3-21G* and HF/6-31G* methods. Kwon *et al.* (2000) used DFT and AM1 methods for thiophene oligomer geometries. They found that DFT-optimized geometries are in excellent agreement with the solid state structure. In their work, calculated C-C inter-ring distances (~1.45 Å) and C-S distances (~1.75 Å) at B3LYP/6-31G* level are almost equal to experimental data (C-C, 1.45 Å; C-S, 1.75 Å), while AM1 calculated distances (C-C, 1.42 Å; C-S, 1.58 Å) are shorter than experimental data due to the nature of the AM1 parametrization. In this work, C-S distance calculated at B3LYP/6-31G* (1.74 Å) shows a good agreement with the C-S distance of the thiophene unit obtained from the solid state structure. Comparing AM1 and *ab initio* methods, Duan *et al.* (2001) found that the structures obtained from both were similar, the major difference being that the C-S bond was about 0.13 Å longer in the *ab initio* structure. Furthermore, the bond angles (C-S-C) obtained from *ab initio* (91.5°) and density functional theory (91.7°) agree well with the experimental data (Horowitz *et al.*, 1995). In addition, Bongini *et al.* (1999), found that the DFT method in particular the B3LYP functional was carried out better than MP2 method for studying the torsional potential of 3,3-dimethyl-2,2-bithiophene and 3,4-dimethyl-2,2-bithiophene.

Table 3 Ground state geometries of the FET monomer obtained from AM1, HF/3-21G*, HF/6-31G*, and B3LYP/6-31G* methods (bond length in Å; bond angle and torsional angle in degree).

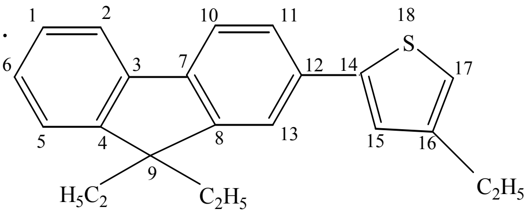

Geometrical parameters	Methods				
	AM1	HF/3-21G*	HF/6-31G*	B3LYP/6-31G*	X-ray
C_1-C_2	1.402	1.387	1.386	1.397	1.40
C_2-C_3	1.385	1.381	1.385	1.397	1.41
C_3-C_4	1.428	1.395	1.394	1.410	1.41
C_4-C_5	1.383	1.377	1.382	1.391	1.38
C_5-C_6	1.403	1.390	1.389	1.400	1.43
C_6-C_1	1.391	1.385	1.388	1.399	1.38
C_3-C_7	1.460	1.474	1.472	1.467	1.48
C_7-C_8	1.427	1.395	1.394	1.401	
C_8-C_9	1.520	1.528	1.527	1.529	
C_9-C_4	1.519	1.528	1.527	1.528	1.47
C_7-C_{10}	1.385	1.380	1.384	1.396	
C_{10}-C_{11}	1.398	1.385	1.385	1.393	
C_{11}-C_{12}	1.402	1.392	1.394	1.409	
C_{12}-C_{13}	1.412	1.396	1.397	1.412	
C_{13}-C_8	1.381	1.375	1.379	1.386	
C_{12}-C_{14}	1.443	1.475	1.479	1.467	
C_{14}-C_{15}	1.384	1.351	1.350	1.375	
C_{15}-C_{16}	1.433	1.440	1.441	1.432	
C_{16}-C_{17}	1.381	1.348	1.346	1.370	
C_{17}-S_{18}	1.664	1.724	1.727	1.735	
S_{18}-C_{14}	1.689	1.735	1.740	1.756	
$\theta(C_{13}$-C_{12}-C_{14}-$C_{15})$	-25.66	-42.12	39.40	26.64	
$\angle(C_{14}$-S_{18}-$C_{17})$	93.98	91.49	91.51	91.71	

Moreover, C-C distances in thiophene unit of the FET monomer are also in good agreement with the thiophene oligomer (Horowitz *et al.* 1995). Therefore, the fluorene unit and ethyl group which is attached at thiophene unit do not significantly effect the thiophene geometries. In case of fluorene unit, the results obtained from AM1, *ab initio*, and DFT are in good agreement with the reported X-ray data (Burns *et al.*, 1955). Normally, C_8-C_9 and C_9-C_4 distances (~1.47Å) obtained from X-ray data are usually shorter than the optimized values. The origin of this difference is due to the crystal packing force. Compared to HF method, DFT calculation yield longer C=C bond and shorter inter-ring distance. Thus, using HF method, π-electrons are more localized, this is due to the neglect of electron correlation. Tirapattur *et al.* (2003) calculated the ground state geometries of fluorene derivatives; 2-(fluoren-2-yl)thiophene (FT) and 2-(fluoren-2-yl)methylthiophene (FMT) at HF/6-31G* level. As compared FET with FT, the addition of an ethyl group at position 4 of the thiophene unit does not significantly affect the bond length of the phenylene and thiophene rings including the inter-ring distance, except for C_{15}-C_{16} distance which becomes longer. This is obviously because of the steric hindrance caused by the ethyl group. Furthermore, those molecules provide non-planar structures which have the torsional angle about 39.0 degrees. The inter-ring distance of FMT is longer than FET due to the steric hindrance caused by the methyl groups, which is evidence from the large torsional angle (55.2 degrees).

Potential energy curves of FEET, FTSO2 and FTSOO were performed by density functional theory at B3LYP/6-31G* level which provides a reliable geometry of FET. Potential energy curves are illustrated in Fig. 6. Moreover, the optimized geometrical parameters of FEET, FTSO2 and FTSOO calculated at B3LYP/6-31G* level were presented in Table 4. According to Fig. 6, it can bring to the fact that FEET, FTSO2 and FTSOO molecules possess non-planar structures. Comparison of the geometry of FET and FEET, it was found that torsional angle of FEET is larger than those of FET because of the steric hindrance of the ethyl group. Whereas, other structural parameters are not different significantly. The potential energy curve of FEET showed two minima which are located at 56° and 134°. Interestingly, the conformer with the torsional angle of 56° showed the steric hindrance generated from ethyl group attached on thiophene unit group at C_9 position of the fluorene unit. Therefore, the energy of this conformer is slightly higher than that of located at 134°. It can bring to the fact that the molecule possesses a non-planar structure in the ground state. In addition, a very low rotational energy barrier (~1.4 kcal/mol) was observed which allows a wide range of non-planar conformations. This obtained result is quite different as compared to those of FET (~3.0 kcal/mol). Therefore, it means that FET structure is more rigid than FEET. Furthermore, it was found that the coplanar energy barrier is a bit higher than the perpendicular energy barrier. The reason might be concerned with the steric hindrance between the ethyl group attached on the thiophene ring and hydrogen at C_{13} and C_{11} of the fluorene moiety.

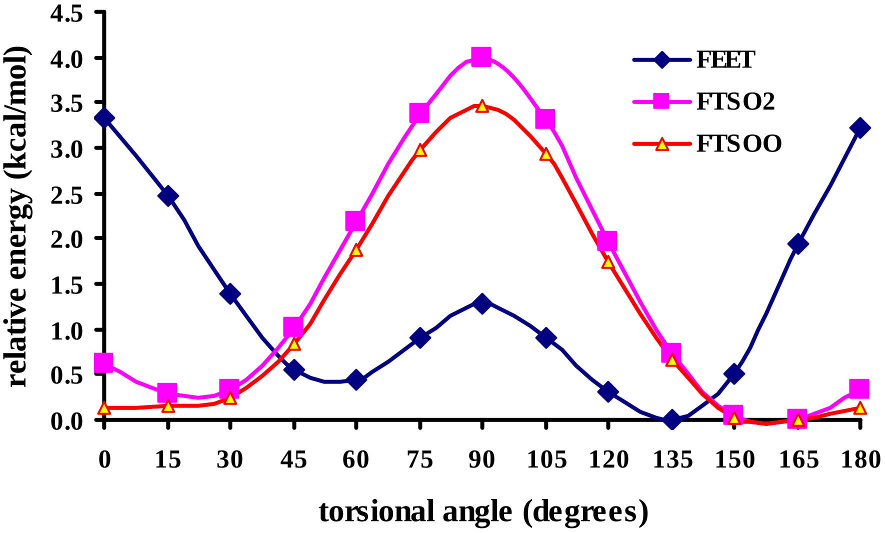

Figure 6 Potential energy curves of FEET, FTSO2 and FTSOO monomers calculated at B3LYP/6-31G* level.

Table 4 Optimized structural parameters of FEET, FTSO2 and FTSOO monomers calculated at B3LYP/6-31G* level. (bond length in Å; bond angle and torsional angle in degree).

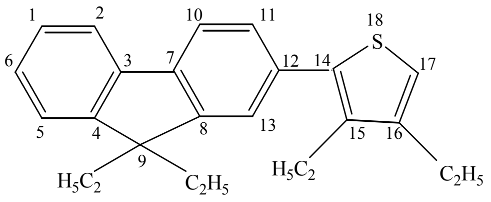

FEET

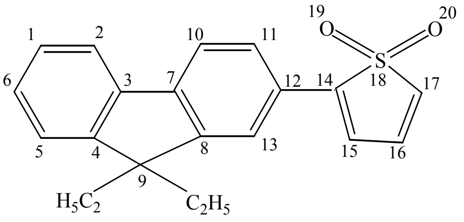

FTSO2

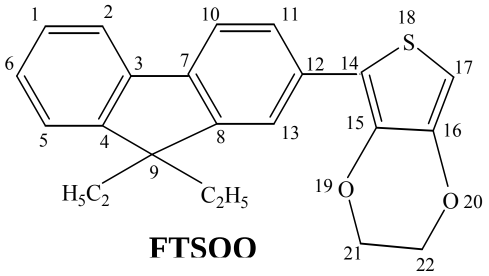

FTSOO

Geometrical parameters	FEET	FTSO2	FTSOO
C_1-C_2	1.396	1.396	1.397
C_2-C_3	1.396	1.397	1.397
C_3-C_4	1.410	1.410	1.411
C_4-C_5	1.391	1.391	1.391
C_5-C_6	1.400	1.400	1.400
C_6-C_1	1.399	1.399	1.399
C_3-C_7	1.468	1.466	1.467
C_7-C_8	1.410	1.412	1.410
C_8-C_9	1.529	1.528	1.529
C_9-C_4	1.528	1.528	1.529
C_7-C_{10}	1.396	1.396	1.396
C_{10}-C_{11}	1.394	1.392	1.393
C_{11}-C_{12}	1.408	1.411	1.412
C_{12}-C_{13}	1.410	1.414	1.413
C_{13}-C_8	1.388	1.383	1.386

Table 4. (cont'd)

Geometrical parameters	FEET	FTSO2	FTSOO
C_{12}-C_{14}	1.478	1.456	1.464
C_{14}-C_{15}	1.381	1.350	1.379
C_{15}-C_{16}	1.446	1.472	1.434
C_{16}-C_{17}	1.370	1.339	1.364
C_{17}-S_{18}	1.728	1.791	1.736
C_{14}-S_{18}	1.752	1.833	1.761
S_{18}-O_{19} **(PFTSO2)**	-	1.474	-
S_{18}-O_{20} **(PFTSO2)**	-	1.471	-
C_{15}-O_{19} **(PFTSOO)**	-	-	1.372
C_{16}-O_{20} **(PFTSOO)**	-	-	1.369
O_{19}-C_{21} **(PFTSOO)**	-	-	1.433
O_{20}-C_{22} **(PFTSOO)**	-	-	1.431
C_{21}-C_{22} **(PFTSOO)**	-	-	1.521
$\theta(C_{13}$-C_{12}-C_{14}-$C_{15})$	56.04	-22.05	-22.58
$\angle(C_{14}$-S_{18}-$C_{17})$	91.52	92.63	92.88
$\angle(O_{20}$-S_{18}-$O_{19})$ **(PFTSO2)**	-	119.10	-

According to Fig. 6, the coplanar energy barrier of FEET was a bit higher than the perpendicular energy barrier. While the coplanar energy barrier of FTSO2 and FTSOO was very low. It means that *S,S*-dioxide functionalized at thienyl sulfur and ethylenedioxide functionalized at the thiophene unit provide a less steric effect. Moreover, the coplanar structures show weak hydrogen bonds. For FTSO2, the weak hydrogen bond (2.22 Å) occurred between O_{19} and H atom at C_{11}. Hydrogen bonding of FTSOO occurred between O_{19} and H atom at C_{13} and the atomic distance was about 2.66 Å. This weak hydrogen bond was found not only the coplanar structures of FTSO2 and FTSOO but also found at the optimized structures. However, the energy difference of PFTSO2 and PFTSOO between the two minima was quite high as compared to FEET. These results indicate that the functionalization of the thienyl sulfur to the corresponding *S,S*-dioxide and the functionalization of the ethylenedioxide at thiophene unit leads to the rigidity of the molecular skeleton. Considering the optimized geometry of FTSO2, it was found that the oxygen atoms of the SO_2 moiety lie roughly at the same distances which were 1.47Å, above and below the pentaatomic ring. In addition, with respect to the thiophene molecule, the loss of the aromatic conjugation by the S atom implies C_{14}-S_{18}, C_{17}-S_{18} and C_{15}-C_{16} bond lengthening as compared with FET, FEET and FTSOO. The optimized geometries of FET, FEET, FTSO2 and FTSOO pentamers obtained from B3LYP/6-31G* are shown in Fig. 7.

2. HOMO-LUMO Energy Gaps and the Lowest Excitation Energies

In theory, the energy gap of polymer $(M)_n$ can be extrapolated by the orbital energy difference between the highest occupied molecular orbital (HOMO) and the lowest unoccupied molecular orbital (LUMO), when $n = \infty$ (Hay, 2002; Hong *et al.*, 2001). Therefore, the calculated HOMO-LUMO energy gaps of FET are shown in Table 5. Moreover, the HOMO-LUMO energy gaps were extrapolated to the infinite chain length of the polymer and the results are depicted in Fig. 8.

Table 5 HOMO-LUMO energy gap of FET oligomers, calculated by B3LYP/6-31G*//AM1, B3LYP/6-31G*//HF/3-21G*, B3LYP/6-31G*//HF/6-31G* and B3LYP/6-31G* methods.

oligomer	HOMO-LUMO energy gap (eV)			
	B3LYP/6-31G* //AM1	B3LYP/6-31G* //HF/3-21G*	B3LYP/6-31G* //HF/6-31G*	B3LYP/6-31G*
n=2	3.60	4.17	4.10	3.54
n=3	3.37	3.93	3.85	3.33
n=4	3.29	3.87	3.79	3.23
n=5	3.19	3.84	3.77	3.23
n=∞	2.93	3.59	3.50	2.92

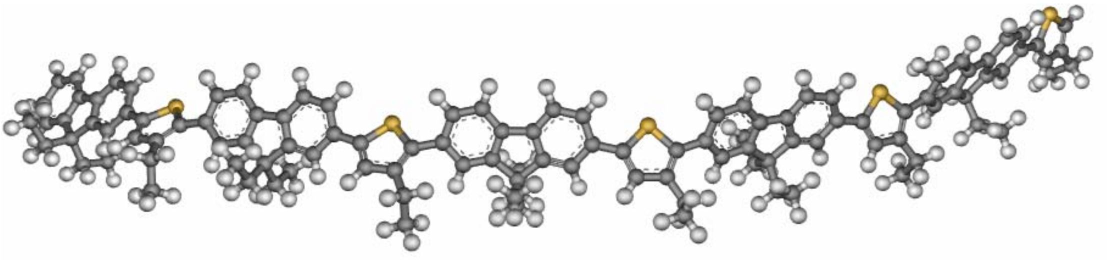

FET

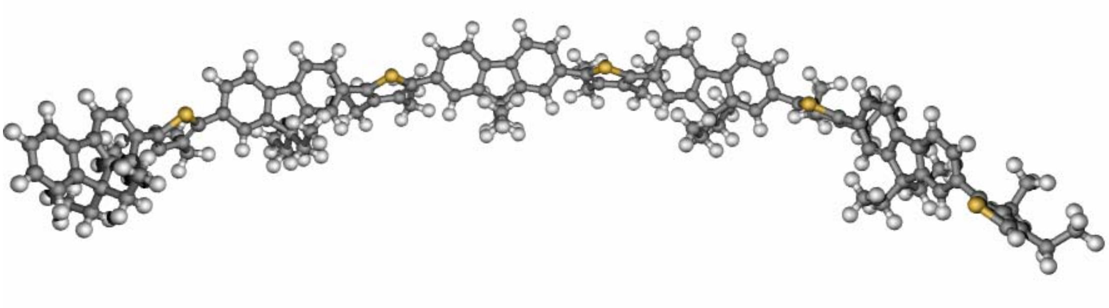

FEET

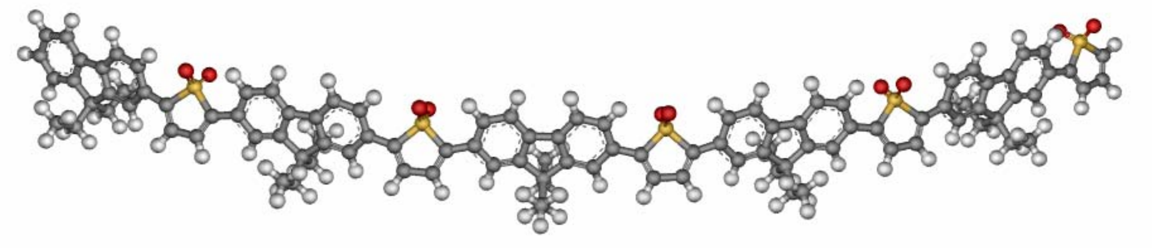

FTSO2

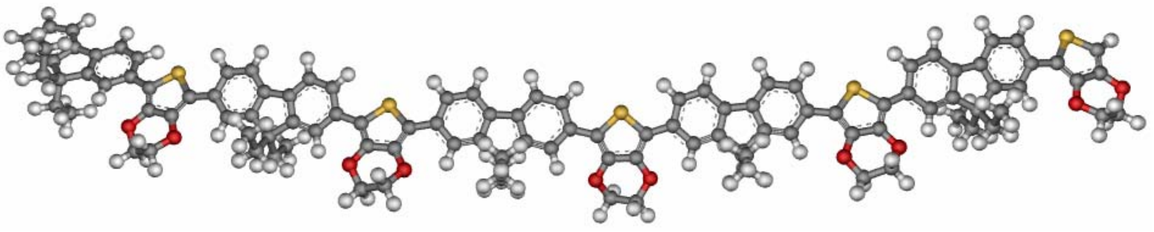

FTSOO

Figure 7 3D-structures of FET, FEET, FTSO2 and FTSOO pentamer, obtained from B3LYP/6-31G*.

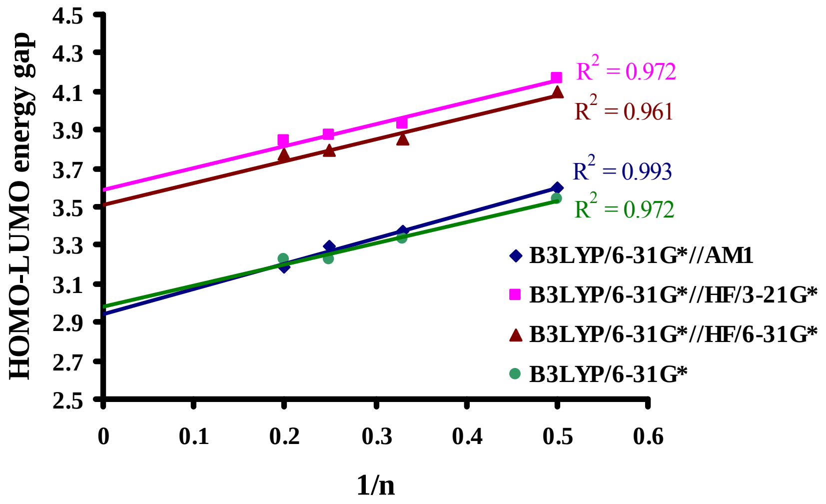

Figure 8 Energy gaps of PFET extrapolated from the plot of HOMO-LUMO energies of the oligomers versus the inverse number of monomer units.

According to Fig. 8, it was found that the obtained energy gaps are far from the experimental data (2.50 eV; Lui *et al*., 2000). This means that estimated HOMO-LUMO energy gap cannot represent the energy gap of this polymer studied. As the result, the orbital energy gap between HOMO and LUMO is still an approximate estimation to the transition energy since the transition energy also contains significant contribution from some two-electron integrals. It is known that HOMO-LUMO energy gaps obtained from HF/3-21G*, HF/6-31G* and B3LYP/6-31G* calculations are the crudest estimation. However, Alguno *et al*. (2000) have studied the energy gaps of the polythiophene using Hartree-Fock and density functional theory methods employing various combinations of exchange and correlation functional with electron core potential (ECP) split valence basis sets. They pointed out that DFT calculations with hybrid functionals (B3LYP and B3P86) gave excellent results (4.06 eV and 4.11 eV) which are in good agreement with the experimental energy gap (4.05 eV).

In order to improve the more accurate energy gaps, the spectrum methods (ZINDO and TDDFT/B3LYP/6-31G*) were applied in this study to calculate the excitation energy. In calculating the excitation energies by both methods, the first excited state with significant oscillator strength ($\pi \rightarrow \pi^*$ transition) was used and it was also the lowest excited state for all oligomers. Extrapolated energy gaps for oligomers by the ZINDO and TDDFT methods, based on AM1-, HF/3-21G*-, HF/6-31G*- and B3LYP/6-31G*-optimized geometries are shown in Fig. 9.

All extrapolated energy gaps as obtained from various methods are summarized in Table 6. The extrapolated energy gap from TDDFT/B3LYP/6-31G* excitation energies using DFT-optimized geometries is in excellent agreement with the experimental data. Considering the geometries obtained from B3LYP/6-31G*, it is found that the geometries are more planar and the inter-ring distances are shorter than those obtained from HF/6-31G* and HF/3-21G* calculations. The optimized geometries of the pentamer as obtained from different methods are shown in Fig. 10. The inter-ring distances of the oligomer as obtained from different methods are also analyzed and plotted against the bond number as shown in Fig. 11. The bond number is defined as following; bond numbers 1, 3, 5, 7 and 9 for inter-ring distance between thiophene-fluorene unit and bond numbers 2, 4, 6 and 8 for inter-ring distance between fluorene-thiophene unit.

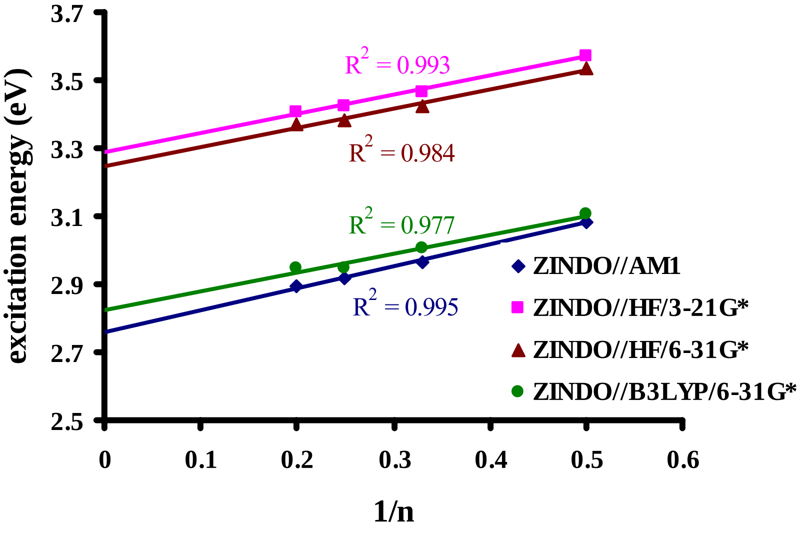

(a)

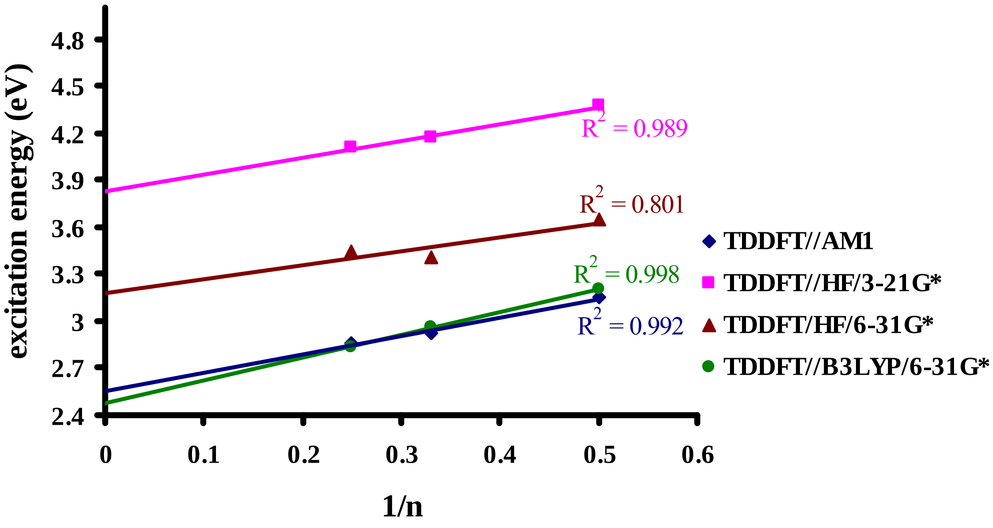

(b)

Figure 9 Energy gap extrapolated from the plot of excitation energies versus the inverse number of FET monomer units; (a) ZINDO (b) TDDFT(B3LYP/6-31G*) methods.

Table 6 Extrapolated energy gaps of FET calculated at various methods.

method	energy gap (eV)
ZINDO//AM1	2.76
ZINDO//HF/3-21G*	3.29
ZINDO//HF/6-31G*	3.24
ZINDO//B3LYP/6-31G*	2.82
TDDFT/B3LYP/6-31G*//AM1	2.56
TDDFT/B3LYP/6-31G*// HF/3-21G*	3.83
TDDFT/B3LYP/6-31G*// HF/6-31G*	3.18
TDDFT/B3LYP/6-31G*// B3LYP/6-31G*	2.47
Experimental optical energy gap	2.50[a]

[a] Lui *et al.*, 2000

Based on the optimized geometries, it was found that the inter-ring distances obtained from AM1 method are shorter than those obtained from DFT and HF methods (Fig. 11). However, this shorter inter-ring distance does not effect the conjugation along the main chain of the structure as compared from the energy gap calculated by the same method; TDDFT/B3LYP/6-31G*//AM1 (Eg = 2.56 eV), TDDFT/B3LYP/6-31G*// B3LYP/6-31G* (Eg = 2.47 eV). On the other hand, the planarity of the oligomer does significantly effect to increase the conjugation along the main chain. Considering the inter-ring torsional angles in Table 7, obtained from the DFT optimized geometry, these are smaller than those obtained from AM1 and HF methods, in particular, the inter-ring torsional angles between thiophene unit attached with ethyl group and fluorene. While, TDDFT excitation energies using AM1-optimized geometries also provide a good energy gap due to the shortening inter-ring distance and planarity of oligomer structure; however, the AM1 geometry of the oligomer, in particular C-S distance of the thiophene unit is shorter than experimental data. Therefore, the geometry of the oligomer obtained from AM1 method is not satisfied as compared to the results obtained from the B3LYP method which are in good agreement with experimental data in terms of both structural parameters and energetic results.

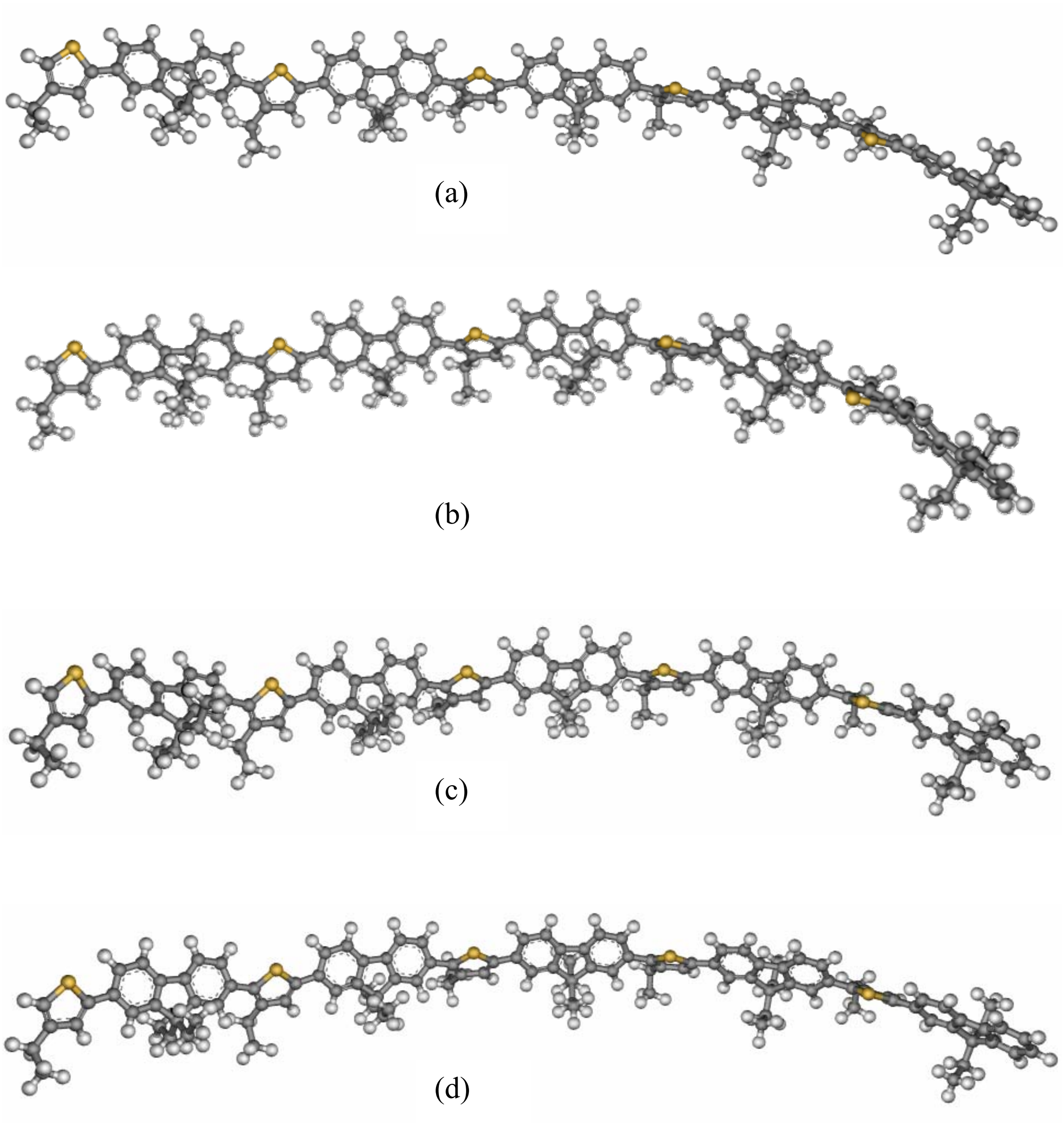

(a)

(b)

(c)

(d)

Figure 10 Optimized geometries of FET obtained from (a) AM1, (b) HF/3-21G*, (c) HF/6-31G* and (d) B3LYP/6-31G* calculations.

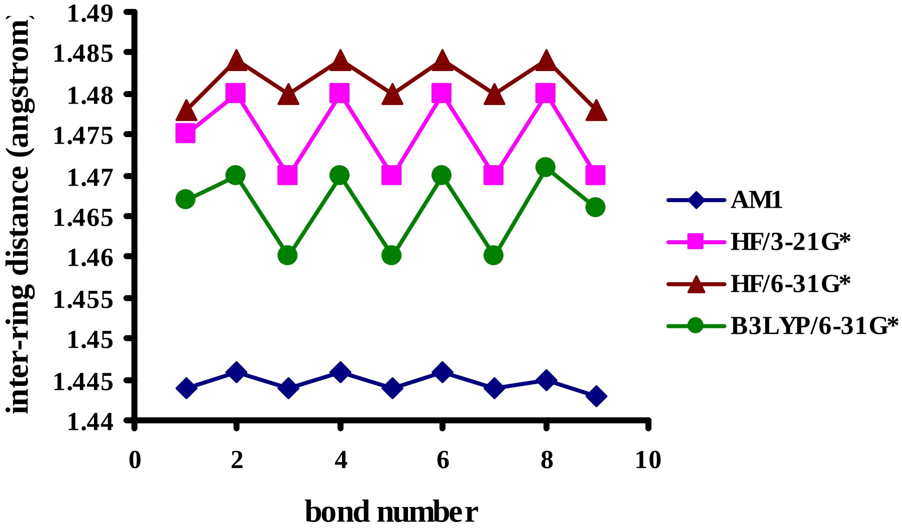

Figure 11 Inter-ring distance of pentamer of FET (bond number started from the left hand side of the optimized geometries as shown in Fig. 10), obtained from different methods.

Table 7 Inter-ring torsional angles of the optimized geometries (started from the left hand side of the optimized geometries as shown in Fig. 10), obtained from the different methods.

Method	Inter-ring torsional angles (degs)
AM1	-25.6, 49.0, -25.4, 49.0, -25.4, 48.9, -25.5, 48.9, -25.5
HF/3-21G*	-42.0, 61.7, -40.7, 61.7, -40.7, 61.6, -40.8, 61.4, -40.5
HF/6-31G*	-38.4, 57.5, -37.3, 57.5, -37.3, 57.5, -37.4, 57.5, -37.4
B3LYP/6-31G*	-27.2, 44.2, -25.6, 45.2, -22.9, 44.6, -23.8, 44.5, -26.0

It was found that the spectrum method (TDDFT) can be used to predict energy gap of FET. In addition, geometry from DFT (B3LYP/6-31G*) provided a reliable geometry. The energy gap of PFEET, therefore, calculated by TDDFT(B3LYP/6-31G*) based on the DFT-optimized geometries. The extrapolated energy gap was

3.07 eV as shown in Fig. 12. It was found that the extrapolated energy gap still agrees with the experimental data (2.76 eV) (Lui *et al.*, 2000).

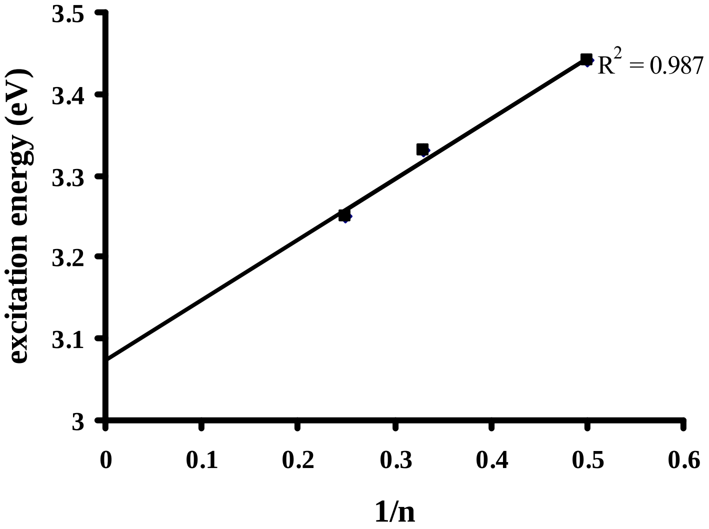

Figure 12 Extrapolated energy gap of PFEET obtained from TDDFT/B3LYP/6-31G*//B3LYP/6-31G*.

In case of PFTSO2, TDDFT(B3LYP/6-31G*)//B3LYP/6-31G* was also performed for obtaining the extrapolated energy gap. The result showed that the extrapolated energy gap is 1.86 eV, as shown in Fig. 13, which is underestimated as compared to the experimental value (2.19 eV) (Charas *et al.,* 2001). This is due to the approximation of exchange potentials from the theory of this method. In practice, the accuracy of TDDFT employing the most widely available exchange-correlation functions, which are approximations to the true functional. Therefore, a disadvantage of this method is the fact that performance can hardly be improved without introduction of better functionals, which are, however, not available in any straightforward way. The deviation between TDDFT-calculated and experimental excitation energies were reported to be between 0.0 and 1.0 eV (Bauernschmitt *et al.*, 1996). The average accuracy for polycyclic hydrocarbons is about 0.3 eV (Heinze, *et al.*, 2000). We found that the HOMO-LUMO difference can represent the energy gap of PFTSO2 as presented in Fig. 14. The extrapolated energy gap is 2.24 eV which is consistent with the experimental data (2.19 eV) (Charas *et al*., 2002). It is worth reminding that Salner *et al*. (1998) performed DFT calculations on a series of oligomers to estimate energy gaps for polyacetylene, polythiophene, polypyrrole, polythiazole, and a thiophene-thiazole copolymer. In their study, they concluded that DFT hybrid methods provide energy gaps in good agreement with vertical excitation energies from UV-absorption spectra. However, the approach to get energy gap from the orbital energy difference between the HOMO and LUMO is crude considering the experimental comparison. The implicit assumption underlying this approximation is that the lowest singlet excited state can be described by only one singly excited configuration in which an electron is promoted from HOMO to LUMO.

In the case of PFTSOO, the results are similar to PFTSO2 in the same method for investigating the extrapolated energy gap. It was found that HOMO-LUMO difference can represent the optical energy gaps derived from the absorption edge of a polymer as shown in Fig. 15. Moreover, we also found that the extrapolated energy gaps from TDDFT excitation energies systematically underestimate the actual energy gap derived from the solid-state data, as shown in Fig. 16. The extrapolated energy gaps obtained from DFT and TDDFT are 2.56 eV and 2.16 eV, respectively, whereas the optical energy gap derived from the absorption edge of a polymer thin film is 2.44 eV (Aubert *et al*., 2004).

The PFTSOO has been investigated by Cornil *et al*. (2003) with semiempirical Hartree-Fock INDO (intermediate neglect of differential overlap) Hamiltonian originally developed by Zerner and co-workers. The excited states of the oligomers have been characterized by coupling the INDO Hamiltonian to a single configuration interaction (the INDO/SCI method). Linear extrapolation of the transition energies yield at the scale of long conjugated chains transition energies is 2.42 eV. Recently, Yang *et al*. (2005) calculated the HOMO-LUMO gaps by DFT(B3LYP/6-31G*) and the lowest excitation energies by TDDFT/B3LYP/6-31G*//B3LYP/6-31G*). The HOMO-LUMO gap is 2.55 eV which is deviated from the optical energy gap (2.44 eV) by 0.11 eV, while energy gap extrapolated from lowest excitation energies is 2.21

eV which is underestimated. In our calculations, the results are almost the same as those of Yang *et al.* (2005).

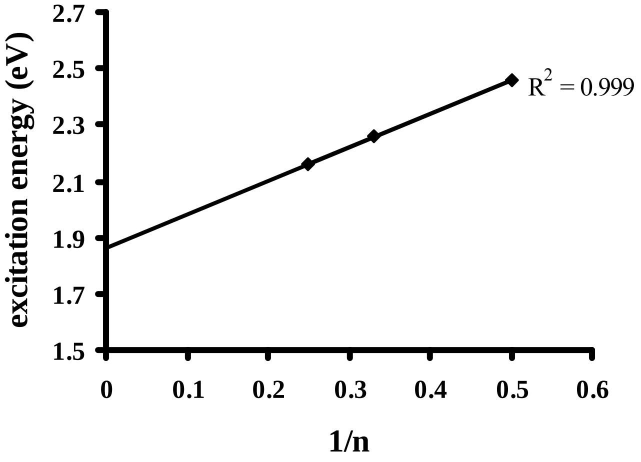

Figure 13 Extrapolated energy gap of PFTSO2 obtained from TDDFT/B3LYP/6-31G*// B3LYP/6-31G*.

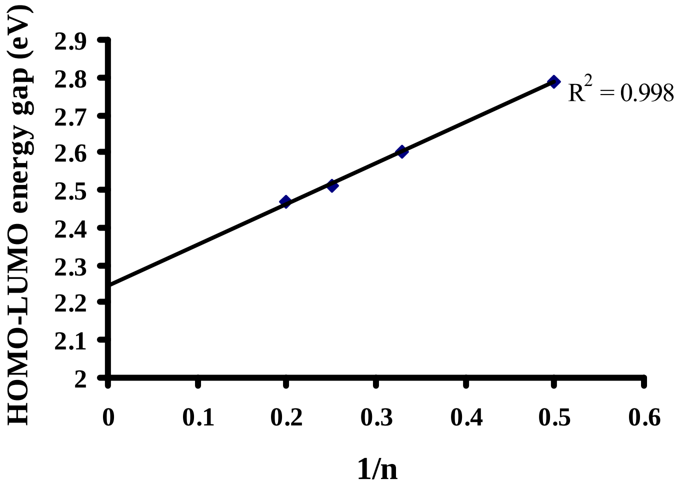

Figure 14 Extrapolated energy gap of PFSTO2 obtained from B3LYP/6-31G*.

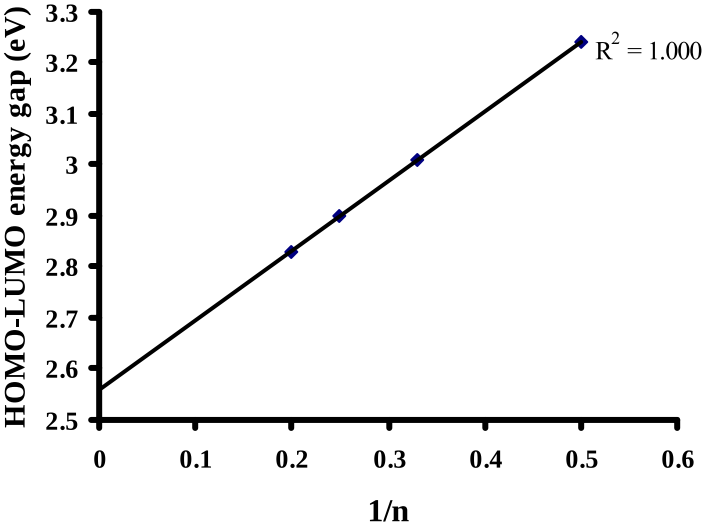

Figure 15 Extrapolated energy gap of PFTSOO obtained from B3LYP/6-31G*.

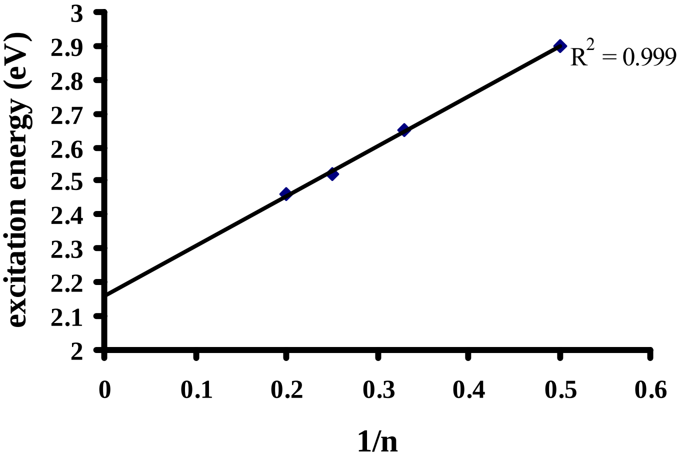

Figure 16 Extrapolated energy gap of PFTSOO obtained from TDDFT/B3LYP/6-31G*//B3LYP/6-31G*.

Therefore, the energy gap has been estimated by two ways; HOMO-LUMO energy difference and the lowest excited energies. However, the deviation from experiment occurred by two factors. One is that the predicted energy gaps are for the isolated gas-phase chains, while experimental energy gaps are measured in the liquid phase where environmental influences may be involved. The second is that solid-state effects (polarization and intermolecular packing forces) have been neglected in the calculations. The latter can be expected to the result in a decreased interring twist and consequently a reduced gap in a thin film compared to an isolated molecule as considered in the calculations.

The energy gaps of PFET, PFEET, PFTSO2 and PFTSOO relative to polyfluorene (PF) were discussed. The calculated energy gaps obtained by HOMO-LUMO energy gap and TDDFT are 3.33 eV and 2.91 eV for PF (Wang *et al.*, 2004), respectively, which are both higher than those of PFET, PFEET (compared to HOMO-LUMO energy gap), PFTSO2 and PFTSOO with the same corresponding methods. It indicates that the energy gap of PF can be tuned by introducing the thiophene derivative units into the backbone of PF. The calculated energy gap of PFET in which monosubstitution of alkyl group on the thiophene unit copolymerized is less than those of PF. This is obvious because the thiophene unit decreases the torsional angle between the fluorene and thiophene units so as to enhance the effective conjugated length along the main chain. Wang *et al.* (2004) found the torsional angle of PF obtained from the optimized ground state geometry using B3LYP/6-31G* is around 37.0°, whereas PFET is around 26.0° obtained from the same method. PFTSO2 which *S,S*-dioxidethiophene copolymerized to be fluorene based copolymer provided the narrow energy gap as compared to PF. The main reason is the reduction of the inter-ring torsional angle. Barbarella *et al.* (1998) synthesized and investigated electronic properties of oligothiophene *S,S*-dioxides relative to the parent oligothiophenes. Oligothiophene *S,S*-dioxides display smaller optical energy gaps than the parent oligothiophenes. Moreover, it also depends on the number and the position of the sulfonyl moieties. In addition, the results of HF/6-31G* calculations on 2,2-bithiophene and its monomer and bis-*S,S*-dioxides indicate that a contribution to such λ_{max} values comes from the more planar conformations of the bithiophene subsystems containing *S,S*-dioxidethiophene moieties and from the smaller inter-ring carbon-carbon distances. In case of PFSTOO, 2,5-ethylenedioxylthiophene which is electron-donating group reduced the inter-ring torsional angle to be 22.0°. However, disubstitution of alkyl group at the thiophene unit of PFEET cannot reduce the energy gap dramatically as compared to PF. They increase the torsional angle between the fluorene and thiophene unit, then to reduce the effective conjugated length along the polymer main chain. Moreover, it was found that the energy barrier between two local minima of FEET was very low. Then, FEET can be varied within the large torsional angle. Therefore, a poor conjugation occurred along the polymer chain leading to a large energy gap. On the other hand, FTSO2 and FTSOO showed the high energy barrier, then, they were constrained to be more planar conformations.

3. Optical Properties

In this study, FT and FMT, which are the model units of the light-emitting diode, were selected to study their excited state properties and optical properties.

3.1 Ground state of FT and FMT

The ground-state potential energy curves of FT and FMT monomers along the torsional angle θ = 0°-90° are shown in Fig. 17. The optimized structure parameters of the stable conformers are summarized in Table 8 for both the ground and S_1 states. FT was stable in the conformation of the torsional angle θ = 27°. However, the energy barrier towards co-planar conformation was calculated to be only 0.25 kcal/mol, while the barrier to the perpendicular conformation was about 3.10 kcal/mol. This very low rotational energy barrier indicates that it allows a wide range of non-planar conformations at room temperature. The ground-state potential energy curve for θ = 90°-180° was calculated to be almost the same energy as θ = 0°-90°, which is expected from the molecular structure. Since the effect of these conformers θ = 90°-180° are nearly same as those of θ = 0°-90°, only the conformers of θ = 0°-90° providing the linear-chain structure in the polymer were considered.

dIn the case of FMT, the torsional angle of the most stable conformation was $\theta = 43°$. The energy barrier to co-planar conformation is higher than that of FT due to the steric interaction between the methyl group and H atom at C_{13} position of fluorene unit. FMT is much more stable in the conformation of large torsional angle than FT; the energy of the conformer at $\theta = 90°$ is 1.90 kcal/mol relative to the most stable conformer at $\theta = 43°$. Thus, the energy barrier along the torsional angle is very small for both FT and FMT and the conformers of wide range of torsional angles should be considered for the excitation spectra of these molecules. It was also found that C-C bond lengths are almost the same between FT and FMT as shown in Table 8, which means the difference of the excitation spectra for these molecules is predominantly determined by the torsional angle.

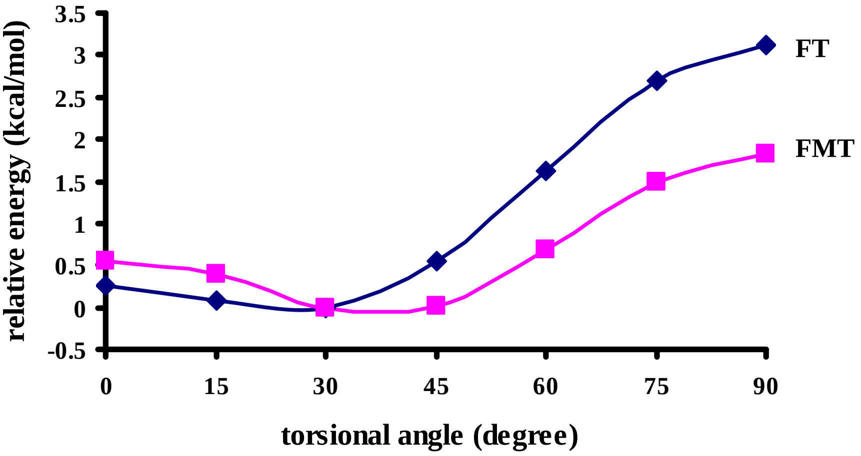

Figure 17 Ground-state potential energy curves of FT and FMT.

3.2 Excited states: effect of torsional angle

The SAC-CI method was used to calculate the first three excited states of FT, which are responsible for the first band observed experimentally. The excitation energy (ΔE) and the oscillator strength (*f*) of FT as a function of torsional angle are shown in Fig. 18. Excitation energy, oscillator strength, and excitation characters of these three excited states are summarized in Table 9, for the conformers of 0°, 30° and 60°.

Table 8 Optimized geometries of FT and FMT in S_0 and S_1 states (bond length in Å; and torsional angle in degree).

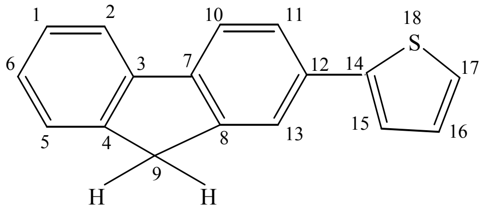

FT

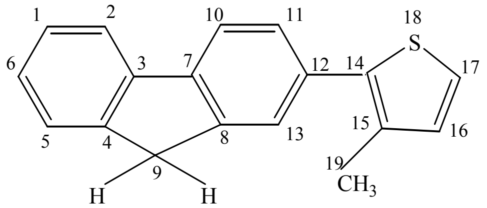

FMT

Geometrical parameters	FT		FMT	
	S_o	S_1	S_o	S_1
C_1-C_2	1.396	1.378	1.396	1.378
C_2-C_3	1.396	1.400	1.396	1.400
C_3-C_4	1.410	1.410	1.410	1.410
C_4-C_5	1.390	1.370	1.390	1.370
C_5-C_6	1.390	1.390	1.390	1.390
C_6-C_1	1.399	1.390	1.390	1.390
C_3-C_7	1.460	1.420	1.460	1.420
C_7-C_8	1.410	1.420	1.410	1.420
C_8-C_9	1.510	1.510	1.510	1.510
C_9-C_4	1.510	1.510	1.510	1.510
C_7-C_{10}	1.390	1.410	1.390	1.410
C_{10}-C_{11}	1.390	1.360	1.390	1.350
C_{11}-C_{12}	1.410	1.440	1.410	1.440
C_{12}-C_{13}	1.400	1.440	1.410	1.440
C_{13}-C_8	1.380	1.350	1.380	1.350
C_{12}-C_{14}	1.460	1.400	1.470	1.400
C_{14}-C_{15}	1.370	1.400	1.380	1.420
C_{15}-C_{16}	1.420	1.390	1.430	1.400
C_{16}-C_{17}	1.360	1.360	1.360	1.360
C_{17}-C_{18}	1.730	1.720	1.730	1.710
C_{18}-C_{14}	1.756	1.770	1.750	1.780
C_{15}-C_{19}			1.500	1.500
θ (C_{13}-C_{12}-C_{14}-C_{15})	26.87°	0°	42.66°	3.05°

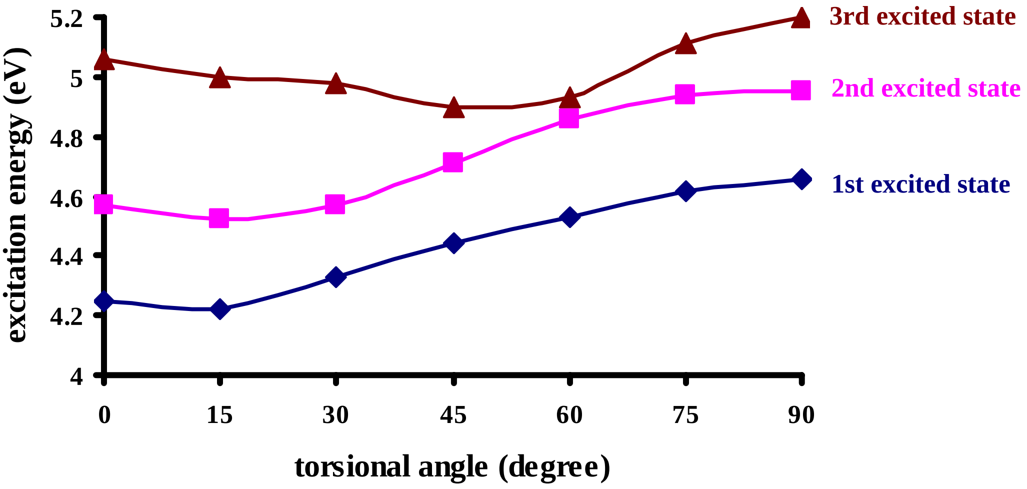

(a)

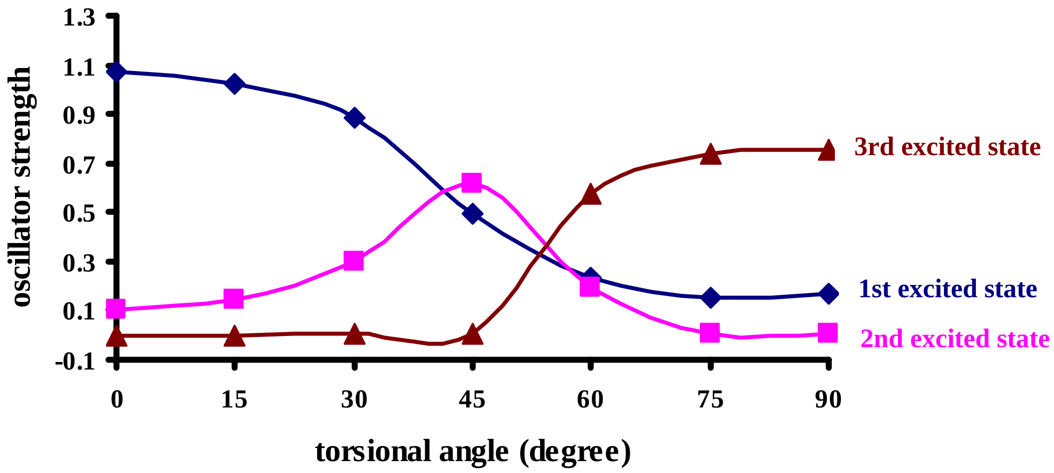

(b)

Figure 18 SAC-CI (a) excitation energy and (b) oscillator strength of the first three excited states for FT versus torsional angle.

Table 9 Excitation energy (ΔE), oscillator strength (*f*), excitation character, and dipole moment ($< r >$) of the excited states of FT at torsional angles 0°, 30°, and 60°.

Torsional angle	State	ΔE (eV)	*f*	Excitation character	$< r >$ (au)
0°					
	S_1	4.25	1.08	0.91(HOMO$\rightarrow$LUMO)	0.65
	S_2	4.56	0.11	0.73(HOMO$\rightarrow$LUMO+1)	0.58
	S_3	5.06	0.00	0.56(HOMO-1$\rightarrow$LUMO)	0.57
30°					
	S_1	4.32	0.89	0.83(HOMO$\rightarrow$LUMO)	0.65
	S_2	4.57	0.30	0.69(HOMO$\rightarrow$LUMO+1)	0.60
	S_3	4.98	0.00	0.56(HOMO-1$\rightarrow$LUMO) +0.50(HOMO-1$\rightarrow$LUMO+3)	0.58
60°					
	S_1	4.53	0.24	0.62(HOMO$\rightarrow$LUMO+1)	0.64
	S_2	4.86	0.19	0.48(HOMO-2$\rightarrow$LUMO) +0.47(HOMO$\rightarrow$LUMO+3)	0.76
	S_3	4.93	0.58	0.68(HOMO$\rightarrow$LUMO)	0.45

The present calculation shows that the excitation energies of the first (S_1) and second (S_2) excited states increase when the planarity between fluorene and thiophene units reduces. It was also found that the excitation characters of the excited states of FT depend on the torsional angle, for instance, the S_1 state of FT at torsional angle $\theta = 0°$ is characterized as the excitation from HOMO to LUMO, while the S_1 state at $\theta = 90°$ is the excitation from HOMO to LUMO+1. The characters of the S_1, S_2 and S_3 (third excited) states change in the region of $\theta = 45°$-60°, which is also clearly seen in the oscillator strength of these states in Fig. 18(b). Namely, the excitation characters are represented as follows;

	$\theta = 0°$	$\theta = 90°$
S_1	HOMO $\rightarrow$ LUMO	HOMO $\rightarrow$ LUMO+1
S_2	HOMO $\rightarrow$ LUMO+1	HOMO-2 $\rightarrow$ LUMO
S_3	HOMO-1 $\rightarrow$ LUMO	HOMO $\rightarrow$ LUMO

From the oscillator strength and the excitation character of the excited states, it can be concluded that the HOMO-LUMO transition is predominantly responsible for the absorption of the first band of FT and FMT. It was also noticed that the excitations to higher states do not contribute to this band; from our calculations, the excited states higher than 5.5 eV have small oscillator strength, whereas the first absorption bands of FT and FMT are centered at 3.90 eV and 4.09 eV, respectively (Belletete, *et al.* 2000).

Previously, the excited states of these molecules have been studied by ZINDO/S and TDDFT methods. We examine the CIS calculation for these states along the torsional angle. The CIS potential energy curves of the three low-lying excited states of FT are shown in Fig. 19. The CIS excitation energies of these states were calculated to be much higher than those of the SAC-CI method. Significantly, the CIS gave wrong excitation characters for these states at the large torsional angles. The character of the S_1 state is not dependent on the torsional angle; it is characterized as the excitation from HOMO to LUMO in all torsional angles and the S_1 state is located apart from other two states.

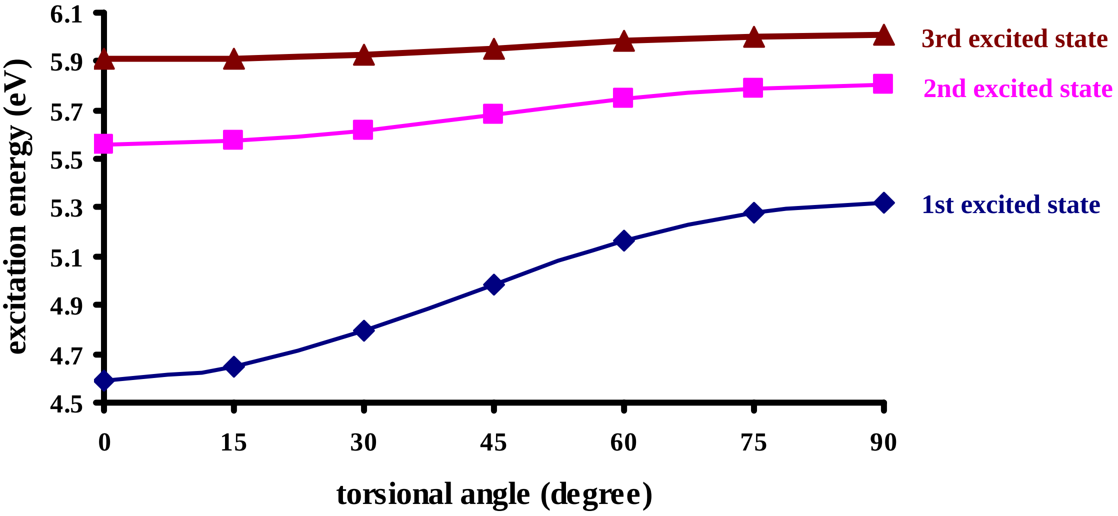

Figure 19 CIS excitation energy of the first three excited states for FT versus torsional angle.

Next, the MOs which are important for these excited states are discussed. From the SAC-CI results, these excited states are mainly described by the linear combination of the transitions from next HOMO (HOMO-1) and HOMO to LUMO and next LUMO (LUMO+1). These four orbitals of FT at torsional angle $\theta = 30°$ are displayed in Fig. 20. The HOMO and LUMO are delocalized over the molecule, while the LUMO+1 is dominantly localized in the fluorene unit. The HOMO shows inter-ring anti-bonding character between two subunits and the LUMO shows inter-ring bonding character. The HOMO-LUMO transition is destabilized as the torsional angle becomes larger, because of the bonding character of LUMO. On the other hand, energy change of HOMO-LUMO+1 transition along the torsional angle is much smaller due to the localized nature of LUMO+1. This situation provides the interchange of the excited states.

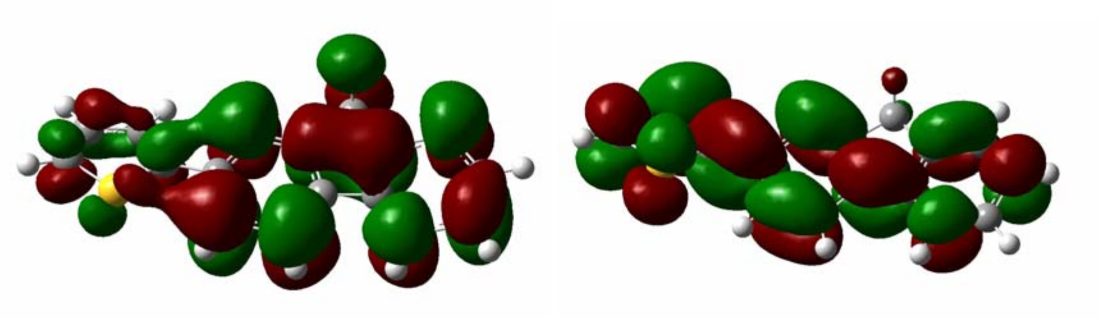

next LUMO (LUMO+1) LUMO

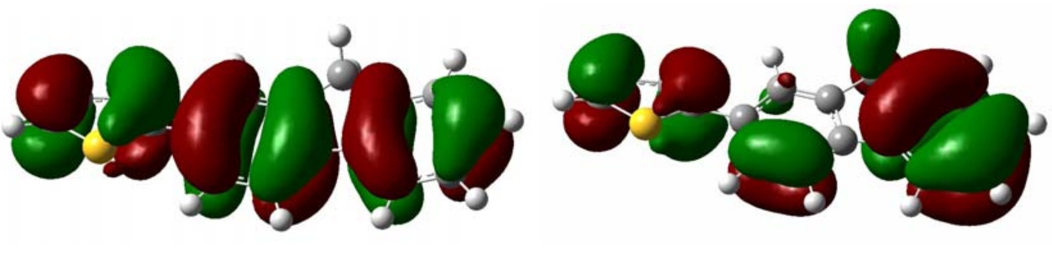

HOMO next HOMO (HOMO-1)

Figure 20 next HOMO (HOMO-1), HOMO, LUMO, and next LUMO (LUMO+1) of FT ($\theta = 30°$).

Next, we discuss the dipole moment of FT in these three excited states. It was found that for the conformers with small torsional angle like $\theta = 0°$ and 30°, the dipole moments of three excited states are not significantly different. On the other hand, dipole moments of the conformers with large torsional angle, e.g. $\theta = 60°$ are different for the S_2 and S_3 states, which is also due to the interchange of the excited states.

3.3 Absorption spectra of FT and FMT

Since the excitation spectra of FT and FMT are dependent on the torsional angle and the ground-state potential energy curves are flat along the torsional angle, thermal distribution of the conformers should be considered in order to simulate the absorption spectra. The SAC-CI absorption spectra of FT for $\theta =$ 0°-60° are compared in Fig. 21. These three excited states shift into higher energy region, as the torsional angle becomes large. The shape of the spectra also changes, for example, the oscillator strength of the S_3 state becomes large at $\theta =$ 60°.

The absorption spectra of FT and FMT were simulated with the simple model; contributions of the conformer of $\theta = 0°$-90° with the interval of $\Delta\theta = 15°$ were averaged with the statistical weights at the room temperature. From the Boltzmann weights, the conformers at $\theta =$ 0°-60°, which have large oscillator strength, predominantly contribute to the absorption spectra; for FT, the weights of the conformers at torsional angle $\theta = 0°$, 15°, 30°, 45°, 60° were evaluated to be 22%, 29%, 33%, 13%, 2%, respectively, and for FMT, they were 12%, 15%, 30%, 30%, 9%, respectively.

The calculated absorption spectra of FT and FMT, in which thermal distribution at 300 K is taken into account, are shown with the experimental spectra in Fig. 22. The spectra without the thermal average correction, namely the spectra at most stable conformers, are also displayed for comparison. The simulated spectra with thermal average showed an excellent agreement with the experimental spectra, while the spectra without thermal average did not reproduce the spectral shape. For FT, the contributions of the conformers whose torsional angle is up to 30° were dominant and the asymmetric spectra were obtained. In the case of FMT, the strong shoulder was observed in the higher energy side of the peak around 4.30 eV. This absorption can be mainly attributed to the S_2 state of the conformer of $\theta = 30°\text{-}45°$. The present results show that it is important to take thermal average for the absorption spectra of these molecules.

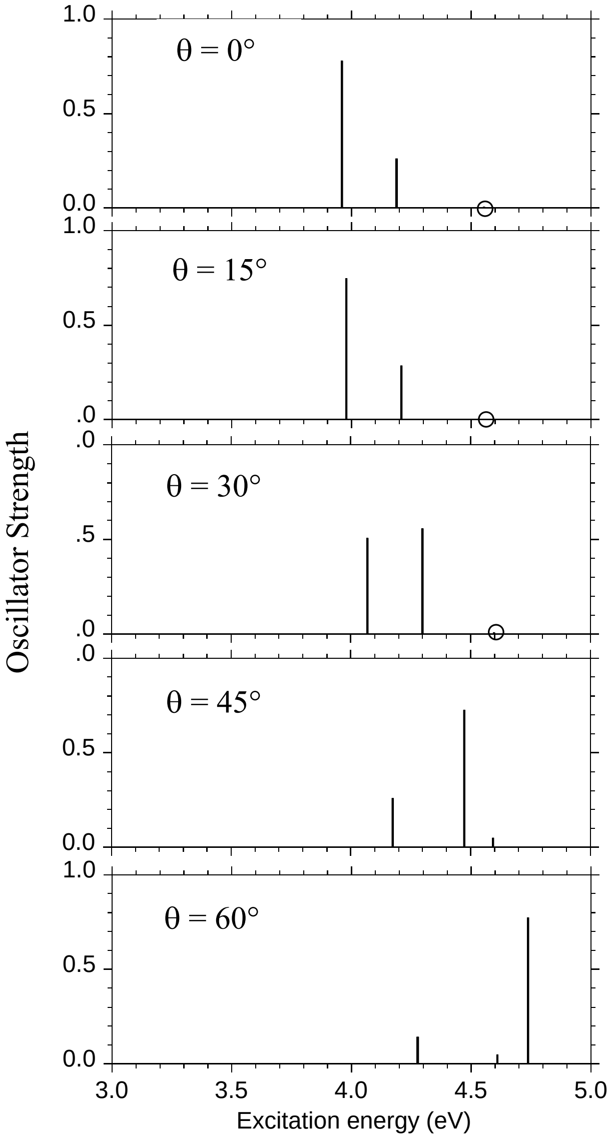

Figure 21 The SAC-CI absorption spectra of FT at torsional angle 0°, 15°, 30°, 45° and 60°.

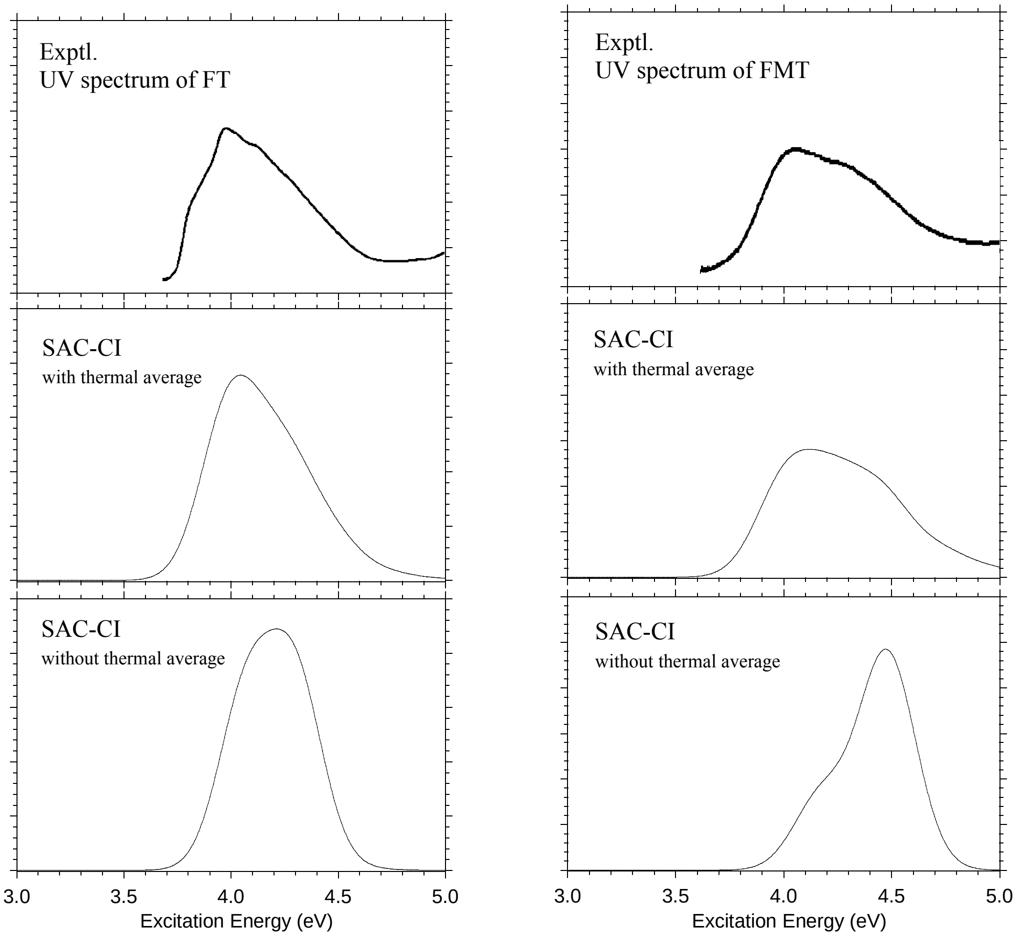

(a) **(b)**

Figure 22 Experimental (Belletete *et al.*, 2000) and SAC-CI absorption spectra of (a) FT and (b) FMT. Theoretical spectra with and without thermal average are shown.

3.4 Absorption spectra of dimer and trimer

The absorption spectra of dimer and trimer of FT were calculated at their ground-state optimized structures for discussing the excited states in copolymer. These spectra are compared with the calculated spectrum of the monomer at the ground state structure in Fig. 23. The excitation energies, oscillator strength, and the excitation character of three low-lying excited states for FT dimer and trimer are summarized in Table 10.

In the case of dimer and trimer, the S_1 state predominantly contributes to the absorption spectrum and other two transitions have small oscillator strength. It is also characterized that the energy separations between the S_1 state and higher excited states are wider than that of monomer. Since the conjugation length increases in the dimer and trimer, red shift occurs for the S_1 state. It can be concluded that the S_1 state also predominantly contributes to the absorption spectra of the polymer of this system. For the quantitative prediction of the absorption spectrum, it should be necessary to take accounts of the thermal average for simulating the observed spectra.

Figs. 24 and 25 show the MOs which are important for the low-lying excited states of dimer and trimer, respectively. In both dimer and trimer, the HOMO shows inter-ring anti-bonding character between two subunits and the LUMO shows inter-ring bonding character; these are similar to those of monomer in Fig. 20. In the case of dimer and trimer, the transitions to S_2 and S_3 have small oscillator strengths and these transitions are related to HOMO-1 and LUMO+1. These HOMO-1 and LUMO+1 have their delocalized amplitude on side units. The bonding character of these MOs between two subunits alternates; namely, anti-bonding, bonding and anti-bonding along the main chain in HOMO-1 of dimer. In the case of LUMO+1 of dimer, bonding, anti-bonding, bonding sequence was found. For trimer, HOMO-1 also shows inter-ring anti-bonding character between the subunits and the bonding character was found in LUMO+1.

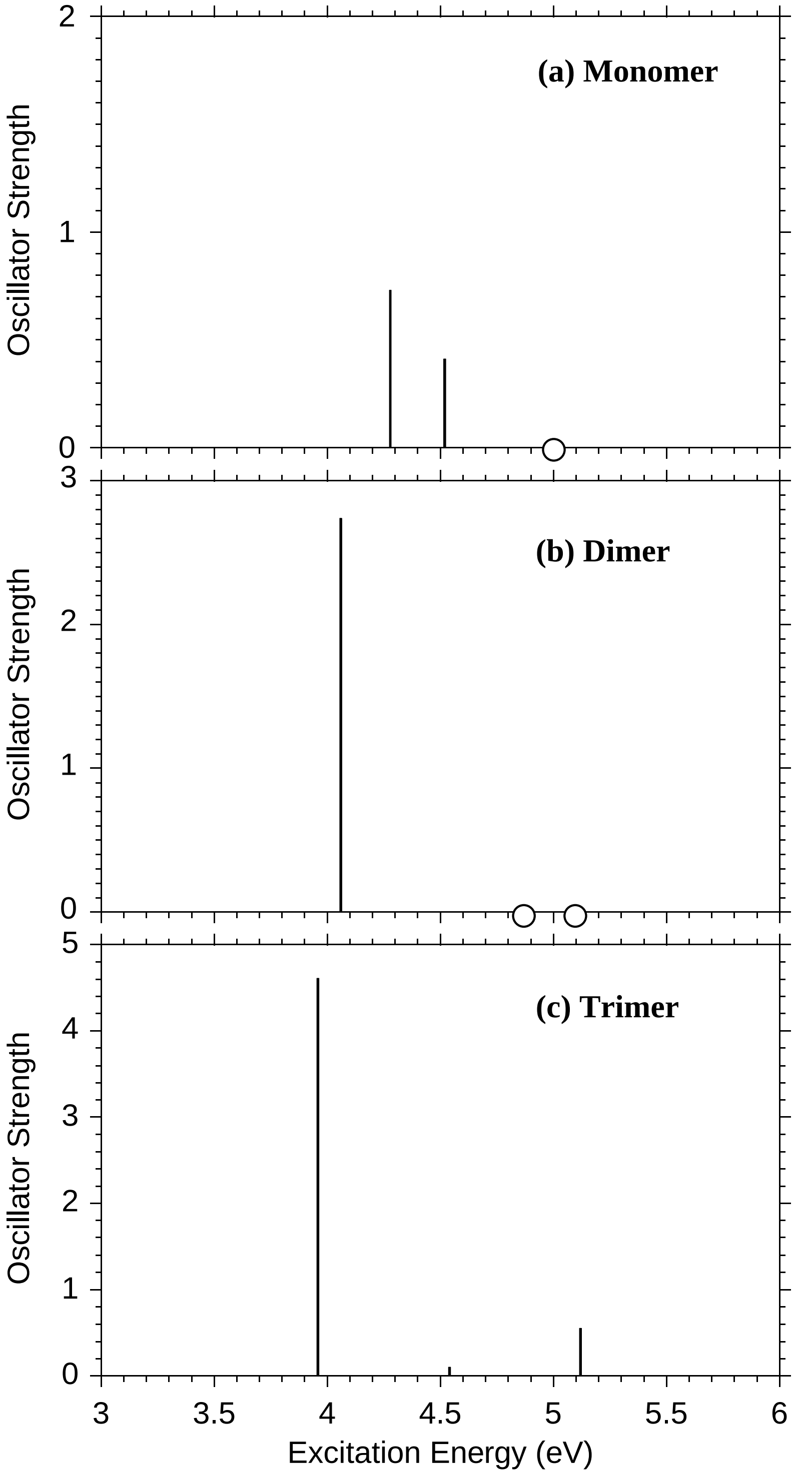

Figure 23 SAC-CI absorption spectra of FT; (a) monomer, (b) dimer, and (c) trimer.

Table 10 Excitation energy (ΔE), oscillator strength (f), and excitation character of the excited states of FT monomer, dimer, and trimer at the ground-state optimized geometry.

State	Monomer			Dimer			Trimer		
	ΔE (eV)	f	Character	ΔE (eV)	f	Character	ΔE (eV)	f	Character
S_1	4.28	0.73	HOMO → LUMO	4.07	2.74	HOMO → LUMO	3.96	4.61	HOMO → LUMO
S_2	4.52	0.41	HOMO → LUMO+1	4.88	0.00	HOMO → LUMO+1	4.54	0.10	(HOMO → LUMO+1) +(HOMO-1 → LUMO)
S_3	4.92	0.00	HOMO-1 → LUMO	5.09	0.01	HOMO-1 → LUMO	5.12	0.55	HOMO-1 → LUMO+1

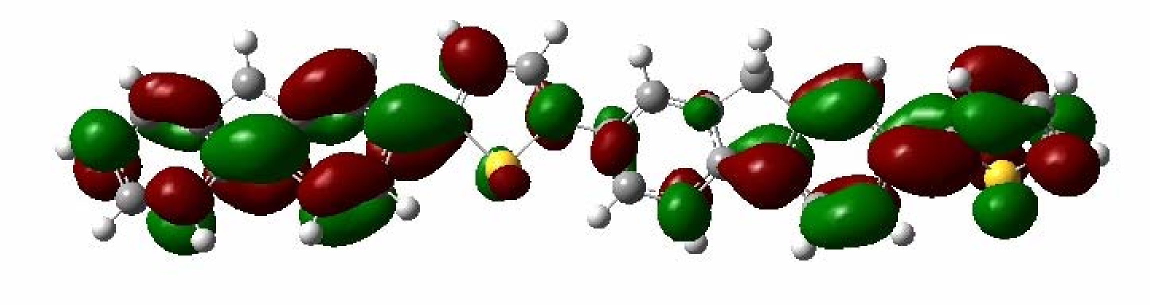

LUMO+1

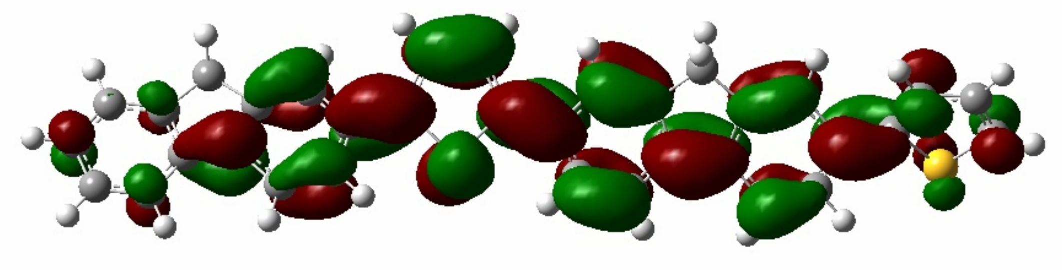

LUMO

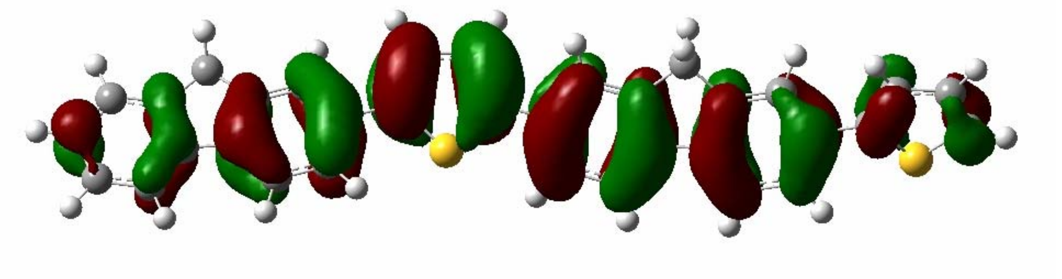

HOMO

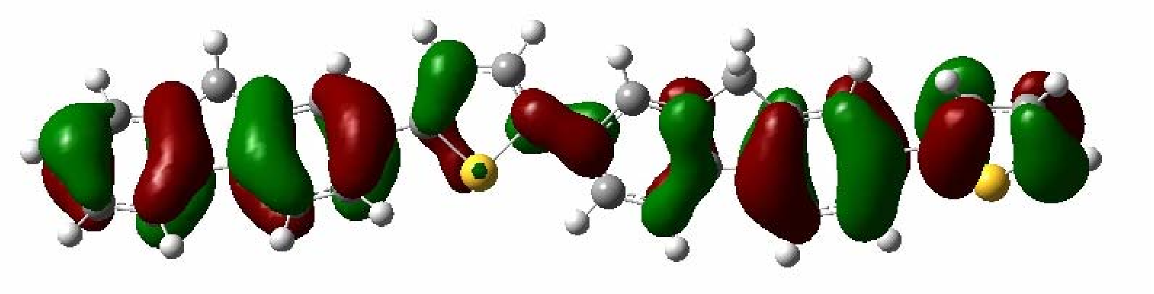

HOMO-1

Figure 24 Next HOMO (HOMO-1), HOMO, LUMO, and next LUMO (LUMO+1) of FT dimer

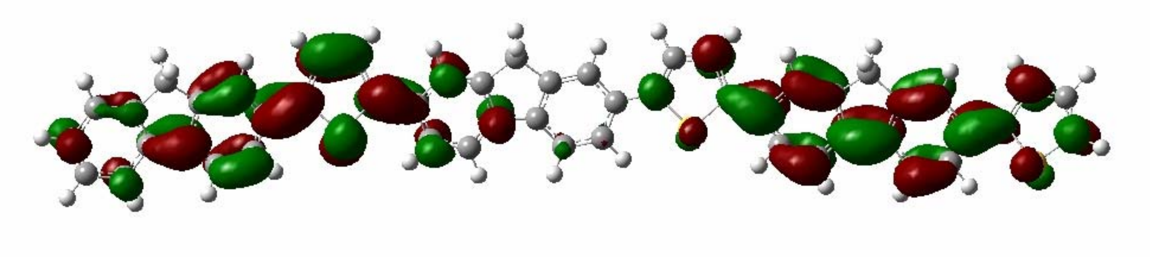

LUMO+1

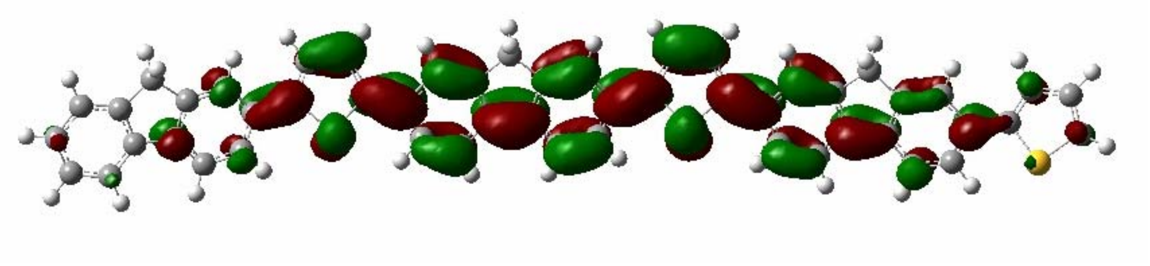

LUMO

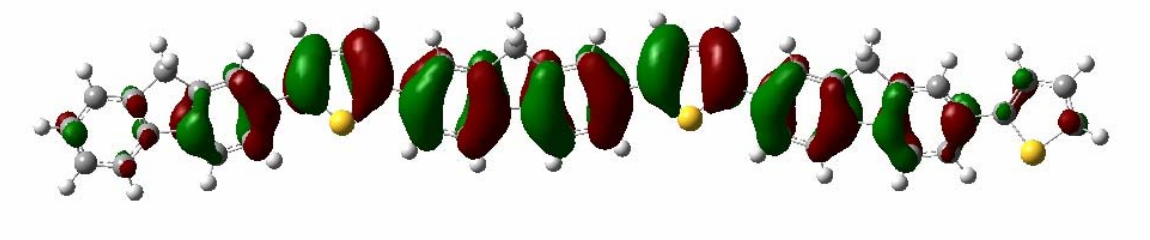

HOMO

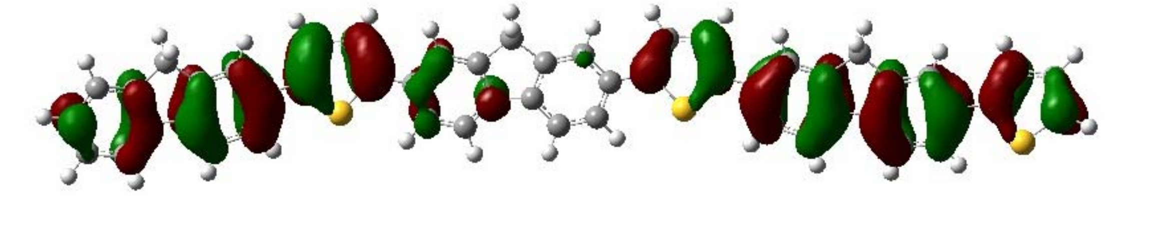

HOMO-1

Figure 25 Next HOMO (HOMO-1), HOMO, LUMO, and next LUMO (LUMO+1) of FT trimer

3.5 Emission spectra of FT and FMT

Next, the excited-state geometries and emission spectra from the S_1 excited state, which are relevant to the light emitting function, are discussed for FT and FMT. As seen in Fig. 18, the conformation of small torsional angle is stable in S_1 state. The equilibrium geometries of S_1 state of these molecules were obtained by CIS/6-31G* and the emission energies were calculated by the SAC-CI calculations at the CIS optimized structures. In Table 8, the optimized structure parameters of the S_1 state are summarized for FT and FMT.

The structures of the S_1 state of FT and FMT were calculated to be almost planar. This is because the S_1 state is HOMO-LUMO transition and the LUMO has the π-bonding character between the fluorene and thiophene units. This geometrical change was found in the previous CIS work (Tirapattur *et al.*, 2003). In the ground state, the torsional angle of the most stable conformation of FMT is larger than that of FT; methyl group causes a twisting of FMT. On the other hand, in the S_1 state, the electronic conjugation effect overcomes the steric effect and the S_1 state structures of FT and FMT are nearly planar. It was also confirmed that the bond lengths along the axis of the molecule, C_1-C_2, C_4-C_5, C_3-C_7, C_{10}-C_{11}, C_{13}-C_8, C_{12}-C_{14} and C_{15}-C_{16} significantly shrink compared with the corresponding bond lengths in the ground state. This indicates that the conjugation over fluorene and thiophene units is enhanced in the S_1 state. In addition, this feature is supported by the fact that the geometries of these two compounds are planar in the S_1 state. This trend was also reported in the previous work (Belletete *et al.*, 2000).

The emission energies of FT and FMT are compared with the experimental values in Table 11. Stokes shift is large for these molecules; the fluorescence energy of FT was calculated to be 3.73 eV in comparison with the absorption energy 4.0-4.2 eV, where absorption energy is estimated with thermal average. Since the stable structures in the S_1 state are nearly planar for both FT and FMT, the emission energies of these molecules are almost the same, 3.73 and 3.69 eV, for FT and FMT, respectively, which is in agreement with the experimental trend, 3.52 and 3.48 eV.

Since the energy barrier along the torsional angle in S_1 state is larger than that of the ground state as shown in Figs. 17 and 18, the effect of the torsional angle must be small in the emission spectra. It was also indicated by the fact that the full width at half-maximum (fwhm) of the fluorescence bands of the FT and FMT are much smaller than those of absorption bands (Belletete *et al.*, 2000).

Table 11 Emission energy (eV) of FT and FMT monomers

Molecule	SAC-CI	Exptl.[a]
FT	3.73	3.52
FMT	3.69	3.48

[a] Belletete *et al.*, 2000

3.6 Effect of electric field

Finally, the effect of applying the electric field on the excitation energy and oscillator strength was examined, since the dipole moments were different between the ground and excited states. In Table 12, the results for applying the electric field $E_x = 0.01$ au in x direction are given for the conformers of $\theta = 0°$ and 60°.

By applying electric field, all the three excited states are stabilized and the excitation energies become smaller; in particular, the HOMO-LUMO transition is stabilized. Since the S_1 state of the conformer $\theta = 0°$ is described as HOMO-LUMO transition, the spectrum shape does not change and performs monotonic red shift. On the other hand, as shown in Table 9, the S_1 state of the conformer $\theta = 60°$ is characterized as HOMO-LUMO+1 transition without electric field, while this state has the character of HOMO-LUMO transition under the electric field. Therefore, the oscillator strength of the S_1 state of the conformer $\theta = 60°$ becomes large compared to that without electric field. In a way, the excitation energy and oscillator strength can be controlled by the electric field in the twisted conformers.

Table 12 Excited states of FT in the electric field $E_x = 0.01$ au.

Torsional angle	State	ΔE (eV)	*f*	Excitation character
0°				
	S_1	3.59	0.89	0.91(HOMO → LUMO)
	S_2	4.14	0.12	0.82(HOMO → LUMO+1)
	S_3	4.74	0.01	0.58(HOMO → LUMO+3)
60°				
	S_1	3.89	0.50	0.89(HOMO → LUMO)
	S_2	4.48	0.02	0.81(HOMO → LUMO+2)
	S_3	4.89	0.29	0.89(HOMO → LUMO+1)

CONCLUSIONS

TDDFT with B3LYP functional using optimized geometry obtained from B3LYP/6-31G* level was found to be a suitable method to estimate both energy gap of poly[2,7-(9,9-dihexylfluorene)-co-alt-2,5-(decylthiophene)], and the reliable structural parameters. On the contrary, extrapolation of HOMO-LUMO energy differences, calculated by DFT(B3LYP/6-31G*) method, based on AM1 and HF-optimized geometries and also full geometrical optimization at B3LYP/6-31G* level, were not reasonable as compared with the experimental data. In addition, the energy gap calculated from the TDDFT(B3LYP/6-31G*) method, based on AM1-optimized geometry provided a good estimated energy gap; however, the structural parameters are not reliable due to the nature of the AM1 parametrization. Poly[2,7-(9,9-dihexylfluorene)-co-*alt*-2,5-(decylthiophene)] and poly[2,7-(9,9-dihexylfluorene)-co-*alt*-2,5-(3,4-didecylthiophene)] are the alkylsubsitution on the thiophene ring of the polymer. It was also found that TDDFT/B3LYP/6-31G*//B3LYP/6-31G* was the appropriate method to estimate the energy gap of poly[2,7-(9,9-dihexylfluorene)-co-*alt*-2,5-(3,4-didecylthiophene)]. Consequently, there is a theoretical approach for evaluating the energy gap which is based on the ground state properties. The energy gap has been estimated from the energy difference between HOMO and LUMO. In case of poly[2,7-(9,9-dihexylfluorene)-co-*alt*-2,5-(*S,S*-dioxidethiophene)] and poly[2,7-(9,9-dihexylfluorene)-co-*alt*-2,5-(3,4-ethylenedioxythiophene)], the HOMO-LUMO energy difference obtained from full geometrical optimization at B3LYP/6-31G* level was found to be a suitable method to estimate the energy gap. Nevertheless, the deviation from the experimental data obtained from those theoretical approaches was found. Two factors are proposed; the former is the isolated gas-phase chains, used to be the model for calculations and the latter is the neglected solid-state effects.

Therefore, the calculated energy gaps of poly[2,7-(9,9-dihexylfluorene)-co-*alt*-2,5-(decylthiophene)], poly[2,7-(9,9-dihexylfluorene)-co-*alt*-2,5-(*S,S*-dioxidethiophene)] and poly[2,7-(9,9-dihexylfluorene)-co-*alt*-2,5-(3,4-ethylenedioxythiophene)] are 2.47, 2.24 and 2.56 eV, respectively. According to this study, it can be concluded that inter-ring torsional angles between fluorene and thiophene units play a very important role for leading to get a narrow energy gap as compared to that of polyfluorene. The inter-ring torsional angles of poly[2,7-(9,9-dihexylfluorene)-co-*alt*-2,5-(decylthiophene)], Poly[2,7-(9,9-dihexylfluorene)-co-*alt*-2,5-(*S,S*-dioxidethiophene)] and Poly[2,7-(9,9-dihexylfluorene)-co-*alt*-2,5-(3,4-ethylenedioxythiophene)] were lower than those of polyfluorene (PF). Hence, the energy gaps of those polymers are significantly lower as compared to PF. In other words, the second alkyl group attached on the thiophene ring of poly[2,7-(9,9-dihexylfluorene)-co-*alt*-2,5-(3,4-decylthiophene)] enhanced the steric hindrance. Therefore, it increases the torsional angle between the fluorene and the thiophene units so as to reduce the effective conjugated length along the polymer main chain. Thus, the large energy gap (3.07 eV) was found. It can be concluded that the modulation of energy gap of polyfluorene can be tuned by insertion of the thiophene derivatives, in particular monoalkyl thiophene, *S,S*-dioxidethiophene and 2,5-ethylenedioxythiophene.

FT and FMT, which are important fragments of the light-emitting devices, have been investigated for the excited state properties and the optical properties. The results pointed out that FT and FMT monomers were stable at the non-planar structures in their ground states, while the rotational energy barriers to their co-planar and perpendicular conformations were calculated to be below 3.00 kcal/mol. The lower rotational energy barrier indicates that FT and FMT allow a wide range of non-planar structures at room temperature.

The excitation energies of the S_1 and S_2 states increase when the planarity between fluorene and thiophene unit reduces. According to the oscillator strength, the component of HOMO-LUMO transition predominantly contributes to the first absorption band of FT and FMT. It was found that the change of the HOMO-LUMO transition energy along the torsional angle causes the interchange of the excitation character between S_1 and S_3 states. This was because the HOMO has an inter-ring anti-bonding character between the two subunits, while the LUMO has inter-ring bonding character. The absorption spectra of FT and FMT in which thermal distributions are taken into account are in good agreement with the experimental spectra.

The structures in the S_1 state were calculated to be nearly planar for both FT and FMT. The calculated emission energies of these molecules are almost the same and in good agreement with the experiment.

For dimer and trimer, only the S_1 state contributes to the absorption spectra and the other two states have small oscillator strength. This tendency must be valid for the polymer of these compounds.

To investigate the energy gap of fluorene-thiophene analogue, the further works can be extended by studying Quantitative Structure-Property Relationship (QSPR). In addition, the inter-chain interaction between the polymer chains of fluorene-thiophene copolymer, which is the important factor for the emission process, should be explored.

LITERATURE CITED

Alguno, A. C., W. C. Chung, R. V. Bantaculo, R. M. Vequizo, H. Miyata, W. E. Ignacio and A. M. Bacala. 2000. *Ab initio* and density functional studies of polythiophene energy band gap. **NECTEC Tech J.** 2: 215-218..

Andersson, M. R., O. Thomas, W. Mammo, M. Sevensson, M. Theander and O. Inganas. 1999. Substituted polythiophenes designed optoelectronic devices and conductors. **J. Mater. Chem.** 9: 1933-1940.

Aubert, P. H., M. Knipper, L. Groenendaal, L. Lutsen, J. Manca and D. Vanderzande. 2004. Copolymers of 3,4-ethylenedioxythiophene and of pyridine alternated with fluorene or phenylene units; Synthesis, optical properties and devices. **Macromolecules.** 37: 4087-4098.

Barbarella, G., L. Favaretto, G. Sotgiu, M. Zambianchi, L. Antolini, O. Pudova and A. Bongini. 1998. Oligothiophene *S,S*-dioxides. Synthesis and electronic properties in relation to the parent oligothiophenes. **J. Org. Chem.** 63: 5497-5506.

______, _____, ______. 2001. Rigid-core oligothiophene-*S,S*-dioxides with high photoluminescence efficiencies both in solution and in the solid state. **Chem. Mater.** 13: 4112-4122.

Bauernschmitt, R. and R. Ahlrich. 1996. Treatment of electronic excitations within the adiabatic approximation of time dependent density functional theory. **Chem. Phys. Lett.** 256: 454-464.

Belletete, M., S. Beaupre, J. Bouchard, P. Blondin, M. Leclerc and G. Durocher. 2000. Theoretical and experimental investigations of the spectroscopic and photophysical properties of fluorene-phenylene and fluorene-thiophene derivatives: Precursors of light-emitting polymers. **J. Phys. Chem. B.** 104: 9118-9125.

______, J. F. Morin, S. Beaupre, M. Ranger, M. Leclerc and G. Durocher. 2001. Spectroscopic and photophysical properties of thiophene-fluorene oligomers as well as their corresponding polyesters. **Macromolecules.** 34: 2288-2297.

______, M. M. Bedard, M. Leclerc and G. Durocher. 2004. Ground and excited states properties of carbazole-based dyads: correlation with their respective absorption and fluorescence spectra. **J. Mol. Struct. (THEOCHEM).** 679: 9-15.

Blondin, P., J. Bouchard, S. Beaupre, M. Belletete, G. Durocher and M. Leclerc. 2000. Molecular design and characterization of chromic polyfluorene derivatives. **Macromolecules.** 33: 8945-8952.

Bouillud, A. D., I. Levesque, Y. Tao and M. D’Iorio. 2000. Light-emitting diodes from fluorene-based π-conjugated polymers. **Chem. Mater.** 12: 1931-1936.

Braun, D. and A. J. Heeger. 1991. Visible light emission from semiconducting diodes. **Appl. Phys. Lett.** 58: 1982-1984.

Briere, J. –F. and M. Cote. 2004. Electronic, structural, and optical properties of conjugated polymers based on carbazole, fluorene, and borafluorene. **J. Phys. Chem. B.** 108: 3123-3129.

Burns, D. M. and J. Iball. 1955. **Proc. Roy. Soc. (London).** A227: 200-214.

Charas, A., N. Barbagallo, J. Morgado and L. Alcacer. 2001. Synthesis and optical properties of poly(fluorene)-based alternating copolymers. **Synth. Met.** 122: 23-25.

_______, J. Morgado, J. M. G Martinho, L. Alcacer and F. Cacialli. 2002. Tuning the optoelectronic properties of polyfluorenes by copolymerization with thiophene moieties. **Synth. Met.** 127: 251-254.

_______, _______, _______, _______, S. F. Lim, R. H. Friend and F. Cacialli. 2003. Synthesis and luminescence properties of three novel polyfluorene copolymers. **Polymer.** 44: 1843-1850.

Chiang, C. K., C. R. Fincher, Jr. Y. W. Park, A. J. Heeger, H. Shirakawa, E. J. Louis, S. C. Gau and A. G. MacDiarmid. 1977. Electrical conductivity in doped polyactylene. **J. Phys. Rev. Lett.** 39: 1098-1101.

Chen, B., Y. Wu, M. Wang, S. Wang, S. Sheng, W. Zhu, R. Sun and H. Tian. 2004. Novel fluorene-*alt*-thienylenevinylene-based copolymers: tuning luminescent wavelength via thiophene substitution position. **Eur. Polym. J.** 40: 1183-1191.

Cornil, J., I. Gueli, A. Dkhissi, J. C. Sancho-Garcia, E. Hennebicq, P. Calbert, V. Lemaur, D. Beljonne and L. J. Bredas. 2003. Electronic and optical properties of polyfluorene and fluorene-based copolymers: A quantum-chemical characterization. **J. Chem. Phys**. 118: 615-6623.

DiCesare, N., M. Belletete, M. Leclerc and G. Durocher. 1999. HF/3-21G* *ab initio* calculations on methoxy-substituted bithiophenes. **J. Mol. Struct**. **(THEOCHEM).** 467: 259-273.

Duan, X., D. S. Dudis and A. T. Yeates. 2001. Electronic structure and energy band gap studies for poly(1,3-thienyl-squaraine) and its dianion. **Synth. Met.** 116: 285-288.

Feng, D., S. Wang, Q. Zhuang, P. Guo, P. Wu and Z. Han. 2004. Joint theoretical and experiment study of the UV absorption spectra of polybenzoxazole. **J. Mol. Struct.** 707: 169-171.

Frisch, M. J., G. W. Trucks, H. B. Schlegel, G. E. Scuseria, *et al*. 2004. **Gaussian03, Inc.** Wallingford CT.

Gong, X., D. Moses, A. J. Heeger and S. Xiao. 2004. White light electrophosphorescence from polyfluorene-based light-emitting diode. Utilization of fluorenone defects. **J. Phys. Chem. B.** 108: 8601-8605.

Grozema, F. C., P. Th. van Duijnen, L. D. A. Siebbeles, A. Goossens and S. W. de Leeuw. 2004. Electronic structure of Thienylene vinylene oligomers: Sinlglet excited states, triplet excited states, cations, and dications. **J. Phys. Chem. B.** 108: 16139-16146.

Hay, J. P. 2002. Theoretical studies of the ground and excited electronic states in cyclometalated phenylpyridine Ir (III) complexes using density function theory. **J. Phys. Chem. A.** 106: 1634-1641.

Heinze, H. H., A. Gorling and N. Rosch. 2000. An efficient method for calculating molecular excitation energies by time-dependent functional-density theory. **J. Chem. Phys.** 113: 2088-2099.

Herguth, P., J. Xuezhong, M. S. Liu and A. K. –Y. Jen. 2002. Highly efficient fluorene- and benzothiadiazole-based conjugated copolymers for polymer light-emitting diodes. **Macromolecules.** 35: 6094-6100.

Hirata, S. and M. Head-Gordon. 1999. Time dependent density functional theory within the Tamm-Dancoff approximation. **Chem. Phys. Lett.** 314: 291-299.

Hong, S. Y., D. Y. Kim, C. Y. Kim and R. Hoffmann. 2001. Origin of the broken conjugation in m-phenylene linked conjugated polymers. **Macromolecules.** 34: 6474.

Horowitz, G., B. Bachet, A. Yassar, P. Lang, F. Demanze, J. –L. Fave and F. Garnier. 1995. Growth and Characterization of sexithiophene single crystals. **Chem. Mater.** 7: 1337-1341.

Hsu, C-.P., S. Hirata and M. Head-Gordon. 2001. Excitation energies from Time-Dependent Density Functional Theory for linear polyene oligomer: butadiene to decapentaene, **J. Phys. Chem. A.** 105: 451-458.

Hutchison, G. R., M. A. Ratner and T. J. Marks. 2002. Accurate prediction of band gaps in neutral heterocyclic conjugated polymers. **J. Phys. Chem. A.** 106: 10596-10605.

Janietz, S., D. D. C. Bradley, M. Grell, C. Giebeler, M. Inbasekaran and E.P. Woo. 1998. Electrochemical determination of the ionization potential and electron affinity of poly(9,9-dioctylfluorene). **Appl. Phys. Lett.** 73: 2453-2455.

Kwon, O. and M. L McKee. 2000. Theoretical calculations of band gaps in the aromatic structures of polythieno[3,4-*b*]benzene and polythieno[3,4-*b*] pyrazine. **J. Phys. Chem. A.** 104: 7106-7112.

______, ________. 2000. Calculations of band gaps in polyaniline from theoretical studies of oligomers. **J. Phys. Chem. B.** 104: 1686-1694.

Kudo. K. 2005. Organic light emitting transistors. **Curr. Appl. Phys.** 5: 337-340.

Lagowski, J. B. and D. Chakraborty. 2001. Configuration interaction study of singlet excited state of thiophene and its cyano derivative oligomers. **J. Chem. Phys**. 115: 184-194.

Levesque, I., A. D. Bouillud, Y. Tao, M. D'Iorio, S. Beaupre, P. Blondin, M. Ranger, J. Bouchard and M. Leclerc. 2001. Organic Tunable electroluminescent diodes from polyfluorene derivatives. **Synth. Met**. 122: 79-81.

Li, Y., G. Vamvounis and S. Holdcroft. 2002. Tuning optical properties and enhancing solid-state emission of poly(thiophen)s by molecular control: A postfunctionalization approach. **Macromolecules**. 35: 6900-6906.

Lim, E., J. B. Jung and K. H. Shim. 2003. Synthesis and characterization of new light-emitting fluorene-thieno[3,2-*b*] thiophene-based conjugated copolymer. **Macromolecules.** 36: 4288-4293.

Liu, B., W. L. Yu, H. Y. Lai and W. Huang. 2000. Synthesis, characterization, and structure-property relationship of novel-fluorene-thiophene based conjugated copolymers. **Macromolecules.** 33: 8945-8952.

_______, Y. H. Niu, W. L. Yu, Y. Cao and W. Huang. 2002. Application of alternating fluorene and thiophene copolymers in light-emitting diodes. **Synth. Met.** 129: 129-134.

Lukes, V., D. Vegh, P. Hrdlovic, M. Stefko, K. Matuszna and V. Laurinc. 2005. Synthesis, theoretical characterization and spectra of thiophene-fluorene π-conjugated derivatives. **Synth. Met**. 148: 179-186.

Ma, J., S. Li and Y. Jiang. 2002. A Time-Dependent DFT study on band gaps and effective conjugation lengths of polyacetylene, polyphenylene, polypentafulvene, polycyclopentadiene, polypyrrole, polyfuran, polysilole, polyphosphole, and polythiophene. **Macromolecules.** 35: 1109-1115.

Meng, H., J. Zheng, A. J. Lovinger, B. -C. Wang, P. G. V. Patten and Z. Bao. 2003. Oligofluorene-thiophene derivatives as high-performance semiconductors for organic thin film transistors. **Chem Mater.** 15: 1778-1787.

Moiorano, V., E. Perrone, S. Carallo, A. Biasco, P. P. Pompa, R. Cingolani, A. Croce, R. I. R. Blyth and J. Thompon. 2005. White, phosphorescent, wet-processed, organic light emitting diode on a window-glass substrate. **Synth. Met.** 151: 147-151.

Nakatsuji, H. 1978. Cluster expansion of the wavefunction, excited states. **Chem. Phys. Lett.** 29: 362-364.

_______, 1979. Cluster expansion of the wavefunction, electron correlations in ground and excited states by SAC (symmetry-adapted-cluster) and SAC-CI theories. **Chem. Phys. Lett.** 67: 329-333.

_______, 1983. Cluster expansion of the wave function. Valence and Rydberg excitations, ionizations, and inner-valence ionizations of CO_2 and N_2O studied by the SAC and SAC-CI theories. **Chem. Phys.** 75: 425-441.

Oliveira, M. A. D, H. A. Duarte, J-. M. Pernaut and W. B. D. Almeida. 2000. Energy gaps of α,α'-substituted oligothiophenes from semiempirical, *ab initio*, and density functional methods. **J. Phys. Chem. A.** 104: 8256-8262.

Ortega, A. V. and I. N. D. Silva. 2005. Application to intelligent systems for specification of automotive equipments using LED. **Appl. Soft. Comput.** 6: 18-25.

Parusel, A. B. J., W. Rettig and W. Sudholt. 2002. A comparative theoretical study on DMABN: Significance of excited state optimized geometries and direct comparison of methodologies. **J. Phys. Chem.** 106: 804-815.

Pei, J., W. L. Yu, W. Huang and A. J. Heeger. 2000. A novel series of efficient thiophene-based light-emitting conjugated polymers and application in polymer light-emitting diodes. **Macromolecules.** 33: 8945-8952.

_______, ________, J. Ni, H. Y. Lai, W. Haung and A. J.,Heeger. 2001. Thiophene-based conjugated polymers for light-emitting diodes: effect of aryl groups on photoluminescence efficiency and redox behavior. **Macromolecules.** 34: 7241-7248.

Poolmee, P., M. Ehara, S. Hannonbua and H. Nakatsuji. 2005. SAC-CI theoretical investigation on electronic structure of fluorene-thiophene oligomers. **Polymer.** 46: 6474-6481.

Ranger, M. and M. Leclerc. 1998. Optical and electrical properties of fluorene-based π-conjugated polymers. **Can. J. Chem.** 76: 1571-1577.

Salzner, U., P. G. Pickup and R. A. Poirier. 1998. Accurate method for obtaining band gaps in conducting polymers using a DFT/hybrid approach. **J. Phys. Chem. A.** 102: 2572-2578.

Suramitr, S., T. Kerdcharern, T. Srikhirin and S. Hannongbua. 2005. Electronic properties of alkoxy derivatives of poly(para-phenylenevinylene), investigated by time dependent density functional theory calculations, computational and theoretical polymer science. **Synth Met.** in press.

Theander, M., O. Inganas, W. Mammo, S. Olinga and R. M. Andersson. 1999. Photophysics of substituted polythiophenes. **J. Phys. Chem**. **B.** 103: 7771-7780.

Tirapattur, S., M. Belletete, N. Drolet, M. Leclerc and G. Durocher. 2002. Spectral and photophysical properties of fluorene-based polyesters in solution and in the solid state. **Macromolecules**. 35: 8889-8895.

_______, __________, M. Leclerc and G. Durocher. 2003. Study of excited stated properties of oligofluorenes by the singles configuration interaction (CIS) theoretical approach. **J. Mol. Struct. (THEOCHEM).** 625: 141-148.

Tsou, C-C., H-T. Lu and M. Yokoyama. 2005. Red, green, blue and white organic electroluminescence devices. **J. Cryst. Growth.** 280: 201-203.

Vardeny, Z. V., A. J. Heeger and A. Dodabalapur. 2005. Fundamental research needs in organic electronic materials. **Synth. Met.** 148: 1-3.

Wan, J., M. Hada, M. Ehara and H. Nakatsuji. 2001. Electronic excitation spectrum of thiophene studied by symmetry-adapted cluster configuration interaction method. **J. Chem. Phys.** 114: 842-850.

_______ and H. Nakatsuji. 2004. Theoretical study of the singlet and triplet vertical electronic transitions of styrene by the symmetry adapted cluster-configuration interaction method. **Chem. Phys.** 302: 125-134.

Wei, H., W. Li, M. Li, W. Su, Q. Xin, J. Niu, Z. Zhang and Z. Hu. 2005. White organic electroluminescent device with photovoltaic performances. **Appl. Surf. Sci.** in press.

Wu, W., M. Inbasekaran, M. Hudack, D. Welsh, W. Yu, Y. Cheng, C. Wang, S. Kram, M. Tacey, M. Bernius, R. Fletcher, K. Kiszka, S. Munger and J. O'Brien. 2004. Recent development of polyfluorene-based RGB materials for light emitting diodes. **Microelectronic J.** 35: 343-348.

Yang, L., Y. Liao, J. -K. Feng and A. -M. Ren. 2005a. Theoretical studies of the modulation of polymer electronic and optical properties through the introduction of the electron-donating 3,4-ethylenedioxythiophene or electron-accepting pyridine and 1,3,4-oxadiazole moieties. **J. Phys. Chem. A.** 109: 7764-7774.

_______, A. -M. Ren, _______ and J. -F. Wang. 2005b. Theoretical investigation of optical and electronic property modulations of π-conjugated polymers based on the electron-rich 3,6-dimethoxy-fluorene unit. **J. Org. Chem.** 70: 3009-3020.

Yang, S., P. Olishevski and M. Kertesz. 2004. Bandgap calculations for conjugated polymer. **Synth. Met.** 141: 171-177.

Yohannes, T., F. Zhang, M. Svensson, M. R. Andersson and O. Inganas. 2004. Polyfluorene copolymer based bulk heterojunction solar cells. **Thin Solid Films.** 449: 152-157.

You, N-. H., J.Y. Lee, H. C. Ko, J. H. Kim and H. Lee. 2005. Light emitting diodes based on alternating copolymers containing fluorene and oligo(p-pheylenevinylene). **Synth. Met.** 151: 218-224.

Yu, J. -S. K., W. -C. Chen and C. -H. Yu. 2003. Time-Dependent Density Functional study of electroluminescent polymers. **J. Phys. Chem. A.** 107: 4268-4275.

Zerner, M. C., G. H. Loew, R. F. Kirchner and U. T. Mueller-Westerhoff. 1979. An Intermediate neglect of differential overlap technique for spectroscopy of transition-metal complexes. Ferrocene. **J. Am. Chem. Soc.** 102: 589-599.

Zhang, X. and S. A. Jenekhe. 2000. Electroluminescence of multicomponent conjugated polymer. 1. Roles of polymer/polymer interfaces in emission enhancement and voltage-tunable multicolor emission in semiconducting polymer/polymer heterojuctions. **Macromolcules.** 33: 2069-2082.

APPENDIX

APPENDIX A

Theoretical Background

The Theory of Quantum Chemical Calculations: Ground State Methods

Molecular orbital theory is concerned with predicting the properties of atomic and molecular systems. It is based upon the fundamental laws of quantum mechanics and uses a variety of mathematical transformation and approximation techniques to solve the fundamental equations, in contrast to semi-empirical models.

1. The Schrödinger Equation

The quantum chemical methods are based on finding solutions to the Schrödinger equation on molecular orbital theory. Quantum mechanics explains how entities like electrons have both particle-like and wave-like characteristics. The time independent Schrödinger equation for a molecule (n-electron and N-nuclei system):

$$H\psi(\vec{r},\vec{R}) = E\psi(\vec{r},\vec{R}) \qquad (1)$$

and the Hamiltonian is (in atomic units):

$$H = T + V$$

$$H = -\sum_{i=1}^{N}\frac{1}{2}\nabla_i^2 - \sum_{A=1}^{M}\frac{1}{2M_A}\nabla_A^2 - \sum_{i=1}^{N}\sum_{A=1}^{M}\frac{Z_A}{r_{iA}} + \sum_{i=1}^{N}\sum_{j>i}^{N}\frac{1}{r_{ij}} + \sum_{A=1}^{M}\sum_{B>A}^{M}\frac{Z_A Z_B}{R_{AB}} \qquad (2)$$

where T and V are the kinetic and potential energy operators, respectively, which separate out the motion of the nuclei from the motion of the electrons, equation (2) can be rewritten as

$$H = -\sum_{A=1}^{M} \frac{1}{2M_A} \nabla_A^2 + H_{el} \tag{3}$$

This focus on the electronic Hamiltonian, H_{el}, and try to solve the electronic Schrödinger equation in the field of the fixed nuclei. The nuclear-nuclear repulsion term (the final in equation (2)) appears as a constant in H_{el}. Further assume the wave function $\psi(\vec{r}, \vec{R})$ to be a product of an electronic and a nuclear part:

$$\psi(\vec{r}, \vec{R}) = \psi_{elec}(\vec{r}, \vec{R})\psi_{nucl}(\vec{R}) \tag{4}$$

The justification for this is that the electrons are much lighter than the nuclei. This is called the Born-Oppenheimer approximation. The parametric $\vec{R}$ dependence of ψ_{elec} arises since the electron distribution depends implicitly on the particular nuclear arrangement for the system under study. The nuclear wave function, ψ_{nucl}, describes the vibrational, rotational and translational motion of the nuclei. From (1), (3) and (4) can obtain;

$$H\psi(\vec{r}, \vec{R}) = H\psi_{elec}(\vec{r}, \vec{R})\psi_{nucl}(\vec{R}) = \left(-\sum_{A=1}^{M} \frac{1}{2M_A} \nabla_A^2 + H_{el} \right)\psi_{elec}(\vec{r}, \vec{R})\psi_{nucl}(\vec{R})$$

$$= \left(-\sum_{A=1}^{M} \frac{1}{2M_A} \nabla_A^2 + E_{el} \right)\psi_{elec}(\vec{r}, \vec{R})\psi_{nucl}(\vec{R}) = E\psi_{elec}(\vec{r}, \vec{R})\psi_{nucl}(\vec{R}) = E\psi \tag{5}$$

The electronic wavefunction $\psi_{elec}(\vec{r}, \vec{R})$ can be divided out from both sides of equation (5), provided that terms in $\nabla^2\psi_{elec}(\vec{r}, \vec{R})$ are small, i.e. the electronic wavefunction changes slowly upon small displacements of the nuclear positions. Thus, if we neglect the influence of the nuclear derivative on the electron wave function (ψ_{el}) (i.e. the nuclei move slowly compared with the electrons) which can separate equation (5) into two equations, an electronic part:

$$H_{el}\psi_{el}\left(\vec{r},\vec{R}\right)=E_{el}\left(\vec{R}\right)\psi_{el}\left(\vec{r},\vec{R}\right) \tag{6}$$

where

$$H_{el}=-\sum_{i=1}^{N}\frac{1}{2}\nabla_i^2-\sum_{i=1}^{N}\sum_{A=1}^{M}\frac{Z_A}{r_{iA}}+\sum_{i=1}^{N}\sum_{j>i}^{N}\frac{1}{r_{ij}}+\sum_{A=1}^{M}\sum_{B>A}^{M}\frac{Z_AZ_B}{R_{AB}} \tag{7}$$

and a nuclear part:

$$H_{nucl}\psi_{nucl}\left(\vec{R}\right)=E\psi_{nucl}\left(\vec{R}\right) \tag{8}$$

where

$$H_{nucl}=-\sum_{A=1}^{M}\frac{1}{2M_A}\nabla_A^2+E_{el}\left(\vec{R}\right) \tag{9}$$

2. Hartree Fock Theory

An exact solution to the Schrödinger equation is not possible for any but the most trivial molecular systems. However, a number of simplifying assumptions and procedures do make an approximate solution possible for a large range of molecules. To simplify the treatment further, the next step is to assume that the electrons are non-interacting. This implies that (apart from the constant nuclear-nuclear repulsion term) which can rewrite the total n-electron Hamiltonian as a sum of n one-electron Hamiltonians,

$$H_{el}=\sum_{i=1}^{N}h(i) \tag{10}$$

$$h(i)=\left(-\frac{1}{2}\nabla_i^2-\sum_{A=1}^{M}\frac{Z_A}{r_{iA}}\right) \tag{11}$$

This is clearly an oversimplification, since have neglected the electron-electron repulsion term $\frac{1}{r_{ij}}$. Equation (10) defines the independent particle model. The one-electron Hamiltonians (equation (11)) are termed core-Hamiltonians, since the only interactions included are those between the electrons and the bare nuclei. Including an average interaction term in the $\{h(i)\}$, these become effective one-electron Hamiltonians. As a consequence of equation (10), the total wave function can be rewritten as a product of n single-particle wave functions,

$$\psi(\vec{r}) = \phi_1(\vec{r}_1)\phi_2(\vec{r}_2)\ldots\phi_n(\vec{r}_n) \qquad (12)$$

or, take the electron spin into account,

$$\psi = \chi_1(\vec{x}_1)\chi_2(\vec{x}_2)\ldots\chi_n(\vec{x}_n) \qquad (13)$$

The spin orbitals $\{\chi_i(\vec{x}_i)\}$ are the products of the spatial orbitals $\phi_i(\vec{r}_i)$ and the spin functions ($\alpha(\omega)$ and $\beta(\omega)$); $\vec{x}_i$ denotes both the space and spin coordinates of electron i. The total independent particle spin-orbital wave function (equation (13)) is called a Hartree-product. This is an eigenfunction of the n-electron model Hamiltonian defined in equation (10), and the corresponding eigenvalue is a sum of the single-particle spin-orbital energies,

$$E_{el} = \sum_{i=1}^{M} \varepsilon_i \qquad (14)$$

A further requirement on the state wave function (13) is that it must be anti-symmetric with respect to the interchange of coordinate r (both space and spin) of any two electrons,

$$\left|\psi\left(\vec{x}_1, \vec{x}_{2,\dots,} \vec{x}_n\right)\right|^2 = \left|\psi\left(\vec{x}_2, \vec{x}_1, \dots, \vec{x}_n\right)\right|^2 \tag{15}$$

$$\psi\left(\vec{x}_1, \vec{x}_2, \dots, \vec{x}_n\right) = \pm\psi\left(\vec{x}_2, \vec{x}_1, \dots, \vec{x}_n\right) \tag{16}$$

It is also possible to write equation (16) in terms of a $n \times n$ determinant, a Slater determinant, which has the same antisymmetric properties:

$$\psi = (n!)^{-1/2} \begin{vmatrix} \chi_1(\vec{x}_1) & \chi_2(\vec{x}_1) & \cdots & \chi_n(\vec{x}_1) \\ \chi_1(\vec{x}_2) & \chi_2(\vec{x}_2) & & \\ \cdots & & \cdots & \\ \chi_1(\vec{x}_n) & \chi_2(\vec{x}_n) & \cdots & \chi_n(\vec{x}_n) \end{vmatrix} \tag{17}$$

Which commonly is written like:

$$|\psi\rangle = (n!)^{-1/2} \left|\chi_1(\vec{x}_1), \chi_2(\vec{x}_2), \dots, \chi_n(\vec{x}_n)\right\rangle \tag{18}$$

It can easily be verified that the Slater determinant obeys the Pauli principle, as the determinant then becomes zero. The pre-factor $(n!)^{-1/2}$ is a normalisation constant, and the $\{\chi_i\}$ are assumed orthonormal. By antisym-metrizing the Hartree-product (13) in the form of a Slater determinant (17), that the probability of finding any two electrons at the same point in space (i.e. $\vec{x}_1 = \vec{x}_2$) is zero.

Through the wave functions, the effective potential is generated. This potential allows to refine wave functions, from which a new potential is obtained. The procedure is repeated until a stable, self-consistent solution is reached. Due to the iterative procedure, the initial guess of the wave function can of course be chosen ad hoc. However, the better the initial guess is, the easier it is to reach a stable solution to the eigenvalue problems in a relatively short computational time, is provided by the variation principle. This can be stated in the following way: Given any approximate wave function, satisfying the correct boundary conditions, the expectation value of the energy obtained by this wave function never lies below the exact energy of the ground state. Expressed in mathematical terms:

$$E_e = \frac{\langle \psi | H_e | \psi \rangle}{\langle \psi | \psi \rangle} \geq E_{exact} \tag{19}$$

A conceptually appealing model for the (trial) wave function of our molecular system is to regard it as being constructed from molecular orbitals (MO). This description in analogous to the model used for the atomic orbitals (AO). The MO's, the elements of the wave function determinant, are in turn thought of as being constructed by a Linear Combination of Atomic Orbitals (LCAO),

$$\psi_i^{MO} = \sum_{\mu} c_{\mu i} \phi_{\mu}^{AO} \tag{20}$$

The variational principle leads to following equations describing the molecular orbital expansion coefficients, c_{vi}, derived by Roothaan and by Hall:

$$\sum_{v=1}^{N} (F_{\mu v} - \varepsilon_i S_{\mu v}) c_{vi} = 0 \quad \mu = 1,2,..., N \tag{21}$$

Equation 21 can be rewritten in matrix form:

$$FC = SC\varepsilon \tag{22}$$

with

$$F_{\mu v} = H_{\mu v}^{core} + \sum_{\lambda\sigma} P_{\lambda\sigma} \left[(\mu v | \lambda\sigma) - \frac{1}{2} (\mu\lambda | v\sigma) \right] \tag{23}$$

$$F_{\mu v} = H_{\mu v}^{core} + G_{\mu v} \tag{24}$$

where $H_{\mu\nu}^{core}$, core-Hamiltonian matrix, defined as

$$H_{\mu\nu}^{core} = \int dr_1 \phi_\mu^*(1) h(1) \phi_\nu(1) \tag{25}$$

The matrix P is the density matrix or charge- and bond-order matrix,

$$P_{\mu\nu} = 2\sum_{a}^{N/2} C_{\mu a} C_{\nu a}^* \tag{26}$$

The matrix S is the overlap matrix, indicating the overlap between orbitals.

$$S_{\mu\nu} = \int dr_1 \phi_\mu^*(1) \phi_\nu(1) \tag{27}$$

The term $(\mu\nu|\lambda\sigma)$ in Equation 23 signified the two-electron repulsion integrals, defined as

$$(\mu\nu|\lambda\sigma) = \int dr_1 dr_2 \phi_\mu^*(1) \phi_\nu(1) r_{12}^{-1} \phi_\lambda^*(2) \phi_\sigma(2) \tag{28}$$

The (initial) wave function is used to generate an effective potential, which apply this potential in order to refine the coefficient matrix. The modified MO's form the new input in the Roothaan or Pople-Nesbet (1986) equations, and a new potential is generated. The iterative procedure is repeated until convergence is reached, i.e. when the changes in energy and/or charge density in two subsequent iterations are below a pre-set threshold value.

Before a more technical description of the SCF-procedure is presented, first need to define a new transformation matrix X, used for orthogonalisation of the basis set. This orthogonalisation can be either symmetric or canonical. A symmetric orthogonalisation implies that X is formed through the relation

$$X = S^{-1/2} = Us^{-1/2}U^{\tau} \tag{29}$$

where S is the overlap matrix, U is an unitary matrix which diagonalizes S, and the diagonal matrix of the eigenvalues of S is given by the relations. In the canonical orthogonalisation procedure, X is instead given by

$$X = Us^{-1/2} \tag{30}$$

Consider a new coefficient matrix C' related to the old coefficient matrix C by

$$C' = X^{-1}C, \qquad C = XC' \tag{31}$$

where assumed that X possesses an inverse. Substituting $C = XC'$ into the Roothaan equations gives

$$FXC' = SXC'\varepsilon \tag{32}$$

Multiplying on the left by X^{τ} gives

$$\left(X^{\tau}FX\right)C' = \left(X^{\tau}SX\right)C'\varepsilon \tag{33}$$

if define a new matrix F^{τ} by

$$F^{\tau} = X^{\tau}FX \tag{34}$$

and use (27),then

$$F'C' = C'\varepsilon \tag{35}$$

The SCF procedure, outlined in Appendix figure A1, is as follows

1. Specify a molecule (a set of nuclear coordinates $\{R_A\}$, atomic numbers $\{Z_A\}$, and number of electron N) and a basis set $\{\phi_\mu\}$.
2. Calculate all required molecular integrals, $S_{\mu\nu}$, $H_{\mu\nu}^{\text{core}}$ and $(\mu\nu|\lambda\sigma)$.
3. Diagonalize the overlap matrix S and obtain a transformation matrix X from either equation $X \equiv S^{-1/2} = Us^{-1/2}U^{\tau}$ or $X = Us^{-1/2}$.
4. Obtain a guess at the density matrix P.
5. Calculate the matrix G of equation $F_{\mu\nu} = H_{\mu\nu}^{\text{core}} + G_{\mu\nu}$ from the density matrix P and the two-electron integral $(\mu\nu|\lambda\sigma)$.
6. Add G to the core-Hamiltonian to obtain the Fock matrix $F = H^{\text{core}} + G$.
7. Calculate the transformed Fork matrix $F^{\tau} = X^{\tau}FX$
8. Diagonalize F^{τ} to obtain C' and ε.
9. Calculate $C = XC'$.
10. Form a new density matrix P from C using $P_{\mu\nu} = 2\sum_{a}^{N/2} C_{\mu a}C_{va}^{*}$.
11. Determine whether the procedure has converged, i.e. determine whether the new density matrix of step (10) is the same as the previous density matrix within a specified criterion. If the procedure has not converged, return to step (5) with the new density matrix.
12. If the procedure has converged, then use the resultant solution, represented by C, P, F, etc., to calculate expectation values and other quantities of interest.

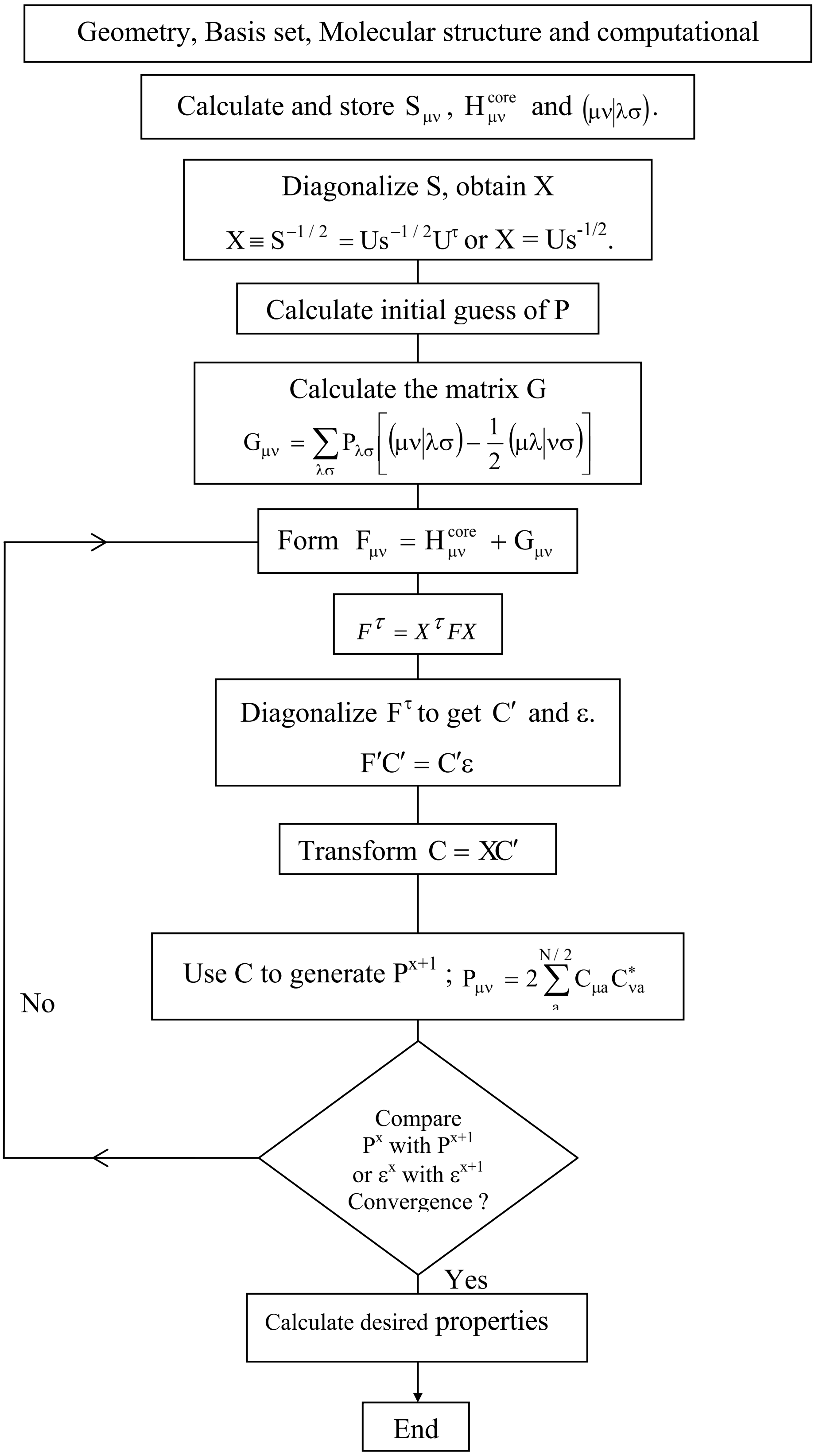

Appendix Figure A1 Schematic view of a Hartree-Fock self consistent field calculation.

3. Basis Set

The basis set most commonly used in quantum mechanical calculations are composed of atomic functions. The next approximation involves expressing the molecular orbitals as linear combinations of a pre-defined set of one-electron functions known as basis function. An individual molecular orbitals is defined as:

$$\phi_i = \sum_{\mu=1}^{N} c_{\mu i}\chi_\mu \tag{36}$$

where the coefficients $c_{\mu i}$ are known as molecular orbital expansion coefficients. The basis function $\chi_1 ... \chi_N$ are also chosen to be normalized. Gaussian-type atomic functions were used as basis functions. Gaussian functions have the general form

$$g(\alpha, \vec{r}) = cx^n y^m z^l e^{-\alpha r^2} \tag{37}$$

where $\vec{r}$ is of course composed of x, y, and z. α is a constant determining the size (radical extent) of the function. In Gaussian function, $e^{-\alpha r^2}$ is multiplied by powers (possibly 0) of x, y, and z and a constant for normalization, so that:

$$\int_{\text{allspace}} g^2 = 1 \tag{38}$$

Thus, c depends on α, l, m, and n.

Here are three representative Gaussian functional (s, p_y and d_{xy} types, respectively):

$$g_s(\alpha, \vec{r}) = \left(\frac{2\alpha}{\pi}\right)^{3/4} e^{-\alpha r^2}$$

$$g_y(\alpha, \vec{r}) = \left(\frac{128\,\alpha^5}{\pi^3}\right)^{1/4} y e^{-\alpha r^2}$$

$$g_{xy}(\alpha, \vec{r}) = \left(\frac{2048\,\alpha^7}{\pi^3}\right)^{1/4} xy e^{-\alpha r^2} \tag{39}$$

Linear combinations of primitive gaussians like these are used to form the actual basis functions; the latter are called contracted Gaussians and have the form

$$\chi_\mu = \sum_P d_{\mu p} g_p \tag{40}$$

where the $d_{\mu p}$'s are fixed constants within a given basis set. Note that contracted functions are also normalized in common practice. A few commonly used basis sets are lists as following.

Minimal Basis Sets: Minimal basis sets contain the minimum number of basis functions needed for each atom, as in these examples:

H: 1s
C: 1s, 2s, $2p_x$, $2p_y$, $2p_z$

Minimal basis sets use fixed-size atomic-type orbitals. The STO-3G basis set is a minimal basis set (although it is not the smallest possible basis set). It used three gaussian primitives per basis function, which accounts for the “3G” in its name. “STO” stands for “Slater-type orbitals,” and the STO-3G basis set approximates Slater orbitals with gaussian functions.

Split Valence Basis Sets

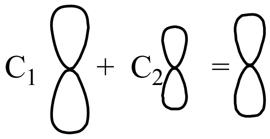

The first way that a basis set can be made larger is to increase the number of basis functions per atom. Split valence basis sets, such as 3-21G and 6-31G, have two (or more) sized of basis function for each valence orbital. For example, hydrogen and carbon are represented as:

H: 1s, 1s’
C: 1s, 2s, 2s’, $2p_x$, $2p_y$, $2p_z$, $2p'_x$, $2p'_y$, $2p'_z$

where the primed and unprimed otbitals differ in size.

The double zeta basis sets, such as the Dunning-Huzinaga basis set (D95), form all molecular orbitals from linear combinations of two sized of functions for each atomic orbital. Similarly, triple split valence basis sets, like 6-311G, use three sizes of contracted functions for each orbital-type.

Polarized Basis Sets

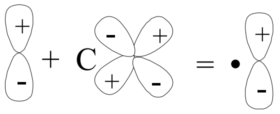

Split valence basis sets allow orbitals to change size, but not to change shape. Polarized basis sets remove this limitation by adding orbitals with angular momentum beyond what is required for the ground state to the description of each atom. For example, polarized basis sets add d functions to carbon atoms and f functions to transition metals, and some of them add p functions to hydrogen atoms.

So far, the only polarized basis set 6-31G(d) is used. Its name indicates that it is the 6-31G basis set with d functions added to heavy atoms. This basis set is becoming very common for calculations involving up to medium-sized systems. This basis set is also known as 6-31G*. Another popular polarized basis set is 6-31G(d,p), also known as 6-31G**, which adds p functions to hydrogen atoms in addition to the d functions on heavy atoms.

Diffuse Functions

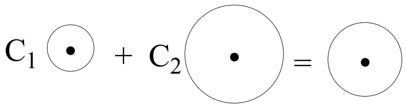

Diffuse functions are large-size versions of s- and p- type functions (as opposed to the standard valence-size functions) which allow orbitals to occupy a larger region of space. Basis sets with diffuse functions are important for systems where electrons are relatively far from the nucleus: molecules with lone pairs, anions and other systems with significant negative charge, systems in their excited states, systems with low ionization potentials, descriptions of absolute acidities. The 6-31+G(d) basis set is the 6-31G(d) basis set with diffuse functions added to heavy atoms. The double plus version, 6-31++G(d), adds diffuse functions to the hydrogen atoms as well. Diffuse functions on hydrogen atoms seldom make a significant difference in accuracy.

High Angular Momentum Basis Sets

Even larger basis sets are now practical for many systems. Such basis sets add multiple polarization functions per atom to triple zeta basis set. For example, the 6-31G(2d) basis set adds two d functions per heavy atom instead of just one, while the 6-311++G(3df,3pd) basis set contains three sets of valence region functions, diffuse functions on both heavy atoms and hydrogens, and multiple polarization funtions:3 d functions and 1 f function on heavy atoms and 3 p functions and 1 d function on hydrogen atoms. Such basis sets are useful for describing the interactions between electrons in electron correlation methods.

4. Semiempirical Calculations

Because both time and storage requirements of an *ab initio* Hartree-Fock calculation increase as the fourth power of the number of basis functions, calculations on large molecules even with the smallest basis sets are apt to be prohibitive. In such situations, the NDDO (neglect of diatomic differential overlap) formalism affords practical methods for calculating the electronic structure of large systems. Here, only one- and two-centre, two-electron integrals are considered, and the Hartree-Fock matrix, consists only of elements for which basis functions μ and ν are on the same atom, and basis functions λ and σ are on another atom. The individual terms are defined below (the sum α is over all other atoms).

$$
\begin{aligned}
F_{\mu\mu} &= H^{\text{core}}_{\mu\mu} + \sum_{\nu} P_{\nu\nu}\left[\langle\mu\mu \mid \nu\nu\rangle - \langle\mu\nu|\mu\nu\rangle\right] + \sum_{\delta}\sum_{\lambda}\sum_{\sigma} P_{\lambda\sigma}\langle\mu\mu|\nu\nu\rangle \\
F_{\mu\nu} &= H^{\text{core}}_{\mu\nu} + P_{\mu\nu}\left[3\langle\mu\nu \mid \mu\nu\rangle - \langle\mu\mu|\nu\nu\rangle\right] + \sum_{\delta}\sum_{\lambda}\sum_{\sigma} P_{\lambda\sigma}\langle\mu\nu|\lambda\sigma\rangle \\
F_{\mu\lambda} &= \beta_{\mu\lambda} - \frac{1}{2}\sum_{\nu}\sum_{\sigma} P_{\lambda\sigma}\langle\mu\nu|\lambda\sigma\rangle \qquad (41)
\end{aligned}
$$

The elimination of three- and four-centre integrals greatly reduces the time and storage requirements for an NDDO calculation (which now increase as the square of the number of atoms) relative to that for a full Hartree-Fock treatment.

Three levels of NDDO theory are included in *SPARTAN'S SEMI EMPIRICAL* module: MNDO Modified Neglect of Diatomic Overlap

AM1 Austin Method 1

PM3 MNDO Parameterization Method 3

In all of these formalisms, only the valence electrons are considered. The one-electron terms are given by,

$$H_{\mu\nu}^{core} = U_{\mu\nu} - Z_A \sum_{B \neq A} Z_B \langle \mu\nu \mid \delta\delta \rangle \tag{42}$$

Here, μ and ν are located on atom A and the summation is over all other atoms. Uνν is related to the binding energy of an electron in atomic orbital ν, and is determined from spectroscopic data. Uνμ is set to zero for ν ≠ μ. The second term in equation 42 represents the attraction on an electron on atom A from the nuclear framework. The two center integral involves only the s function on atom B. Z_A is the charge of atom A without its valence electrons.

All one-centre, two-electron integrals (νν|μμ) and (νμ|νμ) are fitted to spectroscopic data. The two-centre, two-electron repulsion integrals (νμ|λσ) are approximated by classical multipole-multipole charge interactions between atoms A and B. The multipole charge separations within an atom are treated as adjustable parameters, i.e. optimized to fit the experimentally derived one-centre integrals.

The βμλ terms appearing in the Fock matrix (equation 41) are the one-electron, two-centre core resonance integrals and are approximated as,

$$\beta_{\mu\lambda} = \frac{\beta_\mu + \beta_\lambda}{2} S_{\mu\lambda} \tag{43}$$

where $S_{\mu\lambda}$ is the overlap integral between Slater orbitals μ and λ, and $\mu\lambda$ and $\lambda\mu$ are adjustable parameters optimized using experimental thermo chemical data for simple molecules. Because all of the adjustable parameters are rooted in experimental data, these methods are known as semi-empirical. As in *ab initio* Hartree-Fock calculations, an SCF procedure is used to converge on a density matrix, and the electronic energy.

The three methods differ only in the core-repulsion terms (they also differ in the detailed parameterization). Core repulsion includes nuclear repulsion and non-valence electron-electron repulsion, which are not explicitly considered in the calculation of the electronic energy. In the MNDO model, the core repulsion energy is given by,

$$E^{CR} = \sum_{A \neq B} \sum_{B \neq A} Z_A Z_B \langle \delta(A) | \delta(B) \rangle (e^{-\sigma_A R_{AB}} + e^{-\sigma_B R_{AB}}) \qquad (44)$$

where R_{AB} is the internuclear distance and σ_A and σ_B are adjustable parameters fit to give the correct empirical behavior. Details are provided in the original papers. MNDO tends to overestimate core repulsion between two atoms at van der Waals distances. For this reason, the AM1 model was developed.

In AM1 a sum of Gaussians is employed to better represent the core repulsion behaviour at van der Waals distances. PM3 uses a similar core repulsion function, but differs in the parameterisation procedure.

One advantage of methods parameterised using experimental data is their implicit inclusion of electron correlation effects. However, dependence on experimental data means that semi-empirical methods would not be expected to perform well on unusual types of molecules for which no data are available from which to construct parameters.

5. Density Functional Theory

Methods that are rooted in the so-called density functional theory are currently regarded as very promising since are able to include a large amount of correlation effects in a formalism that essentially requires very similar computational resources as the Hartree-Fock procedure. In fact the algorithms of the approach, in which the electron density is described in terms of one-electron basis functions, are very similar to the single-determinant HF algorithm. This property has helped to establish density functional methods as a standard tool for chemistry and physics.

While the concept of expressing part or all of the molecular energy as a functional of the electron density goes back to the early days of quantum theory, Density Functional Theory (DFT) was put on a rigorous theoretical foundation by the Hohenberg-Kohn theorem. It states that there exists unique density ρ that yields the exact ground energy of system. The subsequent work of Kohn and Sham laid the basis for practical computational applications of the DFT to real systems. The basis of their formalism are the so-called Kohn-Sham equations.

$$H\Psi_i = E_i\Psi_i \tag{45}$$

in which the Hamiltonian H is defined as

$$H = \left(-\frac{1}{2}\nabla^2 + V_{KS}\right) \tag{46}$$

where V_{KS} is a local potential defined such that the total density of the non-interacting system

$$\rho = \sum_i |\Psi_i|^2 \tag{47}$$

is the same as the density of the “real” system. V_{KS} has the three components V_{ext}, V_C and V_{XC} containing the nuclear and external, Coulomb potential of the electrons and the exchange-correlation interactions.

$$E_{KS} = V_{ext} + \sum_{\mu\nu} P_{\mu\nu}H_{\mu\nu} + \frac{1}{2}\sum_{\mu\nu\lambda\sigma} P_{\mu\nu}P_{\lambda\sigma}\Im + E_x(P) + E_C(P) \tag{48}$$

In most cases the expressions for E_C and E_X cannot be computed analytically and must be obtained by numerical methods. The key difference between the Hartree-Fock and Kohn-Sham approaches to the SCF methods is the term E_{XC}, which was mostly omitted in above discussion. In HF theory, this E_{XC} is written as

$$E_{XC}^{HF} = \frac{1}{2} \sum_{\mu\nu\lambda\sigma} (P_{\mu\nu}^{\alpha} P_{\lambda\sigma}^{\alpha} P_{\mu\nu}^{\beta} P_{\lambda\sigma}^{\beta})(\mu\nu / \lambda\sigma) \tag{49}$$

while the KS theory introduces a functional

$$E_{XC}^{HF} = \int f(\rho^{\alpha}, \rho^{\beta}, \gamma_{\alpha\alpha}, \gamma_{\alpha\beta}, \gamma_{\beta\beta}) dr \tag{50}$$

for the description. The density gradient invariants γ $(\gamma_{xy} = \nabla\rho_x \nabla\rho_y)$

Density Functionals

It is often customary to make a partition of the density functional into an exchange and correlation part for the separation of

$$E_{XC}(\rho) = E_X(\rho) + E_C(\rho) \tag{51}$$

Although distinction between exchange and correlation contributions is somewhat artificial in the context of DFT, the above separation considerably simplifies the discussion. It should, however, be explicitly noted that the definition of E_C does not correspond to the *ab initio* E_C since correlation has, by definition, meaning only in a mean field approximation and DFT is not using such an approximation. The exchange part, on the other hand, follows closely the HF definition of exchange, does however not necessarily reproduce the exact exchange.

Exchange

The exchange energy of a uniform spin-polarized gas of spin density ρ_σ is

$$E_X^S = -\sum \int \rho^\sigma(r) f_X^S(\rho_\sigma(r))dr \qquad (52)$$

with $f_X^S(\rho_\sigma(r)) = \alpha_X[\rho_\sigma(r)]^{\frac{1}{3}}$ and $\alpha_X = \frac{3}{2}\left(\frac{3}{4\pi}\right)^{\frac{1}{3}}$. The exchange expression is sometimes labeled *Slater exchange*, thus the superscript *S*. This exchange expression serves as a base for other functional, which can be conveniently expressed in terms of their enhancement factor F_X over the exchange of the uniform electron gas

$$E_X = -\sum_\sigma \int \rho_\sigma(r) f_X^S(\rho_\sigma(r)) F_X(\rho_\sigma)(\gamma_{\sigma\sigma}(r))dr \qquad (53)$$

For instance, the exchange functional proposed by Perdew and Wang uses the following factor:

$$F_X^{PW}(s) = \left[1 + 0.0864\frac{s^2}{m} + bs^4 + cs^6\right]^m \qquad (54)$$

with $m = 1/15$, $b = 14$, $c = 0.2$ and $s = (24\pi^2)^{-1/3}\sqrt{(\gamma_{\sigma\sigma}/\rho^{4/3})}$ $\gamma_{\sigma\sigma}$ here is again the squared density gradient ∇_ω^2. One of the most used exchange functionals is that of Becke 1988, which is often labeled B88 or simply B.

$$F_x^B = -\beta\rho^{1/3}\frac{x^2}{1 + 6\beta\sinh^{-1}(x)} \qquad (55)$$

which uses the values $x = \sqrt{(\gamma_{\sigma\sigma}/\rho_\sigma^{4/3})}$ and $\beta = 0.0042$ in order to maintain correct boundary conditions. In a different approach, Perdew and Wang proposed an exchange formula that is designed from purely first principles.

$$F_X^{PW91} = \frac{1+(a_1 s)(a_2 s)\sinh^{-1} + (a_3 + a_4 \exp(-100s^2))s^2}{1+(a_1 s)(a_2 s)\sinh^{-1} + a_5 s^4} \qquad (56)$$

where $a_1 = 0.19645$, $a_2 = 7.7956$, $a_3 = 0.2743$, $a_4 = -0.1508$, $a_5 = 0.004$ and s the same as in eq. 54.

In practice, the three above exchange functionals are very similar, and are in fact based on minor corrections to the previous ones. Therefore they can be expected to produce very similar results. The enhancement over the simple electron gas, however, are significant enough and usually constitute a major improvement.

Correlation

While it is possible to obtain E_C by some numerical methods from E_{XC} and the already known EX (cf. eq. 51) for the uniform electron gas, it is much more common to use separate correlation functionals. Distinction is made between local and gradient corrected functionals, referring to absence or presence of first order terms of the density ρ_σ. The local functional proposed by Vosko, Wilk and Nusair (VWN) was obtained using Pad's approximated interpolations of Ceperley and Alder results of their accurate quantum Monte Carlo calculations for the homogeneous electron gas. The functional is,

$$E_C^{VWN} = \frac{A}{2}\left[\ln\frac{x^2}{X(x)} + \frac{2b}{Q}\tan^{-1}\frac{Q}{2x+b} - \frac{bx_0}{X(x_0)}\left(\ln\frac{(x-x_0)^2}{X(x)} + \frac{2(b+2x_0)}{Q}\tan^{-1}\frac{Q}{(2x+b)}\right)\right] \qquad (57)$$

where the functions $x = r_b^{1/2}$, $X(x) = x^2 + bx + c$ and $Q = (4c - b^2)^{1/2}$ and the constants are $A = 0.0621814$, $x_0 = -0.409286$, $b = 13.0720$ and $c = 42.7189$. r_b represents are the Wigner-radius and is defined by $1/\rho = \frac{4\pi}{3}(r_b)^3$. Together with the exchange expression from eq. 52 this constitutes what is often called the local density approximation (LDA) or local spin density approximation (LSDA) when spin is considered (Gies and Gerhardts, 1987).

Due to the experiences with the LDA and as a consequence of some of its shortcomings, recent developments have resulted in a number of gradient corrections to local functionals like the aforementioned VWN or a completely new class of gradient corrected functionals.

Another frequently used functional has been published by Lee, Yang and Parr. It replaces both the local and the gradient part of the LDA correlation functional.

$$E_C^{LYP} = -a\frac{1}{1+d\rho^{-1/3}}\left\{\rho + b\rho^{-2/3}\left[C_F\rho^{-5/3} - 2t_w + \frac{1}{9}\left(t_w + \frac{1}{2}\nabla^2\rho\right)\right]e^{-2c\rho^{-1/3}}\right\} \tag{58}$$

where $t_w = \frac{1}{8}\left(\frac{|\nabla\rho|^2}{\rho} - \nabla^2\rho\right)$ and $C_F = \frac{3}{10}(3\pi^2)^{2/3}$, $a = 0.04918$, $b = 0.132$, $c = 0.2533$ and $d = 0.349$

Hybrid Functionals

More recently, following an approach proposed by Becke, the combination of DFT functionals with *ab initio* formulations led to a class of expressions which are essentially a mixture of both DFT and HF contributions with fitted coefficients for each contribution. The aim of this approach is to provide expressions that include the full exchange contribution and avoid side-effects arising from a complete replacement of the DFT exchange expression by the HF one. As an example, the B3LYP functional looks like this:

$$E_{XC}^{B3LYP} = a_{X0}E_X^S + (1-a_{X0})E_X^{HF} + a_{X1}\Delta E_X^B + E_C^{VWN} + a_C\Delta E_C^{LYP} \tag{59}$$

with $a_{X0} = 0.80$, $a_{X1} = 0.72$ and $a_C = 0.81$, which are values fitted for a selected set of molecules to reproduce the heat of formation. The term E_X^{HF} is calculated using the Kohn-Sham orbitals in the manner of the HF procedure by computing the exchange integrals $(\mu\nu / \nu\mu)$. The B3LYP functional often uses $\Delta E_C^{3LYP} = E_C^{LYP} - E_C^{VWN}$.

The Theory of Quantum Chemical Calculations: Excited State Methods

1. Excited Slater Determinants

The Hartree-Fock method generates solutions to the Schrodinger equation where the real electron-electron interaction is replaced by an average interaction. In the sufficiently large basis, the HF wave function is able to account for ~ 99% of the total energy, but the remaining ~1% is often very important for describing chemical phenomena. It is therefore clear that in order to improve on HF results, the starting point must be a trial wave function which contains more than one Slater Determinant (SD) Φ. Then electron correlation methods normally use the HF wave function as a starting point for improvements.

A generic multi-determinant trial wave function can be written as

$$\Psi = a_0\Phi_{HF} + \sum_{i=1} a_i \Phi_I \qquad (1)$$

where a_0 usually is close to 1. Electron correlation methods differ in how they calculate the coefficients in front of the other determinants, a_0 being determined by the normalization condition.

How are the additional determinants beyond the HF constructed? With *N* electrons and *M* basis functions, solution of the Roothaan-Hall equations for the RHF case will yield *N/2* occupied MOs and *M* – *N/2* unoccupied (virtual) MOs. A slater determined by *N/2* spatial MOs multiplied by two spin functions to yield *N* spinorbitals. By replacing MOs which are occupied in the HF determinant by MOs which are unoccupied, a whole series of determinants may be generated as shown in Figure A2. These can be denoted according to how many occupied HF MOs have been replaced by unoccupied MOs, i.e. Slater determinants which are *singly, doubly, triply, quadruply* etc. excited relative to the HF determinants, up to a maximum of *N* excited electrons. These determinants are often referred to as *Singles* (S), *Doubles* (D), *Triples* (T), *Quadruples* (Q) etc.

The total number of determinants that can be generated depends on the size of the basis set, the larger the basis, the more virtual MOs, and the more excited determinants can be constructed. If all possible determinants in a given basis set are included, all the electron correlation (in the given basis) is (or can be) recovered. Methods which include electron correlation are thus two-dimensional, the larger the one-electron expansion (basis set size) and the larger the many-electron expansion (number of determinants), the better are the results.

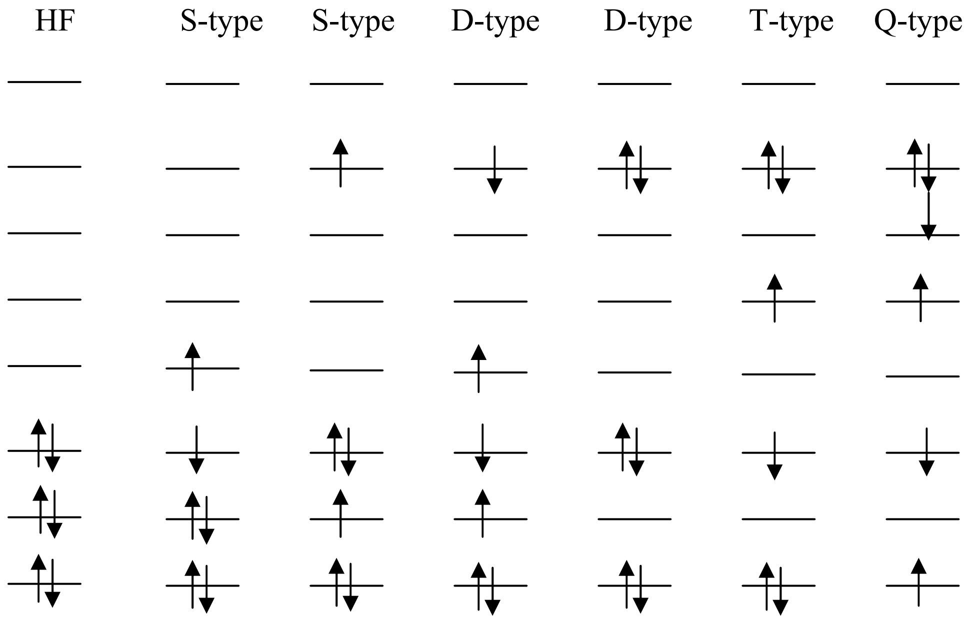

Appendix Figure A2 Excited Slater determinants generated from a HF reference.

2. Molecular Orbital Theories for Excited States

2.1. Configuration Interaction (CI)

The term “configuration” was originally used for the interaction of just a few Slater determinants required for the proper description of some electronic states of atoms and molecules, though the concept of configuration interaction has been known as a tool for obtaining, at least in principle, the exact solution of the Schrodinger equation since the early days of quantum mechanics. The results of CI calculations, and especially the results of full configuration (FCI) calculations, have been used as benchmarks for testing the newly developed methods. FCI is still the only method which is used for the definition of the correlation energy as the difference between the exact nonrelativistic energy (represented by the FCI energy) and the Hartree-Fock (HF) energy:

$$E_{\text{corr}} = E_{\text{exact}} - E_{\text{HF}} \qquad (2)$$

CI is still a standard method for calculation of excited electronic states and its conceptual simplicity makes it the method of choice for qualitative explanation of phenomena for which the single-determinant Hartree-Fock approximation is unsatisfactory because of near-degeneracies or rearrangement of electrons within partly occupied shells.

2.1.1 Definition and the essence of configuration interaction

For any CI calculation, we need first an orbital set, i.e., a set of one-electron functions $\varphi = \{\varphi_i, i = 1, 2, \dots, m\}$, that satisfy the orthonormality

$$\langle \varphi_i \mid \varphi_j \rangle = \delta_{ij} \qquad (3)$$

and the completeness conditions

$$\sum_i |\varphi_i\rangle\langle\varphi_i| = 1 \qquad (4)$$

In the most applications these orbitals are chosen to be Hartree-Fock orbitals, though as will be noted below other types of orbitals (Huckel orbitals, natural orbitals, or even nonorthogonal orbitals) may also be used.

Next that the orbitals are in a certain order, for example in the order of their increasing energy. Then assign to each orbital φ_i an occupation number n_i , which may take the 0, 1, or 2. The sum of the occupation numbers must be equal to the number of electrons. A set of occupation numbers (n_1, n_2, …, n_m) is called a *configuration*. In the ground state configuration of a closed-shell system all the lowest orbitals are doubly occupied. For example, for a ten electron system and the orbital set with m = 7, the ground state configuration is (2222200). The configuration (2222110), corresponding to the excitation of a single electron from orbital 5 to orbital 6, is called a singly excited configuration.

For a configuration having n singly occupied orbitals, we can in general form 2^n spin functions and therefore also 2^n different Slater determinants. A true number of linearly independent spin functions for a given configuration, i.e., for an orbital product function, and a total spin S is given by following formula:

$$f(n, S) = \binom{n}{q} - \binom{n}{q-1} \qquad (5)$$

where

$$q = \tfrac{1}{2}n - S \qquad (6)$$

In general the selected functions are linear combinations of several Slater determinants and, in contrast to individual Slater determinants, they are eigenfunctions of the spin operators S_z and S^2. Therefore they are called spin-adapted configuration fuctions or, most frequently, *configuration state functions* (CSFs). The spin adapted reference configuration is called the reference state function. Because of orthogonality of orbitals and spin functions, the CSFs are also orthogonal, and because of the completeness of the orbital set, a set of all possible CSFs forms a complete set

$$\sum_i \ | \Phi_i > \ < \Phi_i | = 1 \qquad (7)$$

Hence the exact wave function for a particular orbitals set may be expressed as

$$\Psi = \sum_i \ |\Phi_i\rangle\langle\Phi_i|\Psi\rangle \qquad (8)$$

where the overlab intergrals between CSFs and the exact wave function have the meaning of expansion coeffients.

$$\Psi = \sum_i \ C_i \, \Phi_i \qquad (9)$$

Use of a complete set of CSFs in the expansion (8) is referred to as the complete or full configuration (FCI). Since FCI calculations are computationally very demanding, they are only feasible for small sets and a small number of electrons. In chemical applications of the CI method, smaller expansions are used in order to develop a computationally tractable model. Standard levels of the CI method are termed according to the extent of the CI expansion: CIS, CISD, CISDT, and CISDTQ correspond to expansions through singly, doubly, triply and quadruply excited CSFs, respectively. Those methods will be called truncated CI methods. Truncating the excitation level at 1 (CI with Singles, CIS) does not give any improvement over the HF result as all matrix elements between the HF wave function and singly excited determinants are zero. CIS is equal to HF for the ground-state energy, although higher roots from the secular equations may be used as approximations to excited states. It has already been mentioned that only doubly excited determinants have matrix elements with the HF wave function different from zero, thus the lowest CI level which gives an improvement over the HF result is that which includes only doubly excited states, yielding the CID. Although the singly excited determinants have zero matrix elements with the HF reference, they enter the wave function indirectly as they have non-zero matrix elements with the doubly excited determinants. So that the only CI method which is generally applicable for a large variety of systems is CISD. For molecular properties, the singly excited states thus allow the CI wave function to "relax" the MOs, i.e. letting the wave function respond to the perturbation.

2.1.2 Size Consistency, Performance, and Accuracy

Size Consistency

Size consistency is the property that is required for any theoretical model incorporating electron correlation to be applicable to problems of chemical reactivity. It means that the method when applied to an ensemble of isolated molecules should give results which are additive for the energy and other properties. Unfortunately, any incomplete CI does not satisfy this requirement and its applications therefore must be treated with caution if comparison is made for properties of molecule of different size. The origin of this deficiency is well understood and the terms contained in the CI energy, which do not scale linearly with the number of particles, have been identified. The most convenient tool for the examination of size inconsistency in CI is the many-body perturbation theory. It was found that, unlike in the fourth- and higher-order many-body perturbation theory, the unphysical terms in CISD are not canceled and their cancellation is only achieved if quadruply and higher excited CSFs are included in the CI expansion. Complete cancellation is secured only by full CI, though it is believed that CISDTQ properties should be very near the full CI limit for chemical systems which can be well represented by a single restricted HF wave function. For dimer $(H_2O)_2$ and the double zeta basis set the CISDTQ size-inconsistency error amounts to 0.0003 au. which is considerably less than the CISD error of 0.0047 au. In general, we must expect that CISD does not provide results with the accuracy sufficient, for example, for thermochemistry. This stimulated attempts to eliminate unphysical terms in the CISD energy in some computationally simple, though approximate way. Several formulas were suggested for the a posteriori correction of the CISD energy. The most popular among these is the Davidson correction:

$$\Delta E = (1-C_0^2)(E_{CID}-E_{SCF}) \qquad (10)$$

where E_{CID} is the CID energy and C_0 is the expansion coefficient for the ground state CSF. Originally the Davidson correction was developed for CID but it is commonly used for correction of CISD energies.

Performance and Accuracy

It has been stated that CISDTQ properties are very near to the full CI data for systems which can be well represented by a single restricted HF wave function. Unfortunately, in spite of the progress made recently in CISDTQ calculation, the method cannot be advocated for general use because of the immense number of triply and quadruply excited CSFs. The method scales as n^{10}, where n is the number of active molecular orbitals, and it can be used only for the smallest molecular systems. On the other hand, the CISD method scales only as N^6, N being the number of (atomic) basis set functions, which makes the method amenable to routine calculations. In general, the errors in CISD energy predictions (heats of reactions, activation barriers) have to be expected to be considerably larger than that corresponding to the ‘chemical accuracy’ (1 kcal/mol^{-1}), even if the Davidson correction is applied. CISD fails particularly in those cases where the size-inconsistency effect is important.

If a higher accuracy is required, it is recommended to pass to the coupled cluster (CCs) theory, Basically, CCSD is also an N^6 procedure, but the test calculations showed that the timing ratio CCSD/CISD ranged from 4 to 8, though as with any comparison of two different methods, the ratio depends strongly on the efficiency of the two programs.

2.2 Symmetry Adapted Cluster and Symmetry Adapted Cluster Configuration (SAC/SAC-CI) Method

2.2.1 SAC theory for the ground state

SAC is abbreviation for the symmetry adapted cluster, the meaning of which will become clear later. It belongs to the cluster expansion approach, which was originated in the statistical theory of interacting atoms, in the theory of electron correlations in atoms and molecules.

Electron correlation is defined on the basis of the HF theory as

$$E_{corr} = E_{exact} - E_{HF} \tag{11}$$

$$\chi_{\mathrm{corr}} = \Psi_{\mathrm{exact}} - \Psi_{\mathrm{HF}} \tag{12}$$

where ‘exact’ stands for the exact solution of the non-relativistic Schrodinger equation. Since the HF model is independent particle model, electron correlations represent mainly the collisions of electrons scattering into unoccupied orbitals. We introduce an excitation operator T_I^+ which represents such a collision. For example, a collision of two electrons belonging to the occupied orbital $\varphi_{i,}$ resulting in the scattering into the unoccupied orbital $\varphi_{a,}$ is represented by the excitation operator T_{ii}^{aa},

$$T_{ii}^{aa} = a_{a\alpha}^{+}\, a_{a\beta}^{+}\, a_{i\alpha}\, a_{i\beta} \tag{13}$$

$$T_{ii}^{aa}\,|0\rangle = \|\varphi_1\alpha\varphi_1\beta ... \varphi_a\alpha\varphi_a\beta ... \varphi_n\alpha\varphi_n\beta\|\text{, where } |0\rangle = \Psi_g^{HF} \tag{14}$$

Configuration interaction (CI) method is one of the most popular methods for including electron correlations. This method is based on the expansion theorem, and the correlated wave function is expressed as

$$\Psi^{CI} = B_0 \,|0\rangle + \sum_I B_I T_I^{+} \,|0\rangle \tag{15}$$

where B_I are expansion coefficients. This method is simple and exact, but is usually slowly converging, especially for excited states. The dimension of the configurations easily reaches to the order of 10^8, though many efficient algorithms for handling such large matrices are proposed. Further, it is difficult to extract a physical meaning from such a large number of configurations. It is also difficult to solve many lower solutions of such a large matrix, which is necessary for studying shake-up spectra, for example.

The main factor of electron correlation is collisions of two electrons. In many electron systems, however, there is a chance for three, four and more electrons to collide each other. However, the probability for four collisions actually important are the products of pair collisions occurring at different places of the molecule. This is because the fluctuation potential for the electron correlation is very short range. When we introduce a sum of the excitation operation as

$$T = \sum_I C_I T_I^{+} \tag{16}$$

The wave function including higher-order collisional effects is written as

$$\Psi_g = (1 + T + 1/2\, T^2 + 1/6\, T^3 + \ldots..) \,|0\rangle \tag{17}$$

where the terms T^2, T^3, etc., represent two pair collisions, three pair collisions, etc., and the factors 1/2, 1/6, etc., are due to the indistinguishability of pair collisions. Eq. (17) is more compactly written as

$$\Psi_g = \exp(T) \,|0\rangle \tag{18}$$

which is the cluster expansion. The suffix g again stands for the ground state. The theory based on this expansion in called coupled cluster (CC) theory. Hereafter, we call the term, (1+T) $|0\rangle$ as linked term and term, (1/2 T^2 + 1/6 T^3 + …..) $|0\rangle$ as unliked term.

In the above formulation, we have introduced the operators T_I^+ representing two electron excitations (pair collisions). However, generally speaking, this is just an example, and we may take any operators physically important. An important example is to choose T as a sum of all single excitation operators,

$$\mathrm{T}^{(1)} = \sum_{i}^{occ} \sum_{a}^{unocc} C_i^a \, a_a^+ \, a_i \tag{19}$$

where i and a stand for the general spin orbital. Then we get Thouless theorem,

$$\Psi^{\mathrm{SD}} = N \exp (T^{(1)}) \, \Phi^{\mathrm{SD}} \tag{20}$$

where Φ^{SD} and Ψ^{SD} are different single determinants, N a normalization constant. This theorem states that the transformation of single determinants to another one is expressed by the operator N exp ($T^{(1)}$): the cluster expansion includes the *self-consistency of orbitals.*

We note that for open-shell systems, the single determinant Ψ^{SD} on the left hand side of eq. (20) is not a restricted determinant, but an unrestricted one which is not an eigenfunction of the spin-squared operator S^2. Generally, the wave function of the CC theory is not an eigenfunction of S^2, as actually reported for the CCSD wave functions for doublet radicals. In the linear expansions like CI, the solution of the secular equation is always symmetry-adapted, irrespective of the choice of the excited configurations, because the Hamiltonian is totally symmetric. However, this is not the case for the non-linear expansions like cluster expansion. Further, as explained below, coupled cluster expansion may involve a larger number of variables than that necessary for describing the state.

These difficulties do not occur when excitation operations are chosen to be symmetry adapted. Excitation operator S_I^+ are defined to be symmetry adapted when the configuration $S_I^+ |0\rangle$ is symmetry adapted. For totally symmetric singlet states, the symmetry adapted cluster (SAC) expansion are defined as

$$\Psi_g^{SAC} = \exp(S)\ |0\rangle \tag{21}$$

where

$$\mathrm{S} = \sum_I C_I S_I^+ \tag{22}$$

Since S_I^+ is totally symmetric, the unliked terms of eq. (21) are also totally symmetric. For open-shell states like doublet and triplet states, we need a symmetry projector Q as

$$\Psi_g^{SAC} = Q \exp(S)\ |0\rangle = [1 + S + Q\ (1/2S^2 + 1/6S^3 + \ldots)\ ]\ |0\rangle \tag{23}$$

where $|0\rangle$ is a restricted determinant and Q applies only to the unliked terms, since the linked term is already symmetry adapted.

The SAC expansion defined by eq. (21) is thus different from the CC expansion given by eq. (18). Table 1 is summarized the differences in schematic way.

Appendix Table A1 Schematic summary of the differences of the SAC expansion from the conventional cluster expansions[a].

Expansion	Linked term	Unliked term[b]	Number of independent variables[c]	Symmetry[d]
$\exp(T)\ \|0\rangle$	$T\|0\rangle$	$T_I\ T_J\ \|0\rangle$	Larger	Mixed
$Q\exp(T)\ \|0\rangle$	$QT\|0\rangle \rightarrow S\|0\rangle$	$QT_I\ T_J\ \|0\rangle$	Larger	Pure
$Q\exp(S)\ \|0\rangle$	$S\|0\rangle$	$QS_I\ S_J\ \|0\rangle$	Just as required	Pure

[a] The operators T_I are not symmetry-adapted, but the operators S_I are symmetry-adapted.

[b] Only the second-order unliked terms are given

[c] The number of the independent variables included in each expansion is compared with that necessary for the description of the system under consideration.

[d] Symmetry of the total wave function.

Now the solution of SAC theory was considered. In the SAC expansion, the unknown variables C_I are associated to the linked excitation operator S_I^+, so that we require the Schrodinger equation, $H\text{-}E_g\ \left|\Psi_g^{SAC}\right\rangle = 0$, within the space of the linked configurations as

$$\langle 0|\ H\text{-}E_g\ \left|\psi_g^{SAC}\right\rangle = 0 \tag{24a}$$

$$\langle 0|\ S_I(H\text{-}E_g)\ \left|\Psi_g^{SAC}\right\rangle = 0 \tag{24b}$$

We have the same number of equations as the number of the unknown variables, This solution is called non-variational solution.

The variational solution is obtained by applying the variational principle to the SAC wave function and we obtain,

$$\left\langle \Psi_g^{SAC} \right| S_I(H\text{-}E_g) \left| \Psi_g^{SAC} \right\rangle = 0 \tag{25a}$$

$$\left\langle \Psi_g^{SAC} \right| (H\text{-}E_g)\, S_I \left| \Psi_g^{SAC} \right\rangle = 0 \tag{25b}$$

This equation is valid *only* for the SAC expansion, but not for the CC expansion, because of the reason summarized in Table 1. Generally, the variation solution is more difficult than the non-vairational one, because former involves the intergrals between the umliked terms. However, we believe, as long as the wave function itself is accurate, the difference between the variational and non-variational solutions should be small.

It is shown that eq. (25b) is the *generalized Brillouin theorem*. In comparison with eq. (26).

$$\left\langle \Psi_g^{HF} \right| \mathrm{H} \left| \phi_i^a \right\rangle = 0 \tag{26}$$

where Ψ_g^{SAC} corresponds to Ψ_g^{HF} and $S_I^+ \left| \Psi_g^{SAC} \right\rangle$ does to ϕ_i^a. As the Brillouin theorem is a key equation in the HF/SECI theory, the generalized Brillouin theorem given by eq. (25b) is a key equation in the theoretical framework of the SAC/SAC-CI theory. The SAC theory has the following properties. The first three are common to the CC theory.

(1) It effectively involves higher-order effects of electron collisions. It describes dynamic correlations quite effectively.
(2) It is size consistent or size extensive, so that it correctly describes the energy change in the dissociation process such as $X_n \rightarrow nX$. This property is a direct consequence of the exponential, since

$$\exp(A)\exp(B) = \exp(A+B) \tag{27}$$

when the operators A and B are commutable.

(3) It includes self-consistency. This property is best represented by the Thouless' theorem given by eq. (20). It guarantees that the cluster expansion is *independent* of a choice of the reference orbitals, when we include all the single excitation operations.

(4) The SAC theory defines not only the SAC wave function itself Ψ_g^{SAC} for the ground state, but also the excited functions which span the basis for excited states. The SAC-CI theory is based on this property. This property is probably the most important property, among others, and is valid only for the SAC theory.

2.2.2 SAC-CI theory for excited, ionized, and electron attached states

It was thought for a long time that the description of electron correlations in excited states is much more difficult than that in the ground state. Excited states are generally open shells and are not represented by a single Slater determinant. Many different states of many different symmetries and natures are involves in a narrow energy range, which makes it difficult to suppose a single general theory in a useful form. However, this is not the case in the SAC-CI theory. By using the SAC-CI method, we can *easily* calculate the correlated wave function of the excited, ionized and electron attached states, as explained in the following.

The electron correlations in the excited state will be described on the basis of those in the ground state. Approximately, excitations and ionizations involve only one or two electrons, and most other electrons lie essentially in the same orbitals as in the ground state. Therefore, the electron correlations in the excited state should be able to be compactly described by considering only some modifications to the ground-state electron correlations.

The excited functions $\{\Phi_K\}$ by using the SAC wave function was written as

$$\Phi_K = P S_K^{+} \Psi_g^{SAC} \tag{28}$$

where *P* is the operator which projects out the ground state wave function,

$$P = 1 - \left|\Psi_g^{SAC}\right\rangle \left\langle\Psi_g^{SAC}\right| \tag{29}$$

and $\{S_K^+\}$a set of the excitation operations involving the excitations under consideration in a orbital picture. From the generalized Brillouin theorem of the SAC theory, eq. (25b), it is easily shown that the functions $\{\Phi_K\}$ satisfy

$$\left\langle\Phi_K \middle| \Psi_g^{SAC}\right\rangle = 0, \qquad \left\langle\Phi_K \middle| H \middle| \Psi_g^{SAC}\right\rangle = 0 \tag{30}$$

These equation shows, that *the set of the functions spans the space for the excited states.* We therefore describe the excited state by *a linear combination* of the functions $\{\Phi_K\}$,

$$\Psi_e^{SAC-CI} = \sum_K d_K \Phi_K \tag{31}$$

which is the SAC-CI theory.

Obviously, the SAC-CI wave function for the excited state satisfied the correct relations with the SAC ground state,

$$\left\langle\Psi_g^{SAC} \middle| \Psi_g^{SAC-CI}\right\rangle = 0, \quad \left\langle\Psi_g^{SAC} \middle| H \middle| \Psi_g^{SAC-CI}\right\rangle = 0 \tag{32}$$

Applying the variational principle to eq. (32) for solving the unknown variables $\{d_K\}$, we obtain

$$\left\langle\Phi_K \middle| H - E_e \middle| \Psi_g^{SAC-CI}\right\rangle = 0 \tag{33}$$

Different solutions of eq. (32), which correspond to different excited states, satisfy

$$\left\langle \Psi_e^{SAC-CI} \middle| \Psi_f^{SAC-CI} \right\rangle = 0, \qquad \left\langle \Psi_e^{SAC-CI} \middle| H \middle| \Psi_f^{SAC-CI} \right\rangle \tag{34}$$

Since they are the solutions of the common secular equation. Thus, the SAC-CI wave function satisfies the correct relations with the ground state and with the other excited states. This is very important when we consider the properties, like transitions and relaxations, which interconnect different states.

In the above formulation, we have considered implicity the excited states having the same symmetry as the ground state. However, the SAC-CI theory is also valid for the excited states having different symmetries (e.g., triplet), and for the ionized and electron attached states. We generalize eq. (28) as

$$\Phi_K = P R_K^+ \Psi_g^{SAC} \tag{35}$$

where $\{R_K^+\}$ represents a set of excitation, ionization, and/or electron attachment operators. In any cases, eqs. (29)-(34) are valid.

Though the above formulation of the SAC-CI theory is variational and non-variational formulation. The non-variational SAC-CI solution is obtained by projecting the Schrodinger equation onto the space of the linked configurations,

$$\left\langle 0 \middle| R_K (H - E_e) \middle| \Psi_g^{SAC-CI} \right\rangle = 0 \tag{36}$$

Referring to eq. (25), we note that in the non-variational case, the SAC and SAC-CI wave functions satisfy the common set of equations. In particular, when we consider the excited states belonging to the same symmetry as the ground state, the operator $\{R_K^+\}$ in eq. (35) are actually $\{S_I^+\}$. The solutions of the Schrodinger equation belonging to different eigenvalues are orthogonal and Hamiltonian orthogonal. Therefore, we obtain eqs. (32) and (34) within the space of the liked operators under consideration. These equations are quite important for the theoretical consistency of the different states under consideration.

Practically, the non-variational solution is easier than the variational one by the reason similar to that stated for the SAC solution, but we have to diagonalize non-symmetric matrices. When the SAC-CI program was first coded, it was no efficient method for diagonalizing non-symmetric matrices of large dimentions, Therefore, we had to prepare the algorithm of iterative diagonaliztions of non-symmetric, extending the Davidson 's algorithm for symmetric matrices.

As the SAC theory is exact, the SAC-CI theory is also exact. Though the introduction of the SAC-CI theory so far given is rather formal and straightforward, it has some interesting physics. First, omitting the projector, or including the identity operator into $\{ R_K^+ \}$, then the SAC-CI wave function was written as

$$\Psi_e^{SAC-CI} = \Re \ \Psi_g^{SAC} \tag{37a}$$

where the excitatory $\Re$ (a king of reaction operator) is defined as

$$\Re = \sum_K d_K R_K^+ \tag{37b}$$

We already know that the SAC wave function well describes the electron correlation of the ground state. The excitatory $\Re$ describes the excitation starting from the electron correlation involved in the SAC ground state Ψ_g^{SAC}.

Generally, excitation is only one or two electron processes and most other electrons lie in the situation (orbitals) similar to those in the ground state. Therefore, it is clever to start from the ground-state electron correlation and describe only the modifications caused by the excitation. eqs. (37a) and (37b) just represent such as an idea, which is the ***transferability*** of electron correlations between ground and excited states. This method is much easier than calculation all of the electron correlations of each state from the beginning. Since the ground-state electron correlation is easier to calculate than the excited state one, when we calculate from the beginning, we first calculate it by the SAC method and then utilize it in the SAC-CI method for calculating the excited-state correlations based on its transferability. For this reason, the SAC-CI expansion is much easier and more rapidly convergent than ordinary CI.

The SAC-CI wave function is also written in the form

$$\Psi_e^{SAC-CI} = \exp\left(\sum_I C_I S_I^+\right)\sum_K d_K R_K^+ |0\rangle \tag{38}$$

which has the structure of multi-reference CI. The configurations $R_K^+|0\rangle$ represent the reference configurations and the operator $\exp\ (\sum_I C_I S_I^+)$ represents the excitations from these reference configurations. In the latter, we use the coefficients $\{C_I\}$ determined for the ground state, which is based on the transferability of electron correlations between the ground and excited states. The dimension of the SAC-CI method is the number of the reference configurations which are typically in the order of 10^3-10^5, not like limited to ~10. Therefore, in the SAC-CI method, there is almost no ambiguity in the choice of the ‘main reference’ configurations in contrast to the ordinary multireference CI method.

The SAC-CI method can be applied to various kinds of excited states by using appropriate excitation operators. It can be applied to excited states, ionized states, and electron attached states having spin multiplicities of singlet, doublet, triplet and up to septet. An important merit is that we can calculate these different electronics states in a *same accuracy*. We *can directly compare* the energies and the wave functions of different electronic states: a property quite important and useful in actual applications. *Thus using the SAC-CI method, we can study chemistry and physics involving the ground state and excited states of various spin multiplicities.*

2.3. Time Dependent Density Functional Theory

A DFT method that is strongly analogous to RPA is called time-dependent DFT (TDDFT). In this case, the Kohn-Sham (KS) orbital energies and various exchange integrals are used in place of matrix elements of the Hamiltonian. TDDFT is usually most successful for low-energy excitations, because the KS orbital energies for orbitals that are high up in the virtual manifold are typically quite poor. Casida, and Salahub (1998) have suggested that TDDFT results are most reliable if the following two criteria are met: (i) the excitation energy should be significantly smaller than the molecular ionization potential (note that excitations from occupied orbitals below the HOMO are allowed, so this is not a tautological condition) and (ii) promotion(s) should not take place into orbitals having positive KS eigenvalues.

Time-dependent density functional theory is widely used as a reliable method for the prediction of electronic excitation processes and other fast time-dependent phenomena involving the electronic response to an external perturbation. Density functional theory (DFT) accounts for the electron correlation of a system in the ground state by virtue of approximations to the exact but unknown exchange-correlation functional. Thus, TDDFT can also, in principle, incorporate a large fraction of the effects of electron correlation in an excited state within the framework of single-excitation theory. In practice, the accuracy of TDDFT employing the most widely available exchange-correlation functionals, which are approximations to the true functional, and so-called adiabatic approximation has been varied. For vertical excitation energies to low-lying valence excited states, TDDFT with these approximate functionals has proven quite accurate, significantly outperforming the Hartree-Fock based analogues, such as CIS and TDHF. However, for high lying excited states or Rydberg excite states, TDDFT underestimates the excitation energies by up to 1 eV or more.

Ground-state DFT is based on the papers by Hohenberg and Kohn, and by Kohn and Sham. The main results are that the density of system is identical to the density of an associated noninteracting particle system moving in a local potential v_s (r) defined by the Khon-Sham equations (atomic units are used throughout):

$$\left[-\frac{1}{2}\nabla^2 + v_s[\rho(r)]\right]\varphi_i(r) = \varepsilon_i\varphi_i(r) \tag{39}$$

Here the local potential $v_s[\rho](r)$ is the so-call Kohn-Sham potential, consisting of the external potential v_{ext} (the Coulomb field of the nuclei and external field if present), the Hatree potential v_H , which is trivially calculated from the density, and the *xc* potential v_{xc} which is the only unknown part:

$$v_s(r) = v_{ext}(r) + v_H(r) + v_{xc}(r) \tag{40}$$

The Kohn-Sham orbitals ϕ_i move in the effective field v_s which depends upon the electron density $\rho(r)$. This density is exactly obtained by summing the squares of the Kohn-Sham orbitals and multiplying by their occupation numbers n_i.

$$\rho(r) = \sum_i^{occ} n_i |\varphi_i(r)|^2 \tag{41}$$

As the KS potential $v_s(r)$ and the density $\rho(r)$ are inter-dependent, the equation have to be solved in a Self-Consistent Field (SCF) procedure, which means that one iteratively adapts the effective potential v_s and the density ρ until the difference in the energy between two subsequent cycles is sufficiently small. In the most straightforward fashion, this can be performed by mixing the density of the previous cycle with a small part of the density in the present cycle. This “simple damping” approach usually converges very slowly, and in practice the Direct Inversion in the Iterative Subspace (DIIS) procedure by Pulay and co-workers, is much to be preferred. In the DIIS approach, not only the result of previous cycle, but the results of all, or many, previous cycles are taken into account, in order to obtain the optimal guess for the next cycle. If one is close to self-consistency, this procedure converge the SCF equation above.

In order to solve the KS equations an approximation for the exchange-correlation (*xc*) potential $v_{xc}(r)$ is required and the simplest one is the LDA which is based upon the local density of the system. The GGAs go beyond this and take the local gradient of the density into account as well, allowing for a much improved accuracy in the results for energies and geometries. Many other approximations, for examples those based directly on the KS orbitals, are also available.

The usual ground state DFT sheme enables one to determine the density, and consequently the dipole moment, of a molecule with or without external electric fields. This affords the determination of the static polarizability and hyperpolarizability tensors α, β and γ by performing calculations in small electric fields of varying magnitudes and directions. In this so-call finite field (FF) approach, the tensor are then determined from finite difference techniques. The main advantage of this approach is that no programming work is needed. Any standard DFT code will allow the determination of static properties in this manner. However, for the determination of higher order tensors, such as γ, one need very well converged solution to the KS equations in order to make reliable predictions, which may be technically hard to achieve and which will certainly lead to considerable increase in CPU time consuming.

The most fundamental disadvantage of the FF approach, however, is that one has access to static properties only. The frequency-dependent polarizability and hyperpolarizabilty tensors are not accessible. Excitation energies and oscillator strengths can also not be obtained from the FF calculations. This is and important drawback of the FF approach, as it makes a direct comparison with experimental results are impossible. Especially for hyperpolarizabilities, it is known that there are substantial differences between the frequency-dependent and zero frequency results.

If one is interested in the time dependent properties mentioned above, a time dependent theory is required. In the DFT framework, this means that one has to start from the time dependent KS (TDKS) equations as derived by Runge and Gross;

$$\mathrm{i}\frac{\partial}{\partial \mathrm{t}}\varphi_\mathrm{i}(\mathrm{r},\mathrm{t}) = \left[-\frac{\nabla^2}{2} + \mathrm{v}_\mathrm{s}(\mathrm{r},\mathrm{t})\right]\varphi_\mathrm{i}(\mathrm{r},\mathrm{t}) \equiv \mathrm{F}_\mathrm{s}\varphi_\mathrm{i}(\mathrm{r},\mathrm{t}) \tag{42}$$

The time dependent KS potential $v_s(r,t)$ is subdivided in the same manner as its static counterpart:

$$\mathrm{v}_\mathrm{s}(\mathrm{r},\mathrm{t}) = \mathrm{v}_\mathrm{ext}(\mathrm{r},\mathrm{t}) + \mathrm{v}_\mathrm{H}(\mathrm{r},\mathrm{t}) + \mathrm{v}_\mathrm{xc}(\mathrm{r},\mathrm{t}) \tag{43}$$

the Hatree potential being explicitly given by:

$$\mathrm{v}_\mathrm{H}(\mathrm{r},\mathrm{t}) = \int \mathrm{dr}'\frac{\rho(\mathrm{r}',\mathrm{r})}{|\mathrm{r}-\mathrm{r}'|} \tag{44}$$

and the time dependent *xc* potential $v_{xc}[\rho](r,t)$ being an unknown functional of the time dependent density $\rho(r,t)$ now given by:

$$\rho(r,t) = \sum_i^{occ} n_i |\varphi_i(r,t)|^2 \tag{45}$$

If a certain approximation for the time dependent *xc* potential v_{xc} (r,t) has been chosen, the TDKS equations can be solved iteratively to yield the time dependent density of system, which may be exposed to an external time dependent electric field. If one is interested in the effects due to extremely large laser fields, the perturbative expansion of the dipole moment become meaningless, and the TDKS equations have to be solved non-peturbatively. This has until now been performed for atoms, by Ullrich and gross (Hirata *et al.*, 1999), and more recently also by others, and gives access to such effects as higher harmonic generation (HHG), which are not accessible in a perturbative approach. The drawback of this is that the calculations are very time consuming, forbidding the treatment of medium-sized molecules. If one restricts oneself to properties which are accessible through perturbative methods, as we will do here, a much more efficient approach is possible, allowing the treatment of large molecules (>100 atoms).

2.4 An Intermediate Neglect of Differential Overlap (INDO) Technique for Spectroscopy

The intermediate neglect of different overlap (INDO) is based on the simplest molecular orbital theory that properly accounts for the two-electron terms required in spectroscopy. INDO/s, where the one-center core integrals are obtained from ionized potentials only, rather than from ionization potentials and electron affinities, is used to calculate the ground-state configuration in terms of molecular orbital coefficients and eigenvalues.

In the molecular orbital model, using the unrestricted Hartree-Fock theory, we are interested in solving the Hartree-Fock equations

$$F^{\alpha}C^{\alpha} = C^{\alpha}E^{\alpha} \tag{46}$$

for an orthogonalized atomic basis set $\{\phi_{\mu}\}$, where E^{α} is the diagonal matrix of eigenvalues for the α spin molecular orbital, C^{α} is a square matrix the *i* th column of which is the molecular orbital coefficients of the *i* th molecular orbital ϕ_i^{α}

$$\phi_i^{\alpha} = \Sigma c^{\alpha}_{i\mu}\, \phi_{\mu} \tag{47}$$

F^{α} is the Fock or energy matrix

$$F^{\alpha} = H + J - K^{\alpha} \cong H + G^{\alpha} \tag{48}$$

and similar expressions are appropriate for β spin matrices and orbitals. In the above, H is the one-electron matrix, and $G^{\alpha} = J - K^{\alpha}$ is the two-electron matrix consisting of Coulomb terms minus exchange. The one-electron matrix H is specified by

$$H^{AA}{}_{\mu\mu} = U^{AA}{}_{\mu\mu} - \sum_{B\neq A} Z_B(\phi_\mu \left| R_B{}^{-1} \right| \phi_\mu) \tag{49}$$

$$U^{AA}{}_{\mu\mu} \cong (\phi_\mu \left| -\nabla^2/2 - Z_A/R_A \right| \phi_\mu) \tag{50}$$

$$H_{\mu\nu} = (\phi_\mu \left| -\nabla^2/2 - \sum_{A} Z_A/R_A \right| \phi_\mu) \tag{51}$$

Using the INDO model of Pople, Santry, and Segal we obtained

$$H^{AA}{}_{\mu\mu} = U^{AA}{}_{\mu\mu} - \sum_{B\neq A} Z_B\gamma_{AB} \tag{52}$$

$$H^{AA}{}_{\mu\nu} = 0 \tag{53}$$

$$H^{AB}{}_{\mu\nu} = (\beta^0{}_{A,\mu} + \beta^0{}_{A,\mu})\,\overline{\Delta}_{\mu\nu}/2 \tag{54}$$

$$\gamma_{AB} = \left\langle \overline{\phi}_\mu \overline{\phi}_\mu \middle| \overline{\phi}_\nu \overline{\phi}_\nu \right\rangle \cong \int d\tau(1)d\tau(2)\overline{\phi}_\mu(1)\overline{\phi}_\mu(1)r_{12}{}^{-1}\overline{\phi}_\upsilon(2)\overline{\phi}_\upsilon(2) \tag{55}$$

$\{\beta^0{}_{A,\mu}\}$ are atomic parameters, chosen empirically to give best agreement with experiment. The same parameter is used for either an s or p atomic orbital, $\beta^0{}_{A,s} = \beta^0{}_{A,p}$, but a different parameter is chosen for the d orbitals. $\overline{\Delta}_{\mu\nu}$ is a proportionality constant, usually the orbital overlap calculated treating ϕ_μ and ϕ_ν as Slater-type orbitals, or an integral simply related to the overlap. γ_{AB} is the two-electron Coulomb integral calculated treating ϕ_μ of atom A and ϕ_ν of atom B as if both were of s symmetry. Such an approximation is required by rotational invariance. Since the orbital exponents of s and p atomic orbitals are chosen the same for a given atom,

$\gamma^{AB}{}_{ss} = \gamma^{AB}{}_{sp} = \gamma^{AB}{}_{pp} = \gamma_{AB}$. However, the exponent of a d atomic orbital is not the same as an s and p.

In the unrestricted Hartree-Fock formalism that is used here, the G matrix elements are given by

$$G^{\alpha}{}_{\mu\nu} = \sum_{\sigma\lambda} P_{\sigma\lambda} \langle \mu\nu | \sigma\lambda \rangle - P^{\alpha}{}_{\sigma\lambda} \langle \mu\sigma | \nu\lambda \rangle \tag{56}$$

with a similar expression for the β electron G^{β} matrix. Here P^{α} is the first-order α spin density matrix or, in the orthogonalized set envisioned here, the α spin charge and bond order matrix

$$P^{\alpha}{}_{\mu\nu} = \sum_{a}^{MO} C^{\alpha}{}_{\mu a} C^{\alpha}{}_{\nu a} n_{a} \tag{57}$$

Where $n_a = 0$ or 1, the occupancy of $\phi^{\alpha}{}_{a}$, and P is the total first-order density

$$P = P^{\alpha} + P^{\beta} \tag{58}$$

Under this formalism, for a closed-shell system

$$P^{\alpha} = P^{\beta} = 1/2P \tag{59}$$

Invoking the INDO model simplifies eq. (55) greatly:

$$G^{\alpha}{}_{\mu\mu} = \sum_{\sigma\lambda}^{A} [P_{\sigma\pi} \langle \mu\mu | \sigma\lambda \rangle - P^{\alpha}{}_{\sigma\lambda} \langle \mu\sigma | \nu\lambda \rangle] + \sum_{\sigma \notin A} P_{\sigma\sigma} \gamma_{\sigma\mu} \; ; \; \mu \in A \tag{60}$$

$$G^{\alpha}{}_{\mu\nu} = \sum_{\sigma\lambda}^{A} [P_{\sigma\pi} \langle \mu\nu | \sigma\lambda \rangle - 1/2 P^{\alpha}{}_{\sigma\lambda} \langle \mu\sigma | \nu\lambda \rangle] \; ; \; \mu, \nu \in A \tag{61}$$

$$G^{\alpha}_{\mu\nu} = - P^{\alpha}_{\mu\nu}\, \gamma_{\overline{\mu\nu}} \;;\; \mu \in A,\, \nu \in B,\, A \neq B \qquad (62)$$

with similar expressions for G^{β}.

The two-electron two-center Coulomb integrals $\gamma_{\overline{\mu\nu}}$ are required for eq. (55) and for eq (62). For spectroscopy, however, a great deal of experience has been gained by using Coulomb integrals chosen semiempirically.

The two-electron Coulomb integrals are evaluated from a modified Mataga-Nishimoto formula

$$\gamma_{AB} = \frac{f_{\gamma}}{2f_{\gamma} / (\gamma_{AA} + \gamma_{BB}) + R_{AB}} \qquad (63)$$

where R_{AB} is the distance between the two centers in Bohr radii, γ_{AA} is obtained from

$$\gamma_{AA} = F^{0}(AA) = I_A - A_A \qquad (64)$$

as the difference between the ionization potential and electron affinity of an s, p or d electron. The formula is modified by the introduction of the parameter f_{γ} as suggested by Weiss, which we set equal to 1.2. This value has been extensively used and has proven very successful in the calculation of spectra of conjugated systems. Since values of $I_A - A_A$ are similar for s and p orbitals, we make the approximation that $\gamma_{\overline{AA}} = \gamma_{\overline{ss}} = \gamma_{\overline{sp}} = \gamma_{\overline{pp}} = F^{0}(AA)$ as before.

The INDO spectroscopic model has been parametrized by comparison of experimental spectra with calculated results obtained after extensive studies with singly excited configurations in a configuration interaction treatment. This basic model has been extended to include members of the first transition series (Zerner *et al.*, 1979), and has been applied to rather large systems in which the role of higher excited configurations (double excited, triple excited, etc., as opposed to higher *energy* configurations) is uncertain. Although use of semiempirical two-electron integrals (γ) and empirical resonance integrals (β) might be expected to include the effect of higher energy excitations in an average way, no such parametrization can be expected to compensate for multiple excited configurations if those configurations are actually in the spectroscopic region of interest, or if a given double excitation heavily mixes with the reference configuration in the mathematical description of the ground state. In these cases, certain higher excitations *must* be included explicitly. Preliminary investigations seem to indicate that higher excitation excitations can be included in the model without extensive reparamitrization. Nevertheless, some systems cannot be well described without these higher excitations, even with the given semiemprical parametrization. The frequency of these more difficult to handle systems is expected to increase with increasing molecular size, and the effect will be aggravated by the presence of a transition metal. The presence of two like transition metals in most complexes will require consideration of higher excitations in the description of both ground and excited states.

In addition to the model being grounded on singly excited configuration interaction, which is not a severe limitation in most cases, the model is founded on basis set of valence-type orbitals. Since Rydberg-type orbitals are not included in the atom basis, Rydberg-type states cannot be described. This is as severe a limitation on small molecules where the Rydberg states are among the lowest lying excited states as exclusion of higher excitations is for very large systems, where they are low lying. For most molecules Rydberg states might be expected to make their appearance 2-3 eV below the first ionization potential. In this region of the spectrum the density of states is quite high. The appearance of broad absorptions usually found within 2-3 eV of the first ionization potential for large systems may have as much to do with the presence of many electronic origins as it has to do with the vibrational broadening usually considered.

The Theory of Photophysic Processes

1. Photophysical Process

If a substance is irradiated with electromagnetic radiation, the energy of the incident photons may be transferred to the atoms or molecules raising them from the ground state to an excited state. This process, known as *absorption*, is accompanied by attenuation of the incident radiation at a particular frequency and can occur only when the energy difference between the two levels is exactly matched by the energy of the photons. The frequency of the radiation is given by

$$E_2 - E_1 = \Delta E = h\nu \qquad (1)$$

where E_1 and E_2 are the energies of the two levels and ΔE is the difference between them. The absorbed energy is rapidly lost to the surrounding by collisions allowing the system to revert or relax to the ground state. Sometimes the energy is not dissipated in this way but is re-emitted a few million seconds later-a process known as *fluorescence*.

A useful way of representing the energies of the electronic states of molecule is a **Jablonski diagram**, such as in Fig. A3. The vertical scale represents potential energy. The horizontal scale has no particular significance; it allows us to separate to singlet and triplet state **manifolds** (sets of energy levels) so that the excited states are more clearly distinguished. Superimposed on each electronic state is a set of vibrational energy levels. For the sake of clarity, a set of rotational energy levels superimposed on each vibrational level is not shown.

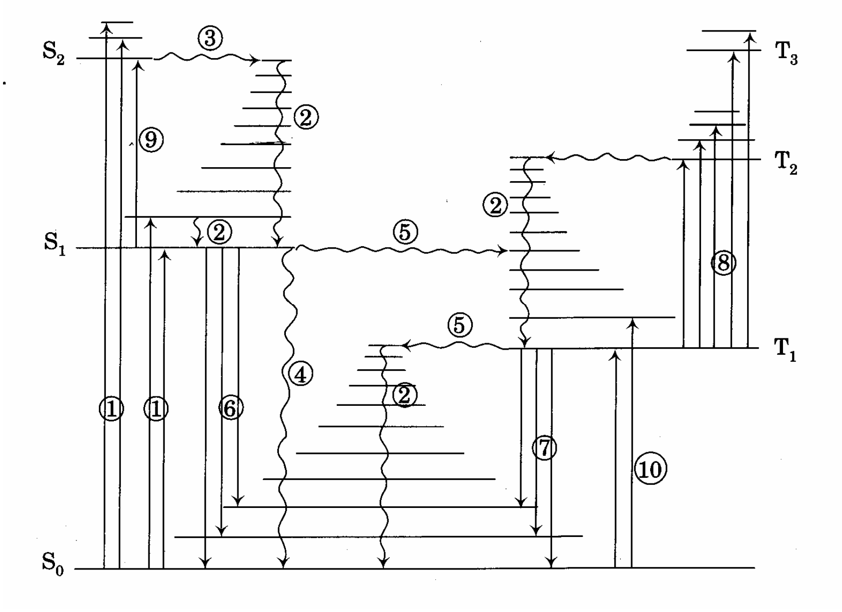

Appendix Figure A3 Generalized Jablonski diagram.

There are two kinds of photophysical processes indicated in Fig. A3. Those interconversions denoted by straight lines are **radiative processes,** which occur through the absorption or emission of light. Those indicated by wavy lines are **nonradiative processes,** which occur without light being absorbed or emitted. The numbers on the lines are keys to the following definitions:

1. **Absorption of Light**. A ground state molecule (S_0) may absorb a photon of light, thus becoming converted to an excited state. The most likely transitions are $S_0 \rightarrow S_1$ or $S_0 \rightarrow S_2$, although S_0 to higher excited singlet state transitions are also possible.

2. **Vibrational Relaxation.** The absorption from S_0 to S_n involves an energy change from the 0^{th} vibrational level of S_0 to any vibrational level of the excited state. However, the $v^{//} = 0$ is also the vibrational level is the level most populated at room temperature for the ground electronic state of molecule, and $v^{/} = 0$ is also the vibrational level of the excited electronic state that is most likely to be populated at equilibrium. Unless the molecule dissociates before equilibrium can be obtained, there

is a very rapid process (with a rate constant of about 10^{12} sec^{-1}) that relaxed the higher vibrational level of the excited state to its 0th vibrational level in condensed phases (i.e., solids or liquids).

3. Internal Conversion is a non radiative process that converts a higher electronic state into a lower state of the same multiplicity (a higher singlet state into a lower singlet state or a higher triplet state into a lower triplet state). The name arises because the process occurs internally, the line for internal conversion is a horizontal one. This means that the the 0th vibrational level of S_2 is converted into a vibrationally excited S_1 can then relax to its 0th vibrational level. The rate constants for internal conversion are fast ($> 10^{10}$ sec^{-1}), especially when the two states are close in energy.

4. Radiationless Decay is a process by which electronically excited states are returned to ground states (typically from S_1 to S_0) without the emission of light. Radiationless decay often has a slower rate constant (ca. $<10^6$ sec^{-1}) than other forms of internal conversion because the energy gap between S_1 and S_0 is usually greater than that between S_2 and S_1 or other pairs of excited states.

5. Intersystem Crossing, the conversion of a singlet state into a triplet state (or vice versa), requires a spin flip of an electron. The probability of intersystem crossing depends, among other things, on the energy gap between the singlet and triplet states, so values of k_{isc} vary from 10^6 to 10^{10} sec^{-1}. The T_n states is lower in energy than the corresponding S_n state because of the lower electron repulsion for unpaired electrons.

Processes 2-5 are nonradiative processes. The following are radiative processes.

6. Fluorescence is the emission of light from an excited state to a ground state with the same multiplicity. Usually the emission is $S_1 \rightarrow S_0$, and generalization to that effect is known as Kasha's rule. However, **anomalous fluorescence** ($S_2 \rightarrow S_0$) occurs in some compound, among them azulene, thiocarbonyl compounds, and some gaseous polyenes.

7. Phosphorescence is the emission of light from an excited state to a ground state with different multiplicity (usually from a triplet excited state to singlet ground state). This process involves both an electronic state change and a spin flip so, like $S_0 \rightarrow T_n$ absorption, phosphorescence is a spin-forbidden process.

8. Triplet-Triplet Absorption. A molecule in a triplet excited state may absorb a photon to give a higher triplet state, so a UV-Vis spectrum may be obtained, and the time-dependence of the excited state decay may be monitored. Flash spectroscopy is triplet-triplet absorption spectroscopy that can be an important technique for detecting triplet excited states.

9. Singlet-Singlet Absorption. Because triple states may persist longer than singlet states, the only excitation of excited states possible during much of the development of photochemistry was triplet-triplet absorption. With the advent of picosecond and femtosecond spectroscopy, it has become possible also to measure transitions from one excited singlet state to another, higher energy excited singlet state.

10. Singlet-Triplet Absorption, like phosphorescence, is a spin-forbidden process, so ordinarily $S_0 \rightarrow T_n$ transitions are not observed in UV-Vis spectroscopy. However, these transitions can be seen under certain conditions.

For ultraviolet and visible wavelengths, one should expect that the absorption spectrum of a molecule (i.e., a plot of its degree of absorption against the wavelength of the incident radiation) should show a few very sharp lines. Each line should occur at a wavelength where the energy of an incident photon exactly matches the energy required to excite an electronic transition as shown in Fig. A4.

In practice it is found that the ultraviolet and visible spectrum of most molecules consists of a few humps rather than sharp lines. These humps show that the molecule is absorbing radiation over a band of wavelengths. One reason for this band, rather than line absorption is that an electronic level transition is usually accompanied by a simultaneous change between the more numerous vibrational levels. Thus, a photon with a little too much or too little energy to be accepted by the molecule for a 'pure' electronic transition can be utilize for a transition between one of the vibrational levels associated with the lower electronic state to one of the vibrational levels of a higher electronic state.

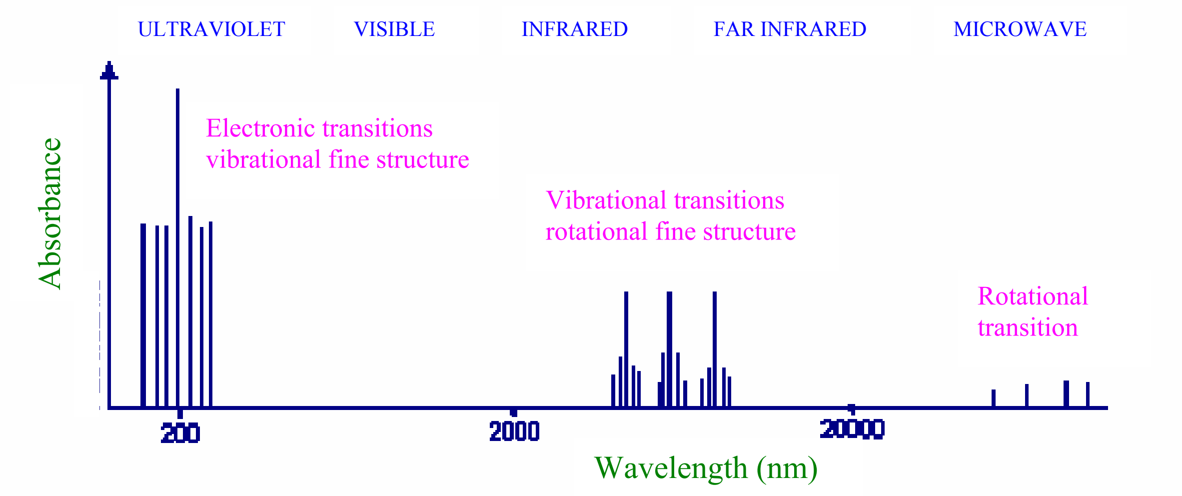

Appendix Figure A4 Idealized absorption spectrum.

If the difference in electronic energy is 'E' and the difference in vibrational energy is 'e', then photons with energies of E, E+e, E+2e, E-e, E-2e, etc. will be absorbed.

Furthermore, each of the many vibrational levels associated with the electronic states also has a large number of rotational levels associated with it. Thus a transition can consist of a large electronic component, a smaller vibrational element and an even smaller rotational change. The rotional contribution to the transition has the effect of filling in the gaps in the vibrational fine structure. In addition, when molecule are closely packed together as they normally are in solution, they exert influences on each other which slightly disturb the already numerous, and almost infinite energy levels and blur the sharp spectral lines into bands.

2. Fluorescence and Phosphorescence

For most organic molecules, fluorescence is the spontaneous emission of light from the $\nu^{/} = 0$ vibrational level of the first excited singlet state to some vibrational level ($\nu^{//} = 0, 1, 2, \ldots$) of the (singlet) ground electronic state. As indicated in the top portion of Fig. A5, the energy of the photon emitted in the $\nu^{/} = 0$ to $\nu^{//} = 0$ fluorescence is the same as the energy of the photon absorbed in the $\nu^{//} = 0$ to $\nu^{/} = 0$ transition if the geometry of the photoexcited molecule is nearly the same as that of the ground state molecule. However, all other fluorescence lines are at longer wavelengths (lower energy). Thus, the fluorescence and emission spectra should overlap at the 0,0 transition, providing confirmation of the 0,0 energy of the electronically excited state. In molecules such as anthracene, the σ bonding provides a molecular framework for the planar π system, and the π bonding results from population of many bonding MOs. Therefore promotion of one electron to an antibonding MO may not seriously distort the molecular geometry. In such cases there can be a nearly mirror image relationship between the absorption and fluorescence spectra of organic molecules, particularly when the spectra are plotted as intensity versus energy (cm^{-1}) instead of wavelength. The similarity arises because the factors that make some $\nu^{//} = 0$ to $\nu^{/} = x$ transitions more probable than others also make some $\nu^{/} = 0$ to $\nu^{//} = x$ emissions more probable.

For some molecules, however, the geometry of the ground and excited states may be very different. As a result, there may be a large difference between λ_{max} for absorption and λ_{max} for emission, and the 0,0 transition may be weak or not present.

A similar relationship between geometry and a mirror image appearance of singlet-triplet absorption and phosphorescence is expected, but this is often difficult to determine experimentally, In fluid solution phosphorescence is usually reduced by diffusion-limited bimolecular interaction of the excited triplet compound and one or more ground state species. However, phosphorescence can often be observed by irradiating the compound in environments in which diffusion is quite slow, such as in an organic glass at liquid nitrogen temperature.

Singlet-triplet absorption is ordinary difficult to detect because the transition is spin-forbidden. Heavy atom solvents or oxygen perturabation have been used to induce singlet-triplet absorption, but absorptions observed in this manner are weak, and it is important to establish that the observed absorption is not due to artifacts resulting from the solvent or additive.

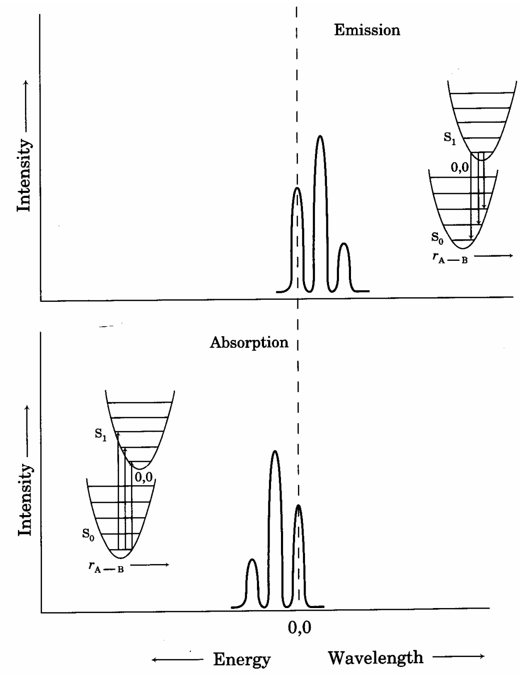

Appendix Figure A5 Schematic representations of the origins of UV-Vis absorption (bottom) and fluorescence (top) spectra.

3. Franck-Condon principle

The different electronic states of a molecule are often associated with different shapes of molecule because the different electron distribution around the molecule changes the electrostatic Coulombic forces that maintain the nuclei in specific relative positions. Since nuclei are considerably more massive than electrons, the **Franck-Condon principle** states that:

an electronic transition takes place sufficiently rapidly that the nuclei do not change their internuclear positions during the transition.

Consequently, when energy is absorbed in an electronic transition, the nuclei suddenly find themselves in a new force field and at positions which are not in equilibrium for the new electronic state. This is shown schematically in Fig. A6, in which an electronic absorption from the ground state appears as a vertical line because of the Franck-Condon principle. The internuclear separation of the ground state becomes a **turning point,** the extent of maximum displacement, in a vibration of the excited state.

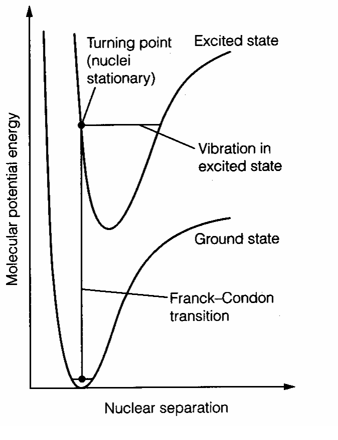

Appendix Figure A6 Illustration of the Franck-Condon principle for vertical electronic transitions.

The vertical transition has the greatest **transition probability** but transitions to nearby **vibrational levels** also occur with lower intensity. Therefore, instead of an electronic absorption occurring at a single, sharp line, electronic absorption consists of many lines each corresponding to the stimulation of different vibrations in the upper state. This vibrational structure (or progression) of an electronic transition can be solved for small molecules in the gas-phase, but in a liquid or solid **collision broadening** of the transitions cause the lines to merge together and the electronic absorption spectrum is often a broad band with limited structure (Fig. A7). The Franck-Condon principle also applies to downward transitions and accounts for the vibrational structure of a **fluorescence** spectrum.

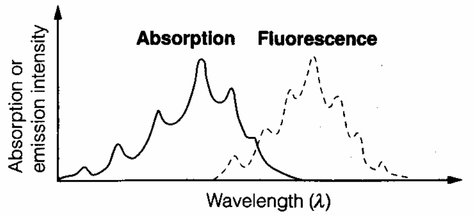

Appendix Figure 7 Relationship between the broad electronic absorption and fluorescence bands of liquids and solids.

APPENDIX B

Oral Presentation and Poster Contributions to Conferences

Oral Presentation

Poolmee, P. and S. Hannongbua. **Structural and Electronic Properties of Fluorene-Thiophene Copolymer.** 8th Annual National Symposium on Computational Science and Engineering, Suranaree University of Technology, Nakhon Ratchasima, Thailand, July 21-23, 2004.

Structural and Electronic Properties of Fluorene-Thiophene Copolymer

Potjaman Poolmee and Supa Hannongbua

Department of Chemistry, Kasetsart University, Bangkok 10900, Thailand.
E-mail : faaspmp@ku.ac.th

Abstract

Nowadays, conductive polymers are widely used in many applications, in particular, light emitting diode. Fluorene-thiophene copolymer is one of a conductive polymers which are prepared, aiming at achieving color tunability over the visible spectrum. Furthermore, the objective is tuning of the frontier levels energetic position in order to minimize the anodic and cathodic injection barriers of the light emitting diode structures. In this work, potential energy surface and energy gap of fluorene-thiophene copolymer (as shown in Figure 1) are studied.

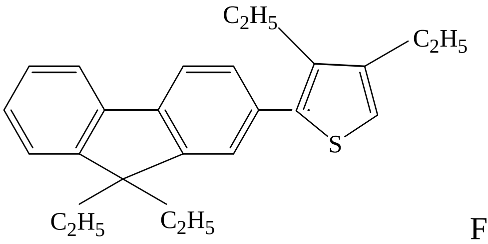

Figure 1. Fluorene-Thiophene Coplymer

Potential energy surface was investigated at the HF/ 6-31G* and B3LYP/6-31G* level of calculations. Conformational analysis was done by changing the torsional angle θ by 15° steps between θ = 0° and θ = 180°. To obtain the final torsional angles of the conformers in each minima, calculations of these geometries were performed without constraint on the dihedral angle. It is found that this molecule shows two minima located at 66° and 118° at the HF/6-31G* level of calculations. In the case of B3LYP/6-31G*, it also shows two minima located at 56° and 134°. A very low rotational energy barrier at 90° is observed which allows a wide range of non-planar conformations for this molecule.

Energy gaps of fluorene-thiophene copolymer were calculated at B3LYP/6-31G* level and ZINDO calculations of the excitation energies performed at the optimized geometries of the ground states using semi-empirical (AM1) and HF/6-31G* level of calculations. Energy gaps of polymers were obtained by plotting the energy of monomer through pentamers against reciprocal chain lengths and extrapolating to infinite chain length. It is found that energy gaps calculated from B3LYP/6-31G*//HF/6-31G* and B3LYP/6-31G*//AM1 are 4.15 eV and 3.66 eV, respectively. Meanwhile energy gaps calculated from ZINDO//HF/6-31G* and ZINDO//AM1 are 3.52 eV and 3.12 eV, respectively. By comparing these calculated results with a experiment data (2.76, optical energy gap), it shows that these calculated results are not good agreement with experimental data. Therefore, TDDFT have to be employed in this system studied.

Poster Presentations

Poolmee, P., S. Suramitr, K. Sriwichitkamol and S. Hannongbua. **Conformational Analysis and Electronic Property of Fluorene-Thiophene Copolymer.** 29th Congress on Science and Technology of Thailand (STT 2003), Khon Kaen University, Khon Kaen, Thailand, October 20-22, 2003.

การศึกษาโครงสร้างคอนฟอร์เมชันและหาค่าทางทฤษฎีของสมบัติอิเล็กโทรนิกส์ของฟลูโอลีน-ไทโอฟีน

พจมาลย์ พูลมี ทรงวุฒิ สุรมิตร เกรียงศักดิ์ ศรีวิตรกลม และสุภา หารหนองบัว
ภาควิชาเคมี คณะวิทยาศาสตร์ มหาวิทยาลัยเกษตรศาสตร์ กรุงเทพ 10900 ประเทศไทย

บทคัดย่อ ได้ศึกษาโครงสร้างคอนฟอร์เมชันและสมบัติอิเล็กโทรนิกส์ของ Poly [2,7-(9,9-dihexylfluorene)-co-alt-decylthiophene] โดยใช้ระเบียบวิธี HF/6-31G* และ B3LYP/6-31G*[redacted]าแถบพลังงานของพอลิเมอร์นี้สามารถทำนายได้โดยการประมาณค่าพลังงานที่ได้จากส่วนกลับของจำนวน monomer ถึง trimers และประมาณค่าไปสู่พอลิเมอร์ ค่าแถบพลังงาน (energy gap) ที่ได้จากการปรับโครงสร้างที่เสถียรที่สุดโดย HF/6-31G* และ B3LYP/6-31G*//HF6-31G* ของพอลิเมอร์นี้มีค่าเท่ากับ 8.2 eV และ 3.6 eV ตามลำดับ

บทนำ ในปัจจุบันคอนจูเกตพอลิเมอร์มีความสำคัญเนื่องจากถูกนำมาใช้ใน light emitting diode หรือ flat control panel display แทนสารจำพวกอนินทรีย์ เหตุผลที่สำคัญอย่างหนึ่งคือโครงสร้างของพอลิเมอร์นั้นสามารถถูกปรับเปลี่ยนให้มีสมบัติตามที่ต้องการได้ง่าย พอลิฟลูโอลีนและอนุพันธ์เป็นคอนจูเกตพอลิเมอร์ที่มีการศึกษาวิจัยอย่างกว้างขวางเนื่องจากมีประสิทธิภาพในการเปล่งแสงสีฟ้า ซึ่งเป็นสีที่มีความสำคัญนอกจาก สีแดงและสีเขียว ดังนั้นโครงการนี้จึงสนใจที่จะศึกษาโครงสร้างและสมบัติทางอิเล็กโทรนิกส์ของโคพอลิเมอร์ระหว่างฟลูโอลีน-ไทโอฟีน เพื่อเป็นแนวทางที่จะออกแบบคอนจูเกตพอลิเมอร์ตัวอื่นๆ ให้มีสมบัติทางอิเล็กโทรนิกส์ที่ดีขึ้นและเปล่งแสงสีต่าง ๆ ตามที่ต้องการ

วิธีการคำนวณ

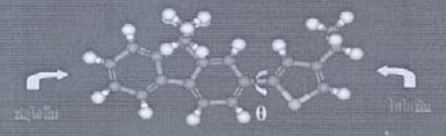

Fluorene-co-alt-ethylthiophene (P1)

รูปที่ 1 โครงสร้างทางเคมีของ **Fluorene-co-alt-ethylthiophene (P1)** ที่ใช้ในการศึกษา

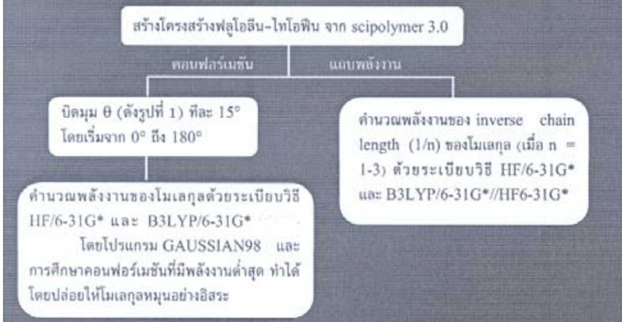
สร้างโครงสร้างฟลูโอลีน-ไทโอฟีน จาก scipolymer 3.0

คอนฟอร์เมชัน

แถบพลังงาน

บิดมุม θ (ดังรูปที่ 1) ทีละ 15° โดยเริ่มจาก 0° ถึง 180°

คำนวณพลังงานของโมเลกุลด้วยระเบียบวิธี HF/6-31G* และ B3LYP/6-31G* โดยโปรแกรม GAUSSIAN98 และการศึกษาคอนฟอร์เมชันที่มีพลังงานต่ำสุด ทำได้โดยปล่อยให้โมเลกุลหมุนอย่างอิสระ

คำนวณพลังงานของ inverse chain length (1/n) ของโมเลกุล (เมื่อ n = 1-3) ด้วยระเบียบวิธี HF/6-31G* และ B3LYP/6-31G*//HF6-31G*

ผลการทดลองและวิจารณ์ผลการทดลอง

การศึกษาโครงสร้างคอนฟอร์เมชัน

การศึกษาโครงสร้างคอนฟอร์เมชันของ P1 โดยการปรับโครงสร้างให้เสถียรที่สุดด้วยระเบียบวิธี HF/6-31G* และ B3LYP/6-31G*[redacted]ว่า P1 มีโครงสร้างที่มีพลังงานต่ำสุด 2 ตำแหน่ง แสดงดังรูปที่ 2 และพบว่าทั้ง 2 ระเบียบวิธีนี้ให้โครงสร้างของโมเลกุลที่วงของฟลูโอลีนจัดวางตัวไม่อยู่ในระนาบเดียวกับวงไทโอฟีน โดย B3LYP/6-31G*[redacted]ห้โครงสร้างของโมเลกุลมีความเป็นระนาบมากกว่าโครงสร้างที่ได้จากระเบียบวิธี HF/6-31G*

ค่าแถบพลังงาน (energy gap)

ค่าแถบพลังงานที่ได้จากกราฟแสดงค่าพลังงานของส่วนกลับของโมเลกุลโดยใช้ระเบียบวิธี HF/6-31G* และ B3LYP/6-31G*//HF/6-31G* มีค่า 8.62 eV และ 3.60 eV ตามลำดับ แสดงดังรูปที่ 3 (ค่าที่ได้จากการทดลองเท่ากับ 2.50 eV, เอกสารอ้างอิง 1) ซึ่งพบว่าค่าที่ได้จากทั้ง 2 วิธีนี้ยังให้ค่าที่แตกต่างจากการทดลอง ซึ่งจะต้องศึกษาต่อไปโดยเพิ่มจำนวนของโมเลกุลหรือใช้ระเบียบวิธีที่สูงขึ้น

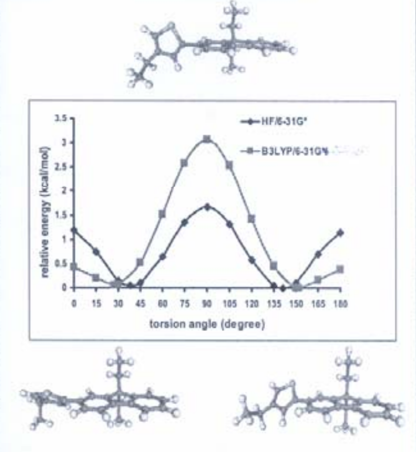

รูปที่ 2 พลังงานศักย์ของ P1 เมื่อปรับมุม θ และคำนวณด้วย HF/6-31G* และ B3LYP/6-31G*//HF/6-31G*

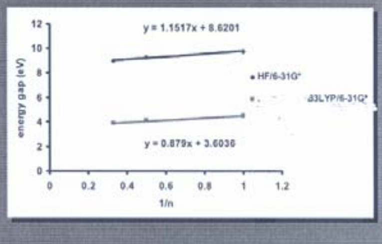

รูปที่ 3 กราฟแสดงค่าพลังงานของส่วนกลับจำนวนโมเลกุลเมื่อ n=1-3

สรุปผลการทดลอง

จากการทดลองโดยใช้ระเบียบวิธี HF/6-31G* และ B3LYP/6-31G*//HF/6-31G* พบว่าทั้งสองวิธีให้โคร้างสร้างที่มีพลังงานต่ำสุด 2 ตำแหน่งที่สอดคล้องกัน และสามารถทำนายค่าแถบพลังงานของ P1 ได้ แต่ยังมีความแตกต่างจากค่าจากการทดลอง

เอกสารอ้างอิง

1. B. Liu., et al. (2000), *Macromolecules*, 33, 8945.
2. P. Blondin., et al. (2000), *Macromolecules*, 33, 5874.

กิตติกรรมประกาศ

งานวิจัยนี้ได้รับการสนับสนุนจาก :

โครงการพัฒนาบัณฑิตศึกษาและวิจัยทางด้านปิโตรเลียมและเทคโนโลยีปิโตรเคมี (ADB-MUA)

Poolmee, P. and S. Hannongbua. **Theoretical Investigation on Electronic Property of Fluorene-Thiophene.** 1st Asia Pacific Conference on Theoretical & Computational Chemistry, Institute of Molecular Science, Okazaki, Japan, May 12-15, 2004

Calculations of Electronic Property of Fluorene-Thiophene Copolymer

P. Poolmee and S. Hannongbua

Laboratory for Computational and Applied Chemistry, Chemistry Department, Kasetsart University,
Bangkok 10900, Thailand : email : faaspmp@ku.ac.th

Introduction

Conjugated polymers are widely used in many applications such as light-emitting diode. One of the characteristics is their structure can be easily modified to provide the appropriate properties. Fluorene-based copolymers have been studied, aiming at achieving color tunability over the visible spectrum and tuning of the frontier levels energetic position in order to minimize the anodic and cathodic injection barrier of the light-emitting diode structures. Therefore, energy gap is one of the important properties. The objective of this study is to calculate the energy gap of the fluorene-thiophene copolymer. Obviously, a theoretical investigation on the energy gaps of the polymer is very useful in guiding the experimental synthesis.

Model

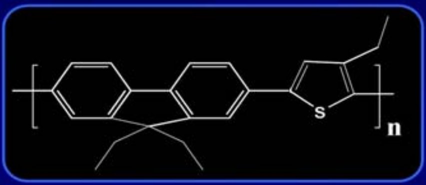

Fluorene-Thiophene Copolymer

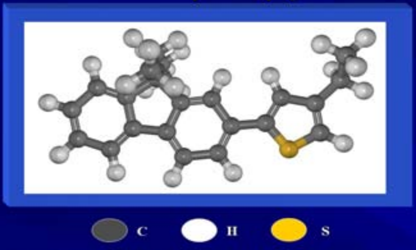

Computational Details

Construct the structure from Scipolymer 3.0

ground state geometries of oligomer (monomer to pentamer) are fully optimized by AM1, HF/3-21G*, HF/6-31G* by Guassian03

B3LYP/6-31G*, ZINDO, and TDDFT(B3LYP/6-31G*) were performed at the optimized geometries.

HOMO-LUMO energy gaps and excitation energies are calculated and plotted with the inverse chain length of the monomer then extrapolated to infinite chain length

Results and Discussion

The calculated energy gaps of fluorene-thiophene copolymer are shown in Table 1.

Table 1. Energy gaps obtained from various methods

method	energy gap (eV)
AM1	6.88
HF/3-21G*	8.78
HF/6-31G*	8.58
B3LYP/6-31G*//AM1	3.10
B3LYP/6-31G*//HF/3-21G*	3.58
B3LYP/6-31G*//HF/6-31G*	3.58
ZINDO//AM1	2.76
ZINDO//HF/3-21G*	3.28
ZINDO//HF/6-31G*	3.23
TDDFT(B3LYP/6-31G*)//AM1	2.53
TDDFT(B3LYP/6-31G*)//HF/3-21G*	3.85
TDDFT(B3LYP/6-31G*)//HF/6-31G*	3.10

the experimental energy gap obtained from the onset of UV is 2.50 eV [Ref. 1.]

The HOMO-LUMO energy gaps obtained from AM1, HF/3-21G*, and HF/6-31G* are far from the experimental energy gap. The orbital energy difference between HOMO and LUMO is still and approximate to the transition energy since the transition energy also contains significant contributions from some two-electron integrals. The real situation is that an accurate description of the lowest singlet excited state requires a linear combination of a number of excited configurations. Therefore, it was found that TDDFT(B3LYP/6-31G*)//AM1 provided the better energy gap. Then it indicated that the geometry from AM1 can be used to predict the energy gap of this polymer. Consequently, the bond length and dihedral angle between fluorene and thiophene unit (in monomer) from AM1 are 1.44 Å and 28 degrees, respectively. Whereas the results obtained from HF/3-21G* are 1.48 Å and 42 degrees, and from HF/6-31G* are 1.48 Å and 38 degrees. In addition, based on our study, a long wavelength transition with higher oscillator strength (>0.7) was obtained.

Conclusions

The energy gaps extrapolated by TDDFT can be compared with the experimental data. The obtained results indicated that TDDFT with B3LYP functional is expected to be a relatively reliable tool for evaluating the excitation energies of low-lying excited states.

Actknowledgements

Postgraduate on Education and Research in Petroleum and Petrochemical Technology (MUA-ADB) for research facilities and The Commission on Higher Education for supporting grant.

Reference :

1. Liu, B.; Yu, W –L.; Lai, Y –H.; Huang, W.; *Macromolecules* 2000, 33, 8945.

Poolmee, P., M. Ehara, S. Hannongbua and H. Nakatsuji. **SAC-CI Investigation on Electronic Structure of Fluorene-Thiophene Oligomer**. 2nd Asia Pacific Conference on Theoretical & Computational Chemistry, Chulalongkorn University, Thailand, May 2-5, 2005.

SAC-CI Theoretical Investigation on Electronic Structure of Fluorene-Thiophene Oligomers

Potjaman Poolmee [a], Masahiro Ehara [b], Supa Hannongbua [a] and Hiroshi Nakatsuji [b,c]
[a]Department of Chemistry, Faculty of Science, Kasetsart University, Bangkok 10900, Thailand
[b]Department of Synthetic Chemistry and Biological Chemistry, Graduate School of Engineering, Kyoto University, Kyoto-Diagaku-Katsura, Nishikyo-ku, Kyoto 615-8510, Japan
[c]Fukui Institute for Fundamental Chemistry, Kyoto University, 34-4 Takano-Nishihiraki-cho, Sakyo-ku, Kyoto 606-8103, Japan

INTRODUCTION: The SAC (symmetry adapted cluster)/SAC-CI (configuration interaction) method has been established as a reliable and useful method for investigating a wide variety of molecular spectroscopy through many successful applications [1-2]. Recently, the SAC-CI method is emerging in the Gaussian03 to be useful method for studying molecular excited states. The purposes of this work are to investigate the electronic excited-state and optical properties of 2-(fluoren-2-yl)thiophene (FT) and 2-(fluoren-2-yl)-3-methylthiophene (FMT) which are the model unit compounds of the light-emitting diodes by using SAC-CI calculations. In my previous work, the energetic properties of fluorene-thiophene copolymer were also investigated by TDDFT (B3LYP) with 6-31G*) [3].

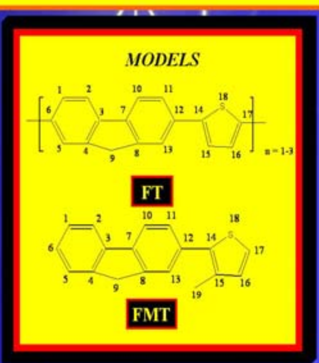

METHOD: The ground-state potential energy curves of FT and FMT monomers along the torsion angle (13-12-14-15) were calculated by using B3LYP/6-31G*. In the calculations, the torsional angle was changed by 15° degrees, whereas all the other geometrical parameters were fixed. The SAC-CI SD-R calculations were performed for the excited spectra of FT and FMT at each torsional angle. Double zeta basis set of Huzinaga-Dunning [4s2p/2s] were adopted. For monomer, the resultant SAC-CI active space consists of 43 occupied and 125 unoccupied MOs. For dimer and trimer, the active space is 129 occupied and 247 unoccupied MOs and 193 occupied and 256 unoccupied MOs, respectively.

RESULTS AND DISCUSSION

From Fig. 1 the energy barrier along the torsional angle is very small for both FT and FMT providing conformers of wide range of torsional angles can exist at room temperature. Moreover, it was found that the excitation character of the excited states of FT depend on the torsional angle as shown in Fig. 2. For instance, the S_1 state of FT at torsional angle of 0° is characterized as the excitation from HOMO to LUMO, while the S_1 state at 90° is from HOMO to LUMO+1. According to the ground-state potential energy surface is flat along the torsional angle, therefore, in order to simulate the absorption spectra, the Boltzmann distribution of the conformers should be considered. The calculated absorption spectra of FT and FMT in which Boltzmann distribution was taken into account are shown in Fig. 3. In addition, the oscillator strength of S_1 state of the dimer and trimer was very high (in Fig. 4) and the red shift occurs due to the π-conjugation. It indicates that the energy separations between the S_1 state and the other excited states are wider than that of monomer.

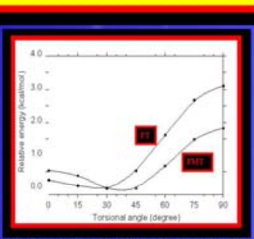

Fig. 1 Ground-state potential energy curves of FT and FMT monomers

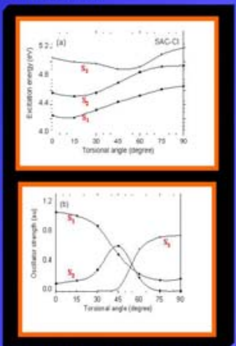

Fig. 2 The SAC-CI (a) excitation energies (b) oscillator strength of FT versus torsional angle.

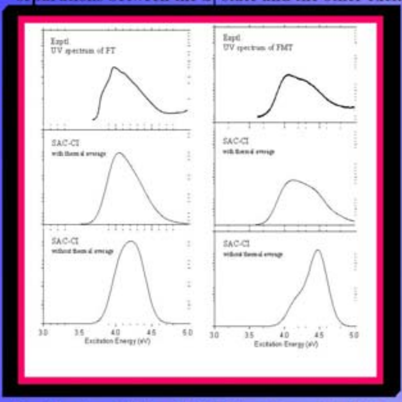

Fig. 3 Experimental [4] and SAC-CI absorption spectra of FT and FMT. Theoretical spectra with and without thermal average are shown.

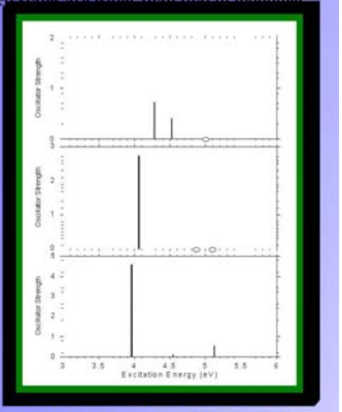

Fig. 4 The calculated absorption spectra of FT; monomer, dimer, and trimer

CONCLUSION: FT and FMT monomers are most stable in the non-planar structures in their ground states. It also allows a wide range of non-planar structure. It was found that the excitation energy of the HOMO-LUMO transition along the torsional angle changes caused the interchange of the character between the S_1 and S_3 excited states. The absorption spectra of FT and FMT in which Boltzmann distributions are taken into account are in common agreement with the experiment spectra. For dimer and trimer, only the S_1 state contributed to the absorption spectra with a large oscillator strength, the other two states have very small oscillator strength.

REFERENCES

1. Wan J., Hada M., Ehara M., Nakatsuji H., *J. Chem. Phys.* 2001; 114 : 842.

2. Wan J., Nakatsuji H., *Chem. Phys.* 2004; 302 : 125.

3. Poolmee P., Hannongbua S., *J. Theo. Comp. Chem.* 2004; 3: 481.

4. Belletete M., Bedard M., Leclerc M., Durocher G., *J. Mol. Struct. (THEOCHEM)* 2000; 104 : 9118.

ACKNOWLEDGEMENTS: This study was supported by a Grant for Creative Scientific Research from the Ministry of Education, Science, Culture, and Sports of Japan. The Postgraduate on education and research in Petroleum and Petrochemical Technology.

Poolmee, P., S. Suramitr, R. Chidthong and S. Hannongbua. **Theoretical Investigation on Blue-light Emitting Conducting Polymer.** 11th Asia Chemical Congress, Korea University, Seoul, Korea, August 24-26, 2005.

Kasetsart University

Theoretical Investigation on Electronic Property of Blue-Light Emitting Conducting Polymers

Potjaman Poolmee, Songwut Suramitr, Rungtiwa Chidthong and Supa Hannongbua
Department of Chemistry, Faculty of Science, Kasetsart University, Bangkok 10900, Thailand

Introduction

Intensive research has been dedicated to explore novel conjugated polymer with narrow energy gap (Eg). There are widely theoretical studies on investigation of the energy gaps. Obviously, a theoretical investigation on the energy gaps of these polymers is very useful in guiding the experimental synthesis. Polydialkylfluorene derivatives (PFs) are one of the most widely investigated PLEDs due to their high efficient blue emission in both photoluminescence (PL) and electroluminescence (EL). However, one of the drawbacks of PFs is that there is a high energy barrier for the hole injection from the anode which limits their application in PLEDs. The main feature of this work is extrapolating the resultant linear relationship to infinite chain length to obtain the energy gap (Eg) and the ionization potential (IP) of polyfluorene derivatives, as shown in Fig. 1.

Polyfluorene (P1)

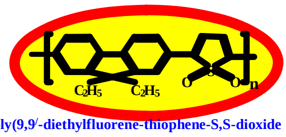

Poly(9,9′-diethylfluorene-thiophene-S,S-dioxide (P2)

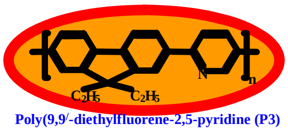

Poly(9,9′-diethylfluorene-2,5-pyridine (P3)

Fig. 1. Molecular structures studied.

Methods of Calculation

The energy gap (Eg) and vertical ionization potential (IP) of polymer were obtained by employing the oligomer extrapolation technique, which has been successfully employed in investigating several series of polymer [1,2]. HOMO-LUMO differences of P1 and P2 were calculated by using density functional theory at B3LYP/6-31G* level. Time-dependent density functional theory (TDDFT) at B3LYP/6-31G* level was performed to calculate excitation energy of P3 at the optimized ground state geometries by using density functional theory at B3LYP/6-31G* level. IP was calculated by using density functional theory at B3LYP/6-31G* level based on the ground state geometry which calculated at B3LYP/6-31G* level. Then IP can be obtained from the difference of the total energy between cation and neutral molecules.

Results and Discussion

1. Ground-State Structural Geometries : The optimized geometries of P1, P2 and P3 calculated by using B3LYP/6-31G* level are presented in Fig. 2. The results of the optimized structures for the oligomeric molecules (n = 1-5) of P1, P2 and P3 showed that the inter-ring distance and inter-ring torsional angles do not variation with the oligomer size. This suggests that they can describe the basic structures of polymer as their oligomers. The optimized torsional angles (represented in the circles shown in Fig. 2) and bond distances are summarized in Table 1.

Table 1. Inter-ring torsional angle (θ, deg)[a] and inter-ring distance (L, Å)[b] of P1, P2 and P3 obtained by using B3LYP/6-31G* level of calculations.

P1	θ	L	P2	θ	L	P3	θ	L
n=1	-	-		22.1	1.46		18.6	1.48
n=2	37.4	1.48		21.3	1.46		13.7[c], 37.6[d]	1.48
n=3	37.3	1.48		22.1	1.46		17.8, 36.3	1.48
n=4	37.3	1.48		21.3	1.46		16.5, 36.5	1.48
n=5	37.2	1.48		22.0	1.46		15.3, 36.1	1.48

[a,b] averaged value

[c] torsional angle composed of atom in the red circle (moderate hydrogen bond occurred in this side)

[d] torsional angle composed of atom in the yellow circle

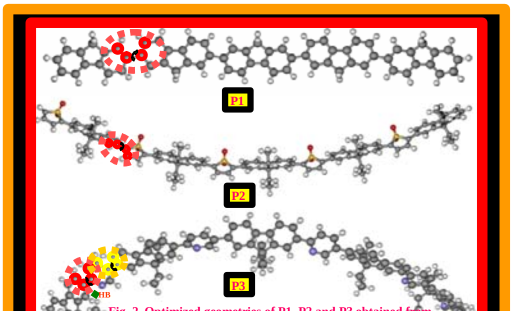

Fig. 2. Optimized geometries of P1, P2 and P3 obtained from B3LYP/6-31G* level of calculations.

2. HOMO-LUMO Gaps and Lowest Excitation Energies :

In these calculations, HOMO-LUMO gaps of P1 and P2 were obtained from density functional theory and shown in Fig. 3. It was found that HOMO-LUMO gaps of P1 and P2 are 3.26 eV and 2.20 eV respectively which are consistent with experiment (3.20 eV [3] and 2.19 eV [4] respectively). However, it was found that the orbital energy difference between HOMO-LUMO is still an approximate estimate to the transition energy because the transition energy contributions from some two-electron integrals. Therefore, in the case of P3, the lowest excitation energy which showed the high oscillator strength will be presented the energy gap as also shown in Fig. 3. The energy gap of P3 is 2.71 eV which is good agreement with the experiment (2.87 eV [5]).

3. Ionization potentials (IPs)

Fig. 4. showed IP of P2 and P3 which are polyfluorene derivatives. The calculated IP of P2 and P3 are 5.63 and 5.70 eV respectively. It was found that the calculated IP of P2 showed the excellent agreement with experimental data (5.62 eV) [6]. In the case of P3 there is not experimental data for comparing. However, it was found that these calculated IP are lower than that of PF which is reported to be 5.87 eV [7]. Therefore, it is clear from these results that the thienyl-S,S-oxide and pyridine units allow the modulation of the IP and make them decrease and thus result in the reduction of the energy barrier to create holes.

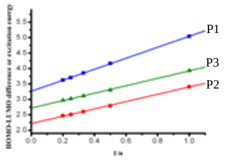

Fig. 3. Energy gaps extrapolated from the plot of HOMO-LUMO difference (P1 and P2) and excitation energy (P3) of oligomers versus the inverse number of monomer units.

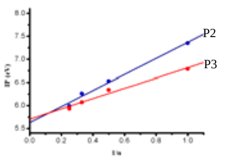

Fig. 4. Ionization potential of P2 and P3 versus the inverse number of monomer units.

Conclusion

The extrapolation results of Eg and IP of oligomers are good agreement with the experimental data. In addition, polyfluorene derivatives (P2 and P3) give a lower energy gap as compared with polyfluorene (P1). Furthermore, polyfluorene derivatives can enhance the injection hole.

References

1. Suramitr S., Kerdcharoen T., Srihiirin T., Hannongbua S., *Synth Met* 2005, in press.
2. Poolmee P., Hannongbua S., *J Theor Comp Chem* 2004, 3, 481.
3. Klaerner G., Miller, R. D., *Macromolecules* 1998, 31, 2007.
4. Charas A., Morgado J., Martinho G.M.J., Alcacer L., Cacialli F., *Synth Met* 2002, 127, 251.
5. Aubert P.H., Knipper M., Groenendaal L., Manca J., Vanderzande D., *Macromolecules* 2004, 37, 4098.
6. Charas A., Barbagallo N., Morgado J., Alcacer L., *Synth Met* 2001, 122, 23.
7. Wang J. F., Feng J. K., Ren A. M., Liu X. D., Ma Y. G., Lu P., Zhang H. X., *Macromolecules* 2004, 37, 3451.

Acknowledgements

We thank the Postgraduate Education and Research on Petroleum and Petrochemical Technology (MUA-ADB), and the Center of Nanotechnology, Kasetsart University Research and Development Institute (KURDI) for financial support and LCAC and computing center of KU are grateful for computing facilities.

APPENDIX C

Publications

Publication I

Theoretical Investigation on Energy Gap of Fluorene-Thiophene Copolymer.

Poolmee, P. and Hannongbua, S.

Journal of Theoretical and Computational Chemistry
Vol. 3, No. 4 (2004) 481–489
© World Scientific Publishing Company

THEORETICAL INVESTIGATION ON ENERGY GAP OF FLUORENE-THIOPHENE COPOLYMER

P. POOLMEE and S. HANNONGBUA
Department of Chemistry, Faculty of Science, Kasetsart University
Bangkok, Thailand, 10900

Received 6 July 2004
Accepted 9 September 2004

In this work, HOMO-LUMO energy gap and the lowest excitation energy of poly [2,7-(9,9-dihexylfluorene)-*co*-alt-2,5-(decylthiophene) were performed by different methods. The obtained results indicate that TDDFT(B3LYP/6-31G*)//B3LYP/6-31G* calculations can be useful to provide reliable energetic and structural results of this polymer. The HOMO-LUMO predictions were not accurately obtained as compared to the experimental results. The inverse chain length approximation by using TDDFT(B3LYP/6-31G*)//B3LYP/6-31G* calculations provides energy gap of 2.50 eV, which is in an excellent agreement with the experimental data. However, it was found that the HOMO-LUMO energy gaps obtained from B3LYP calculations were still far from the experimental data.

Keywords: Fluorene-thiophene copolymer; oligomer plot; excitation energy; HOMO-LUMO energy.

1. Introduction

Intensive research has been dedicated to exploring novel conjugated polymer with narrow band gaps (Eg),[1–1] a property that is essential for high conductivity upon doping, high nonlinear optical response, and the possible transparency in the visible region of the absorption spectrum, etc. In addition, there are widely theoretical studies on investigation of the energy gaps.[5–10] Obviously, a theoretical investigation on the band gaps of these polymers is very useful in guiding the experimental synthesis. To evaluate the energy gap, there are two different theoretical approaches. One is the polymer approach in which the periodic structures are assumed for infinite polymers. Another one is the oligomer extrapolation technique that is popular in this field. In this approach, a sequence of increasing longer oligomer is calculated, and extrapolation to infinite chain length is followed. A distinct advantage of this approach is that it can provide the convergence behavior of the structural and electronic properties of oligomers.

Ab intio and density functional theory, the methods that can be used to estimate the HOMO-LUMO energy gap, sometimes agree fairly well with the experimental band gap in many cases.[5] It may perhaps due to the error cancellations. Nowadays, time-dependent density functional theory (TDDFT) is a recently developed tool for calculation excitation energies. Ma *et al.*[11] employed time-dependent DFT to calculate band gaps and effective conjugation lengths of polyacetylene, polyphenylene, polypentafulvene, polycyclopentadiene, polypyrrole, polyfuran, polysilole, polyphosphole and polythiophene. They obtained band gaps of the corresponding polymers by extrapolating vertical excitation energies of the trimers through pentamers to infinite chain length. Time-dependent DFT was applied to calculate vertical excitation energies of linear polyene oligomers: butadiene to decapentaene by Hua *et al.*[12] In addition, this method is also used to study electroluminescent polymer.[13]

In this study, we employed semi-empirical, *ab initio*, and density functional theory to investigate the HOMO-LUMO energy gap. Moreover, TDDFT with B3LYP functional and semi-empirical ZINDO are used to investigate the vertical excitation energies of poly [2,7-(9,9-dihexylfluorene)-*co*-alt-2,5-(decylthiophene) (Fig. 1.).

2. Methods of Calculations

The ground state geometry of the monomer was fully optimized using the semi-empirical (AM1), *ab initio* (at HF/3-21G* and HF/6-31G* levels), and density functional theory (B3LYP/6-31G*). The hexyl groups at the 9 position have been replaced by ethyl groups to reduce calculating time. The length of the side chain at thiophene unit is also reduced to ethyl group as it was found that longer side chain does not significantly effect on the electronic properties of the polymer. Consequently, the excitation energies were obtained by using ZINDO and TDDFT(B3LYP/6-31G*) calculations at the optimized ground state geometries.

Estimated energy gaps of the polymer were obtained by plotting the vertical excitation energies for the dipole-allowed excited states of oligomer against reciprocal chain lengths and extrapolating to infinite chain length. In the case of *ab intio* method, HOMO-LUMO energy gaps were also performed in the similar plot. All calculations were done by using GAUSSIAN 03, running on a Linux PC 2.4 GHz.

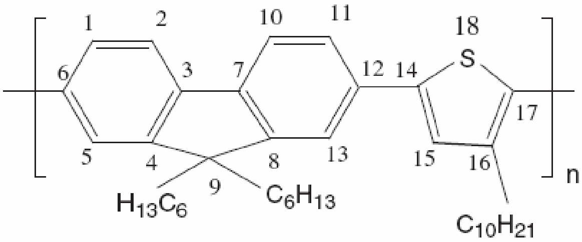

Fig. 1. Structure of poly [2,7-(9,9-dihexylfluorene)-*co*-alt-2,5-(decylthiophene). (FET for monomer.)

3. Results and Discussion

3.1. *Geometry of FET at ground state*

The ground state geometries of monomer (FET) as obtained from AM1, *ab intio* density functional theory are shown in Table 1. Accordingly, it was found tha the geometries obtained from AM1 and B3LYP/6-31G* are not significantly different as compared with those obtained from HF/3-21G* and HF6-31G* methods Kwon *et al.* used DFT and AM1 methods for thiophene oligomer geometries. They found that DFT-optimized geometries are in excellent agreement with the solid state structure. In their work, calculated C–C inter-ring distances (~ 1.45 Å) and C–S distances (~ 1.75 Å) at B3LYP/6-31G* are almost equal to experiment (C–C 1.45 Å; C–S 1.74 Å), while AM1 calculated distances (C–C, 1.42 Å; C–S 1.58 Å) are shorter than experiment due to the nature of the AM1 parametrization. In this work, C–S distance calculated at B3LYP/6-31G* (1.74 Å) shows good agreemen with the C–S distance of the thiophene unit obtained from solid state structure.

Moreover, C–C distances in thiophene unit of the FET monomer are also in good agreement with the thiophene oligomer.[14] Therefore, the fluorene unit is no significantly effected on the thiophene geometries. In the case of fluorene unit

Table 1. Ground state geometries of the FET monomer, obtained from AM1, HF/3-21G*, HF/6-31G*, and B3LYP/6-31G* methods.

	Methods			
Geometry Parameters	AM1	HF/3-21G*	HF/6-31G*	B3LYP/6-31G*
C_1–C_2	1.402	1.387	1.386	1.397
C_2–C_3	1.385	1.381	1.385	1.397
C_3–C_4	1.428	1.395	1.394	1.410
C_4–C_5	1.383	1.377	1.382	1.391
C_5–C_6	1.403	1.390	1.389	1.400
C_6–C_1	1.391	1.385	1.388	1.399
C_3–C_7	1.460	1.474	1.472	1.467
C_7–C_8	1.427	1.395	1.394	1.401
C_8–C_9	1.520	1.528	1.527	1.529
C_9–C_4	1.519	1.528	1.527	1.528
C_7–C_{10}	1.385	1.380	1.384	1.396
C_{10}–C_{11}	1.398	1.385	1.385	1.393
C_{11}–C_{12}	1.402	1.392	1.394	1.409
C_{12}–C_{13}	1.412	1.396	1.397	1.412
C_{13}–C_8	1.381	1.375	1.379	1.386
C_{12}–C_{14}	1.443	1.475	1.479	1.467
C_{14}–C_{15}	1.384	1.351	1.350	1.375
C_{15}–C_{16}	1.433	1.440	1.441	1.432
C_{16}–C_{17}	1.381	1.348	1.346	1.370
C_{17}–S_{18}	1.664	1.724	1.727	1.735
S_{18}–C_{14}	1.689	1.735	1.740	1.756
$\theta(13, 12, 14, 15)$	25.66	42.12	39.40	26.64

the results obtained by AM1, *ab initio*, and DFT are in good agreement with the reported X-ray data.[15] Normally, C_8–C_9 and C_9–C_4 distances (~1.47 Å) obtained from X-ray data are unusually shorter than the optimized values. The origin of this difference is due to the crystal packing force. Compared to the HF method, DFT calculations yield longer C=C bonds and shorter inter-ring distances. Thus, using HF method, π-electrons are more localized; this is due to the neglect of electron correlation. Tirapattur *et al.*[16] calculated the ground state geometries of fluorene derivatives; 2-(fluoren-2-yl)thiophene (FT) and 2-(fluoren-2-yl)methylthiophene (FMT) at HF/6-31G* level. When FET is compared with the FT, the addition of a ethyl group at position 4 of the thiophene unit does not significantly affect the bond length of the phenylene and thiophene rings, including the inter-ring distance, except for C_{15}–C_{16} distance, which becomes longer. This is obviously because of the steric hindrance caused by the ethyl group. Furthermore, those molecules provide non-planar structures, which have the torsional angle about 39.0°. In the case of FMT, inter-ring distance is longer than FET due to the steric hindrance caused by the methyl group, which is evidence from the larger torsional angle (55.2°).

3.2. *HOMO-LUMO energy gaps and the lowest excitation energies*

The calculated HOMO-LUMO energy gaps are shown in Table 2. The HOMO-LUMO energy gaps were extrapolated to the infinite chain length of the polymer and the results are depicted in Fig. 2.

According to Fig. 2, it was found that the obtained energy gaps are far from the experimental data (2.50 eV; Lui *et al.*).[17] This means that estimated HOMO-LUMO energy gap cannot represent the energy gap of this polymer studied. As the result, the orbital energy gap between HOMO and LUMO is still approximate estimate to the transition energy since the transition energy also contains significant contribution from some two-electron integrals. It is known that HOMO-LUMO energy gaps obtained from *ab initio* and density functional theory calculations are the crudest estimate. However, Arnold C. *et al.* have studied the energy gaps of the polythiophene using *ab initio* and density functional theory methods. They

Table 2. HOMO-LUMO Energy Gaps of the oligomers, calculated by B3LYP/6-31G*//AM1, B3LYP/6-31G*//HF/3-21G* and B3LYP/6-31G*//HF/6-31G* methods.

	HOMO-LUMO Energy Gaps (eV)		
Oligomer	B3LYP/6-31G* //AM1	B3LYP/6-31G* //HF/3-21G*	B3LYP/6-31G* //HF/6-31G*
$n = 1$	4.14	4.50	4.47
$n = 2$	3.60	4.17	4.10
$n = 3$	3.37	3.93	3.85
$n = 4$	3.29	3.87	3.79
$n = 5$	3.19	3.84	—

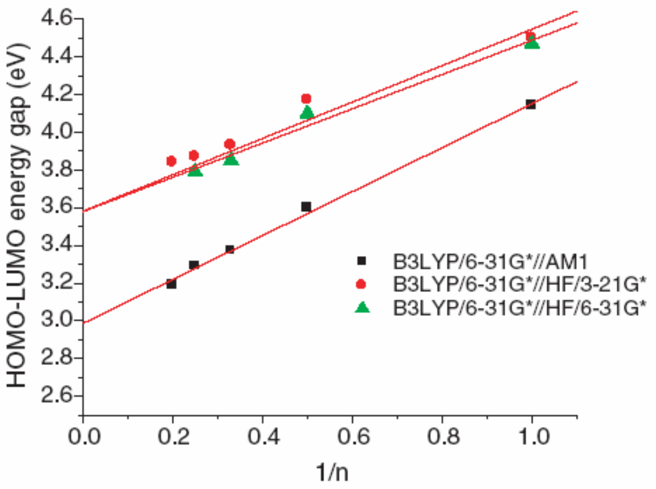

Fig. 2. Energy gaps extrapolated from the plot of HOMO-LUMO energies of the oligomers versus the inverse number of monomer units.

pointed out that DFT calculations with hybrid functionals (B3LYP and B3P86) gave excellent results (4.06 eV and 4.11 eV) that are in good agreement with the experiment energy gap (4.5 eV).[18]

In order to improve the more accurate energy gaps, the spectrum methods (ZINDO and TDDFT/B3LYP/6-31G*) were applied in this study to calculate the excitation energy. In calculating the excitation energies by both methods, the first excited state with significant oscillator strength (a π–π^* transition) was used and it was also the lowest excited state for all oligomers. Extrapolated energy gaps for oligomers by the ZINDO and TDDFT methods, based on AM1-, *ab initio*-, and DFT-optimized geometries, are shown in Fig. 3.

All extrapolated energy gaps as obtained from various methods are summarized in Table 3. The extrapolated energy gap from TDDFT/B3LYP/6-31G* excitation energies using DFT-optimized geometries is in excellent agreement with the experimental data. Considering the geometries obtained from B3LYP/6-31G*, it is found that the geometries are more planar and the inter-ring distance are shorter than those obtained from HF/6-31G* and HF/3-21G* calculations. The optimized geometries of the tetramer as obtained from different methods are shown in Fig. 4. The inter-ring distances of the oligomer as obtained from different methods are also analyzed and plotted against the bond number as shown in Fig. 5. The bond number is defined as following; bond numbers 1, 3, 5, and 7 for inter-ring distance between thiophene-fluorene unit and bond numbers 2, 4, and 6 for inter-ring distance between fluorene-thiophene unit.

Based on the optimized geometries, it is found that the inter-ring distances obtained from AM1 method are shorter than those obtained from DFT and HF methods (Fig. 5). However, this shorter inter-ring distance does not effect

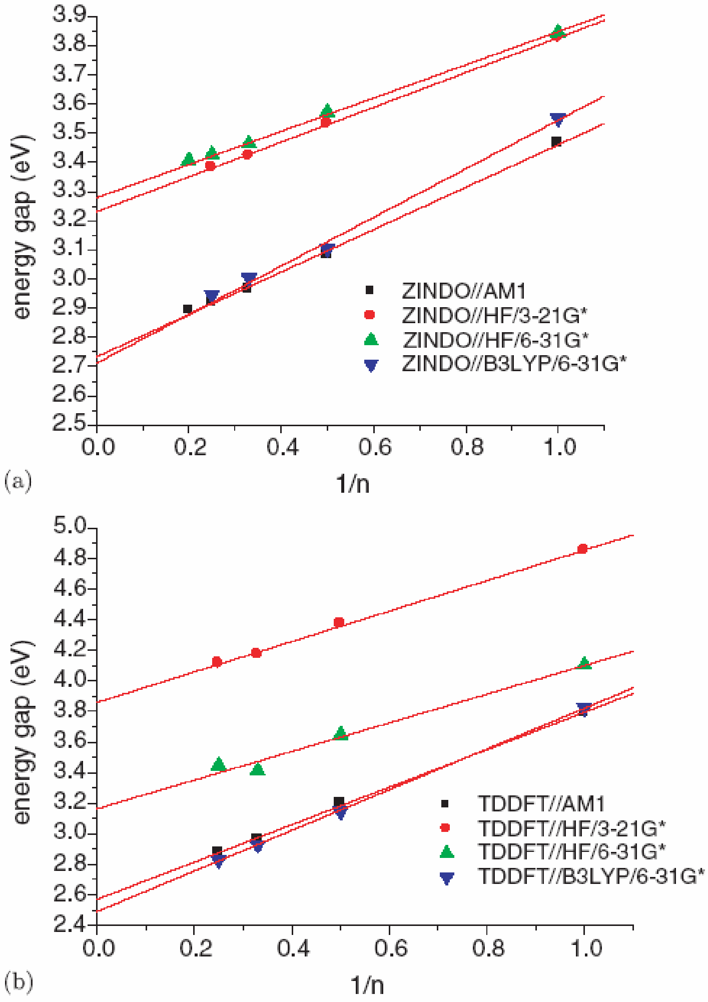

Fig. 3. Energy gaps extrapolated from the plot of excitation energies versus the inverse number of monomer units.

Table 3. The extrapolated energy gaps calculated at various methods.

Method	Energy Gap (eV)
ZINDO//AM1	2.74
ZINDO//HF/3-21G*	3.27
ZINDO//HF/6-31G*	3.23
ZINDO//B3LYP/6-31G*	2.71
TDDFT/B3LYP/6-31G*//AM1	2.56
TDDFT/B3LYP/6-31G*//HF/3-21G*	3.86
TDDFT/B3LYP/6-31G*//HF/6-31G*	3.16
TDDFT/B3LYP/6-31G*//B3LYP/6-31G*	2.50
Experimental optical energy gap	**2.50**[*]

[*] Lui *et al.*

(a) AM1–optimized geometry

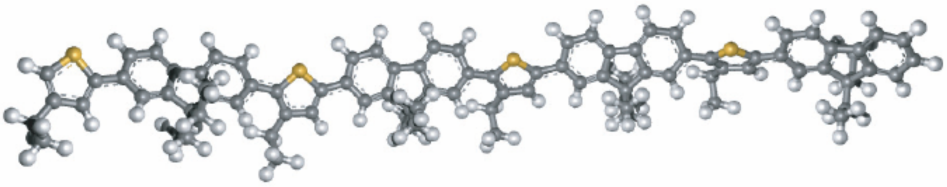

(b) HF/3-21G* –optimized geometry

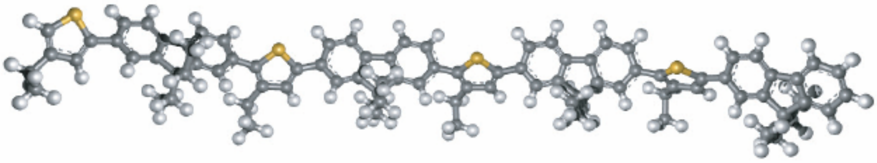

(c) HF/6-31G*–optimized geometry

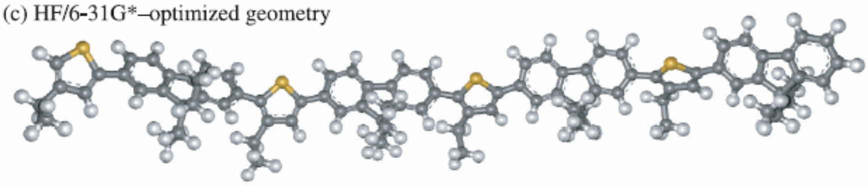

(d) B3LYP/6-31G* –optimized geometry

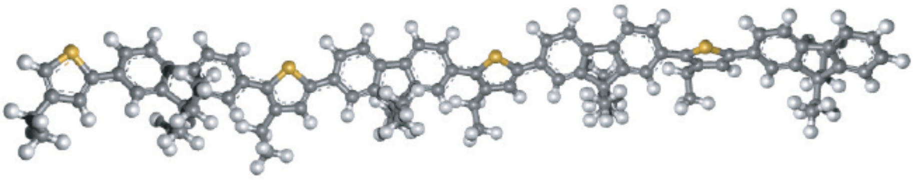

Fig. 4. Optimized geometries obtained from AM1, *ab initio*, and DFT methods.

to the conjugation along the main chain of the structure as compared from the energy gap calculated by the same method; TDDFT/B3LYP/6-31G*//AM1 (Eg = 2.56 eV), TDDFT/B3LYP/6-31G*//B3LYP/6-31G* (Eg = 2.50 eV) and ZINDO//AM1 (Eg = 2.74 eV), ZINDO//B3LYP/6-31G* (Eg = 2.71 eV). On the other hand, the planarity of the oligomer is significantly effect to increase the conjugation along the main chain. Note that the inter-ring torsional angles obtained from the DFT optimized geometry are smaller than those obtained from AM1 and HF methods, in particular, the inter-ring torsional angles between thiophene unit attached with ethyl group and fluorene. While TDDFT excitation energies using AM1-optimized geometries also provide a good energy gap due to the shortening inter-ring distance and planarity of oligomer structure, however, the AM1 geometry of the oligomer, in particular C–S distance of the thiophene unit, is shorter than experimental data. Therefore, the geometry of the oligomer obtained from AM1 method is not satisfied as compared to the results obtained from the B3LYP

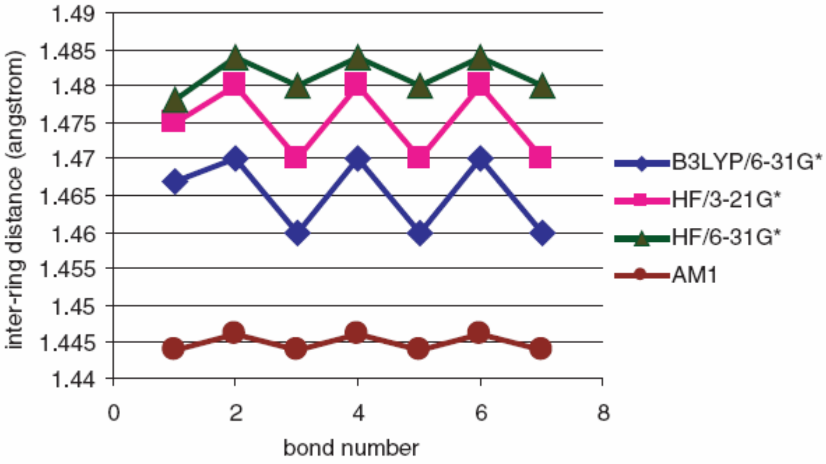

Fig. 5. Inter-ring distances of tetramer of FET (bond number started from the left-hand side of the optimized geometries as shown in Fig. 4), obtained from different methods.

Table 4. Inter-ring torsional angles of the optimized geometries (started from the left hand side of the optimized geometries as shown in Fig. 4), obtained from different methods.

Method	Inter-Ring Torsional Angles (Degrees)
AM1	25.6, 49.0, 25.4, 49.0, 25.4, 48.9, 25.5
HF/3-21G*	42.0, 61.7, 40.7, 61.7, 40.7, 61.6, 40.8
HF/6-31G*	38.4, 57.5, 37.3, 57.5, 37.3, 57.5, 37.4
B3LYP/6-31G*	27.2, 44.2, 25.6, 45.2, 22.9, 44.6, 23.8

method, which are in agreement with experimental data both in terms of structural parameters and energetic results.

4. Conclusions

TDDFT with B3LYP functional using B3LYP/6-31G* geometry was found to be a suitable method to estimate both energy gap of poly [2,7-(9,9-dihexylfluorene)-*co*-alt-2,5-(decylthiophene) and the reliable structural parameters. On the contrary, extrapolation of HOMO-LUMO energy differences, calculated by B3LYP method, based on AM1 and HF-optimized geometries were not reasonable as compared with the experimental data. In addition, the energy gap calculated from TDDFT method, based on AM1-geometry also provides a good estimated energy gap, however, the structural parameters are not reliable due to the nature of the AM1 parametrization.

Acknowledgments

This work is supported by the Postgraduate Education and Research on Petroleum and Petrochemical Technology (MUA-ADB). The Cooperative Research Network of Nanoscience and Nanotechnology under the Commission of Higher Education is grateful for the first APACTC supporting grant. We thank the high performance-computing at Laboratory Computational and Applied Chemistry at Kasetsart University and computing center of KU for research facilities.

References

1. Charas A, Morgado J, Martinho JMG, Alcacer L, Lim SF, Friend RH, Cacialli F, *Polymer* **44**:1843, 2003.
2. Beaupre S, Leclerc M, *Macromolecules* **36**:8986, 2003.
3. Charas A, Morgado J, Martinho JMG, Alcacer L, Cacialli F, *Synth Met* **127**:251, 2002.
4. Bouillud AD, Levesque I, Tao Y, D'Iorio M, Beaupre S, Blondin P, Ranger M, Bouchard J, Leclerc M, *Chem Master* **12**:1931, 2000.
5. Oliveira MAD, Duarte HA, Pernaut, J-M, De Almeida WB, *J Phys Chem A* **104**:8256, 2000.
6. Kwon O, McKee ML, *J Phys Chem A* **104**:7106, 2000.
7. Kwon O, McKee ML, *J Phys Chem B* **104**:1686, 2000.
8. Duan X, Dudis DS, A, Yeates T, *Synth Met* **116**:285, 2001.
9. Cornil J, Gueli I, Dkhissi A, Sancho-Garcia JC, Hennebicq E, Cabert JP, Lemaur V, Beljonne D, Bredas JL, *J Chem Phys* **118**:6615, 2003.
10. Yang S, Olishevski P, Kertesz M, *Synth Met* **141**:171, 2004.
11. Ma J, Li S, Jiang Y, *Macromolecules* **35**:1109, 2002.
12. Hsu C-P, Hirata S, Head–Gordon M, *J Phys Chem A* **105**:451, 2001.
13. Yu J-SK, Chen W-C, Yu C-H, *J Phys Chem A* **107**:4268, 2003.
14. Horowitz G, Bachet B, Yassar A, Lang P, Demanze F, Fave J-L, Garnier F, *Chem Mater* **7**:1337 1995.
15. Burns MD, Iball, *J Proc Roy Soc A* **227**:200, 1955.
16. Tirapattur S, Belletete M, Leclerc M, Durocher G, *J Mol Struct (Theochem)*, **625**:141, 2003.
17. Liu B, Yu W-L, Lai Y-H, Huang W, *Macromolecule* **33**:8945, 2000.
18. Alguno AC, Chung WC, Bantaculo RV, Vequizo RM, Miyata H, Ignacio EW, Bacala AM, *NECTEC Tech J*, **II**(a):2000–2001.

Publication II

SAC-CI Theoretical Investigation on Electronic Structure of Fluorene-Thiophene Oligomers

Poolmee, P., Ehara, M., Hannongbua, S., Nakatsuji. H.,

Available online at www.sciencedirect.com
SCIENCE DIRECT®

ELSEVIER

Polymer 46 (2005) 6474–6481

polymer

www.elsevier.com/locate/polymer

SAC–CI theoretical investigation on electronic structure of fluorene–thiophene oligomers

Potjaman Poolmee[a], Masahiro Ehara[b], Supa Hannongbua[a,*], Hiroshi Nakatsuji[b,c,*]

[a]*Department of Chemistry, Faculty of Science, Kasetsart University, Bangkok 10900, Thailand*
[b]*Department of Synthetic Chemistry and Biological Chemistry, Graduate School of Engineering, Kyoto University, Kyoto-Diagaku-Katsura, Nishikyo-ku, Kyoto 615-8510, Japan*
[c]*Fukui Institute for Fundamental Chemistry, Kyoto University, 34-4 Takano-Nishihiraki-cho, Sakyo-ku, Kyoto 606-8103, Japan*

Received 10 February 2005; accepted 18 March 2005
Available online 22 June 2005

Abstract

The excited states of the fluorene–thiophene compounds whose polymers are useful as a light-emitting diode were studied by SAC–CI method. The effect of the torsional angle on the excited state was examined for the FT and FMT monomers in details. The first three excited states were calculated for the conformers of several torsional angles. These three excited states were found to change their characters by varying the torsional angle from 0 to 90°. The accurate absorption spectra were simulated by taking the thermal average for the conformers of torsional angle from 0 to 90°. The absorption spectra of dimer and trimer were also calculated at the equilibrium structure. It was found that the oscillator strength of $S1$ states of the dimer and trimer was very high and the red shift occurs due to the π-conjugation. The equilibrium structures are planar for both FT and FMT, and the calculated emission energies are in consistent agreement with the experiment. The effect of applying the electric fields to these molecules was examined.

Keywords: Fluorene; Thiophene; Excited states

---

1. Introduction

Recent research has shown that fluorene derivatives emerging as a very promising candidate to develop flexible and tunable light-emitting diode (LEDs) [1–5]. These polymers are soluble in organic solvents and their structure can be controlled to obtain the desired electro–optical properties. Previously, many theoretical works only investigated the structures and electronic properties in the ground state of these polymers or theirs segments. Therefore, theoretical information for the excited states of these molecules are limited. The RCIS/6-31G* calculations were performed to determine the structures of the $S1$ state and excitation energies of fluorene oligomers by Tirapattur et al. [6]. It is not only the structure of the excited state of conjugated polymer which is an important investigation but the optical non-linearities and spectral characteristics are also a major problem in the research. The time-dependent density functional theory (TDDFT) is only one tool to determine the excitation energy, therefore, it was widely common used to investigate the excitation energy of the conjugated system [7–9]. Recently, the electronic spectra of thiophene–fluorene π-conjugated derivatives was interpreted using ZINDO/s by Lukes et al. [10]. In their work the influence of conformation effect on the electronic spectra was studied and Boltzman's distribution was taken into account to simulate the average electronic absorption spectra. Belletete et al. [11] reported the important work on the optical properties of monomers; they observed the absorption and fluorescence spectra of fluorene derivatives and characterized the excited states by ZINDO/s calculations. For the optical properties of 2-(9,9-dioctylfluorene-2-yl)thiophene and 2-(9,9-dioctylfluorene-2-yl)-3-methylthiophene, they concentrated on the vertical transition for the absorption spectra in their theoretical treatment. Many conjugated polymers, such as thiophene

---

* Corresponding author. Tel./fax: +66 2 9428900.
E-mail addresses: fscisph@ku.ac.th (S. Hannongbua), hiroshi@sbchem.kyoto-u.ac.jp (H. Nakatsuji).

0032-3861/$ - see front matter © 2005 Elsevier Ltd. All rights reserved.
doi:10.1016/j.polymer.2005.03.120

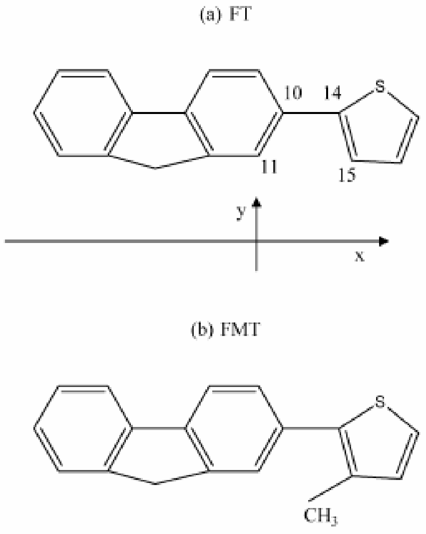

Fig. 1. Structures of FT and FMT.

and its cyano derivative oligomers and carbazole-based dydads were also studied by CIS [12,13].

In our previous work [14], structure and energetic properties of fluorene–thiophene copolymer was investigated, based on quantum chemical calculations. It was found that the energy gap of this copolymer as estimated by TDDFT (B3LYP/6-31G*) was in well agreement with experimental data. Unfortunately, there are no theoretical works that examined the effect of the torsional angle between the fluorene and thiophene units on the optical properties of these compounds, though the rotional barrier has been proven to be very small. Since the LUMO of FT has the bonding character between these units, it is anticipated that the excitation spectrum depends on the torsional angle. For this reason, reliable theoretical work is necessary to elucidate the mechanism of the optical properties.

The SAC (symmetry adapted cluster) [15]/SAC–CI (configuration interaction) method [16,17] has been established as a reliable and useful method for investigating a wide variety of molecular spectroscopy through many successful applications [18–26]. Recently, the SAC–CI method is emerging in the Gaussian03 [27] to be the useful method for studying molecular excited states. This method has clarified the details of the excited states of the π-conjugated system and transition metal complex [28]. In relation to the present study, the excitation spectrum of thiophene has been accurately investigated [26].

The purpose of this paper are to investigate the excited-state electronic structures and optical properties of 2-(fluorene-2-yl)thiophene (FT) and 2-(fluorene-2-yl)-3-methylthiophene (FMT) which are the model unit compounds of the light-emitting diodes by using SAC–CI calculations. We studied the effect of torsional angle on the absorption spectra and gave the accurate absorption spectra of monomer, dimer and trimer. We also addressed the emission spectrum of monomer through the calculation and the accurate characterizations of the excited states are provided.

2. Computational details

Structures of FT and FMT studied in the present work are demonstrated in Fig. 1. The ground-state potential energy curves of FT and FMT monomers along the torsion angle (11-10-14-15) were calculated by using B3LYP/6-31G* [29,30] level. In the calculation, the torsional angle was changed by 15°, whereas all the other geometrical parameters were fixed.

The SAC–CI SD-R calculations were performed for the excitation spectra of FT and FMT at each torsional angle. Double zeta basis set of Huzinaga–Dunning [4s 2p/2s] were adopted [31,32]; the valence excited states were investigated and the consistent calculations up to trimer can be possible with this basis set. In the preliminary calculations, it was found that only the low lying three excited states are important for the first absorption peak in the experimental spectrum. Therefore, we present the results of these three excited states, although we also calculated higher excited states. In the SAC–CI calculation, 1s orbital of C and 1s, 2s, 2p orbitals of S were taken as the frozen core MOs and their counterparts were excluded from the active space. For monomer, the resultant SAC–CI active space consist of 43 occupied and 125 unoccupied MOs. For dimer and trimer, the active space is 129 occupied and 247 unoccupied MOs and 193 occupied MOs and 256 unoccupied MOs, respectively.

To reduce the computational requirements, the perturbation selection procedure was adopted [21]. LevelTwo accuracy in SAC–CI Gaussian03 [27] was adopted as follows. The threshold of the linked terms for the ground state was set to $\lambda g = 5.0 \times 10^{-6}$. The unlink terms were described as the product of the important linked terms whose SDCI coefficient were larger than 0.005. For excited state, the thresholds of the linked doubles were set to $\lambda e = 5.0 \times 10^{-7}$. The thresholds of the CI coefficients for calculating the unlinked operators in the SAC–CI method were 0.05 and 0.0 for the R and S operators, respectively. For the trimer, LevelOne accuracy was adopted.

3. Results and discussion

3.1. Ground state of FT and FMT

The ground-state potential energy curves of FT and FMT monomers along the torsion angle were calculated by using B3LYP/6-31G* level. The calculations were performed for

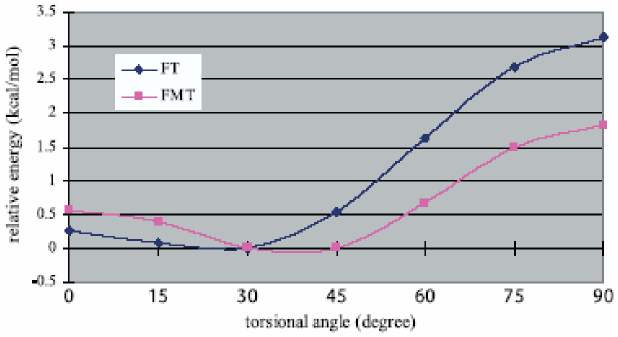

Fig. 2. The ground state potential energy curves of FT and FMT monomers.

the conformers of the torsional angle (11-10-14-15) $\theta=0$–$90°$, with the grid of $\Delta\theta=15°$, whereas all the other geometrical parameters were fixed. The potential energy curves of FT and FMT are shown in Fig. 2.

The torsional angle of the most stable conformation of FT was $\theta=27°$. The energy barrier towards co-planar conformation was calculated to be only 0.25 kcal/mol, while the barrier to the perpendicular conformation was about 3.1 kcal/mol. This very low rotational energy barrier indicated that it allows a wide range of non-planar conformations at the room temperature. In the case of FMT, the torsional angle of the most stable conformation was $\theta=43°$. The energy barrier to co-planar conformation is higher than that of FT due to the steric interaction between the methyl group and the hydrogen atom at the C_{11} position of the fluorene unit. FMT is much more stable in the

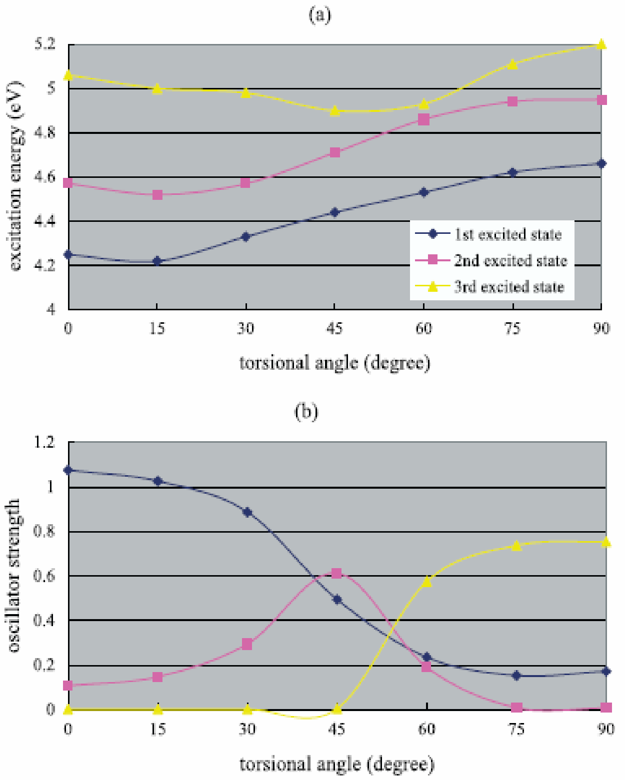

Fig. 3. The SAC–CI (a) excitation energy and (b) oscillator strength of FT versus torsional angle.

Table 1
The excitation energy (ΔE), oscillator strength, excitation character, and dipole moment of FT at torsional angle 0, 30, and 60°

Torsional angle	State	ΔE (eV)	Oscillator strength (*f*)	Excitation character	Dipole moment
0°	1st	4.25	1.08	0.91(H→L)	0.65
	2nd	4.56	0.11	0.73(H→nL)	0.58
	3rd	5.06	0.00	0.56(*n*H→L)	0.57
30°	1st	4.32	0.89	0.83(H→L)	0.65
	2nd	4.57	0.30	0.69(H→*n*L)	0.60
	3rd	4.98	0.00	0.56(*n*H→L)+0.50(*n*H→L+3)	0.58
60°	1st	4.53	0.24	0.62(H→*n*L)	0.64
	2nd	4.86	0.19	0.48(H−2→L)+0.47(H→L+3)	0.76
	3rd	4.93	0.58	0.68(H→L)	0.45

conformation of large angle than FT; the energy of the conformer of $\theta=90°$ is 1.9 kcal/mol relative to the most stable conformer of $\theta=43°$. Therefore, the energy barrier along the torsion angle is very small for both FT and FMT proving conformers of wide range of torsion angles can exist at room temperature as will be shown later.

3.2. Excited states; effect of torsional angle

The SAC–CI/D95 was used to calculate the first three excited states of FT, which are responsible for the first band observed experimentally. The excitation energy (ΔE) and the oscillator strength (*f*) of FT as the function of torsional angle are shown in Fig. 3. Excitation energy, oscillator strength, and excitation characters of these three excited states for the conformer of 0, 30 and 60° are summarized in Table 1.

The present calculation shows that the excitation energies of 1st and 2nd excited states increase when the planarity between fluorene unit and thiophene unit reduces. It was also found that the excitation character of the excited states of the FT depend on the torsional angle, for instance, the *S*1 state of FT at torsional angle 0° is characterized as the excitation from HOMO to LUMO, while the *S*1 state at torsional angle 90° is from HOMO to next LUMO. The avoided crossing occurs between the 1st and 3rd states in the region of $\theta=45$–$60°$ as also seen in the oscillator strength of Fig. 3(b). Namely, the excitation characters are represented as follows;

	Torsional angle 0°	Torsional angle 90°
1st excited state	H→L	H→*n*L
2nd excited state	H→*n*L	H-2→L
3rd excited state	*n*H→*n*L	H→L

From the oscillator strength and the excitation character of the excited states, it can be concluded that the excitation of HOMO–LUMO mainly contributes to the absorption of the 1st peak of the FT and FMT, however, it was found that the excitation to the higher states does not contribute to the 1st peak. The next higher excited states occur higher than 5.5 eV with small oscillator strength, whereas the first absorption bands of FT and FMT are centered at 3.09 eV and 4.04 eV, respectively [11].

The SECI (single excitation configuration interaction) results of FT are shown in Fig. 4 for comparison. The SECI excitation energies of these three excited states were calculated to be much higher than those of the SAC–CI method. Significantly, the SECI gave wrong picture for these excited states. The excitation character of the *S*1 state is not dependent on the torsional angle; it is characterized as

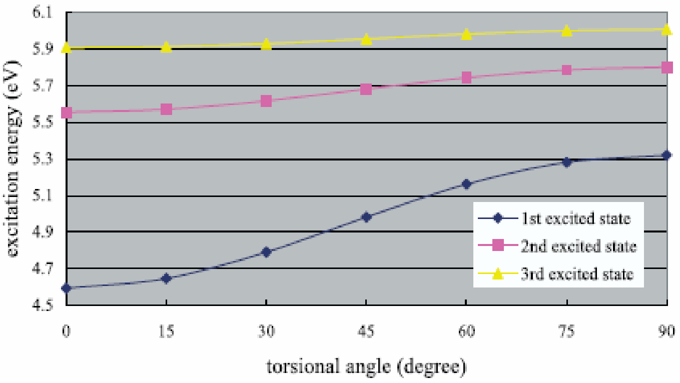

Fig. 4. The SECI excitation energy of FT monomer versus torsional angle.

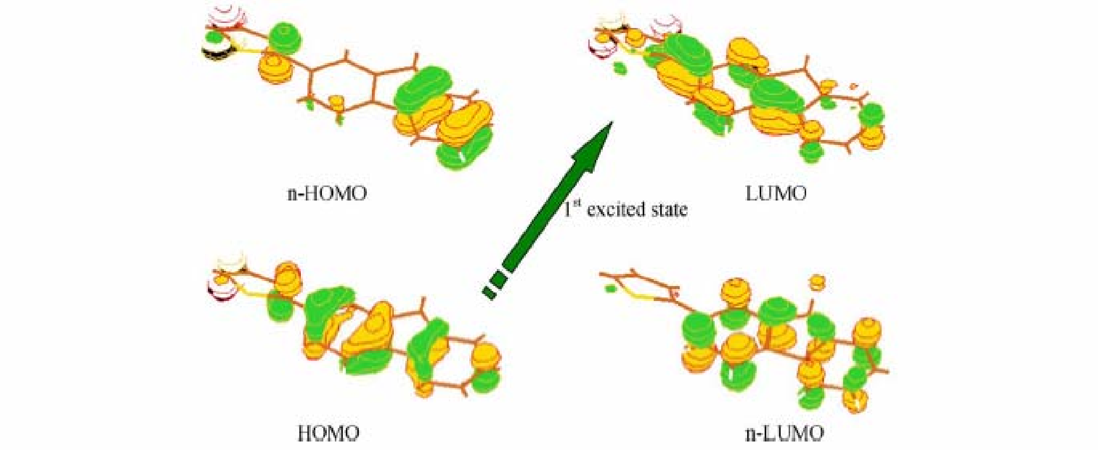

Fig. 5. Schematic representation of MOs of FT monomer ($\theta = 30°$).

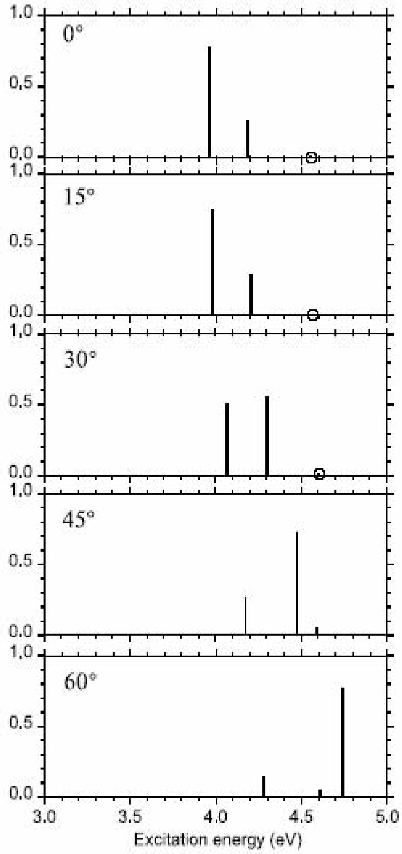

Fig. 6. The calculated absorption spectra of FT at torsional angle 0, 15, 30, 45 and 60°.

the excitation from HOMO to LUMO in all torsional angles and the $S1$ state is located apart from other two states.

Next, the MOs which are important for these excited states are analyzed. From the SAC–CI results, these excited states are mainly described by the linear combination of the transitions from next HOMO and HOMO to LUMO and next LUMO. These four orbitals of FT at torsional angle 30° are displayed in Fig. 5.

As shown in Fig. 5, the HOMO and LUMO delocalized over the molecule, while the next LUMO localized in the fluorene unit. The HOMO shows inter-ring anti-bonding character between the two subunits and the LUMO shows inter-ring bonding character. The HOMO to LUMO transition is destabilized as the torsion angle becomes large, because of the bonding character of LUMO. On the other hand, HOMO to next LUMO transition does not change along the torsional angle. This situation gives rise to the interchange of the excited states.

Next, we discuss the dipole moment of FT in the three excited states. It was found that the dipole moments of three excited states are not significantly different at torsional angle 0 and 30°. On the other hand, dipole moment at torsional angle 60° is different for the 2nd and 3rd excited states.

3.3. Absorption spectra of FT and FMT

The SAC–CI absorption spectra of FT for the torsional angles 0–60° are displayed in Fig. 6. These three excited states shift into high energy region for the conformer of large θ and the oscillator strength of the 3rd excited state becomes large in $\theta = 60°$.

The ground state potential energy surface is flat along the torsion angle, therefore, in order to simulate the absorption spectra, the Boltzmann distribution of the conformers should be considered. The absorption spectra were

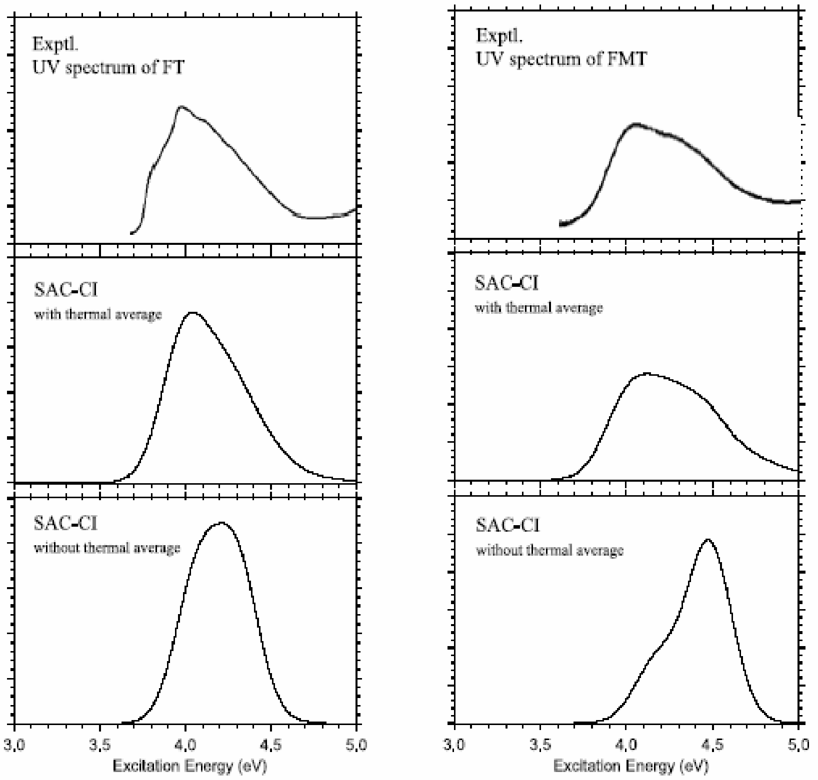

Fig. 7. Experimental [11] and SAC–CI absorption spectra of FT and FMT. Theoretical spectra with and without thermal average are shown.

simulated with the simple model: contributions of the conformer of $\theta = 0$–$90°$ with the interval of $\Delta\theta = 15°$ were averaged with the statistical weights at the room temperature. From the Boltzmann weight, the excitation which has the high oscillator strength at torsional angle 0, 15, 30, 45 and 60° contributed mainly to the absorption spectra of the FT and FMT. The calculated absorption spectra of FT and FMT in which Boltzmann distribution was taken into account are shown with the experimental spectra in Fig. 7. The spectra without the thermal average correction are also displayed for comparison. For FT, the Boltzmann weights at torsion angle 0, 15, 30, 45 and 60° are 22, 29, 33, 13 and 2%, respectively, and for FMT, they are 12, 15, 30, 30 and 9%, respectively.

Table 2
Excited states of FT in the electric field ($E_x = 0.01$ a.u.)

Torsional angle	State	ΔE (eV)	f	Excitation character
0°	1st	3.59	0.89	0.91(H→L)
	2nd	4.14	0.12	0.82(H→*n*L)
	3rd	4.74	0.01	0.58(H→L+3)
60°	1st	3.89	0.5	0.89(H→L)
	2nd	4.48	0.02	0.81(H→L+2)
	3rd	4.89	0.29	0.89(H→*n*L)

For FT the contributions of the conformer whose torsional angle is up to ~30° are dominant and the asymmetric spectra are obtained. In the case of FMT, the strong shoulder was observed in the higher energy side of the peak at about 4.3 eV. This absorption can be mainly attributed to the 2nd excited state of the conformer of $\theta = 30$–$45°$.

3.4. *Effect of electric field*

The effect of the electric field is examined for the conformer of $\theta = 0$ and 60°. The results for applying the electric field of $E = 0.01$ a.u. in the x direction (E_x) are given in Table 2. By applying the electric field, all three excited states are stabilized and the excitation energy becomes small. In particular, the HOMO–LUMO transition is stabilized. Since the 1st excited state of the conformer $\theta = 0°$ is described as HOMO–LUMO transition, the spectrum shape does not change. However, the 1st excited states of the conformer $\theta = 60°$ is characterized as HOMO–LUMO transition under the electric field. Therefore, the oscillator strength of the 1st excited state becomes large compared to that without electric field (Table 1).

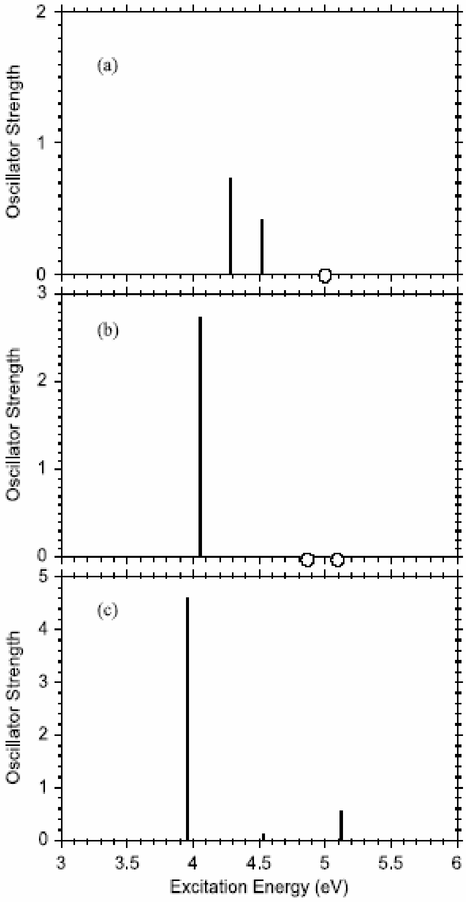

Fig. 8. The calculated absorption spectra of FT; (a) monomer, (b) dimer, and (c) trimer.

3.5. Absorption spectra of dimer and trimer

The absorption spectra of dimer and trimer were calculated at their ground-state optimized structures. These spectra are compared with that of the monomer as shown in Fig. 8. The excitation energies, oscillator strength and the excitation character of three excited states for dimer and trimer are also summarized in Table 3. In the case of dimer and trimer only the 1st excited state contributes to the absorption spectrum with the large oscillator strength. Other two states have small oscillator strength. It is also characteristic that the energy separations between the 1st and the other excited states are wider than that of monomer. Since the conjugation length increases in the dimer and trimer, red shift occurred for the first excited state. It can be concluded that the 1st excited state contributes the absorption spectra not only for the dimer and trimer but also in the case of polymer.

Table 4
The emission energy (eV) of FT and FMT monomers

Monomer	SAC–CI	Exptl.[a]
FT	3.73	3.52
FMT	3.69	3.48

[a] Ref. [11].

3.6. Emission spectra for FT and FMT

We studied the emission spectra from the 1st excited state of FT and FMT. Equilibrium geometries of the 1st excited state were calculated by CIS/6-31G*. It was found that the structures of the 1st excited state of FT and FMT are almost planar. This is because the 1st excited state is HOMO–LUMO transition and the LUMO has the π-bonding character between the fluorene and thiophene units. The emission energies of FT and FMT are given in Table 4 with the experimental values. Since the stable structures in the 1st excited state are planar for both FT and FMT, the emission energies of these molecules are almost identical.

4. Summary

FT and FMT monomers are most stable in the non-planar structures in their ground states. However, the rotational energy barriers to co-planar and perpendicular conformations are well below 3 kcal/mol. This indicates that it allows a wide range of non-planar structure. The excitation energies of 1st and 2nd excited states increase when the planarity between fluorene and thiophene unit reduces. From the oscillator strength, the component of HOMO–LUMO transition mainly contributes to the absorption of the 1st peak of the FT and FMT. It was found that the excitation

Table 3
The excitation energy (ΔE), oscillator strength (f), and character of FT monomer, dimer, and trimer at the optimized geometry

Excited state	Monomer			Dimer			Trimer		
	ΔE (eV)	f	Character	ΔE (eV)	f	Character	ΔE (eV)	f	Character
1st	4.28	0.73	H→L	4.07	2.74	H→L	3.96	4.61	H→L
2nd	4.52	0.41	H→*n*L	4.88	0.00	H→*n*L	4.54	0.10	H→*n*L + *n*H→L
3rd	4.92	0.00	*n*H→L	5.09	0.01	*n*H→L	5.12	0.55	*n*H→*n*L

energy of the HOMO–LUMO transition along the torsional angle changes caused the interchange of the character between the 1st and 3rd exited states. This was found to be because the HOMO has an inter-ring anti-bonding character between the two subunits, while the LUMO has inter-ring bonding character. The absorption spectra of FT and FMT in which Boltzmann distributions are taken into account are in common agreement with the experimental spectra.

For dimer and trimer, only the 1st excited state contributes to the absorption spectra with the large oscillator strength, the other two states have very small oscillator strength. This tendency must be valid for the polymer of these compounds.

The stable structures in the 1st excited state were predicted to be nearly planar for both FT and FMT. The calculated emission energies of these molecules are almost the same and also in common agreement with the experiment.

Therefore, using the SAC–CI method, fine analysis of the excited states of the FT and FMT, which are important fragments of the light-emitting devices, have been achieved.

Acknowledgements

This study was supported by a Grant for Creative Scientific Research from the Ministry of Education, Science, Culture, and Sports of Japan. The Postgraduate on education and research in Petroleum and Petrochemical Technology and KURDI are gratefully acknowledged for financial support and research facilities, and the Graduate School KU, for partial support via Grant-in-Aid for thesis. Thanks are also due to Richard Burgess for reading of the manuscript.

References

[1] Feng L, Zhang E, Bie H, Chen Z. Dyes Pigments 2005;64:31.
[2] Wu FI, Shu CF, Chien CH, Tao YT. Synth Met 2005;148:133.
[3] Hwang DH, Park MJ, Lee JH. Mater Sci Eng C 2004;24:201.
[4] Wu W, Inbasekaran M, Hudack M, Welsh D, Yu W, Chen Y, et al. Microelectron J 2004;35:343.
[5] Chen B, Wu Y, Wang M, Wang S, Sheng S, Zhu W, et al. Eur Polym J 2004;40:1183.
[6] Tirapattur S, Belletete M, Leclerc M, Durocher G. J Mol Struct (THEOCHEM) 2003;625:141.
[7] Ma J, Li S, Jiang Y. Macromolecules 2002;35:1109.
[8] Yu JK, Chen WC, Yu CH. J Phys Chem A 2003;107:4268.
[9] Agalya G, Lv C, Wang X, Koyama M, Kubo M, Miyamoto A. Appl Surf Sci; 2005;244:195.
[10] Lukes V, Vegh D, Hrdlovic P, Stefko M, Matsuzna K, Laurinc V. Synth Met 2005;148:179.
[11] Belletete M, Beaupre S, Bouchard J, Blandin P, Leclerc M, Durocher G. J Phys Chem B 2000;104:9118.
[12] Chakraborty D, Lagowski JB. J Chem Phys 2001;115:187.
[13] Belletete M, Bedard M, Leclerc M, Durocher G. J Mol Struct (THEOCHEM) 2004;679:9.
[14] Poolmee P, Hannongbua S. J Theor Comp Chem 2004;3:481.
[15] Nakatsuji H, Hirao K. J Chem Phys 1978;68:2053.
[16] Nakatsuji H. Chem Phys Lett 1978;59:362.
[17] Nakatsuji H. Chem Phys Lett 1979;67:329 [see also p. 334].
[18] Ishida M, Toyota K, Ehara M, Nakatsuji H. Chem Phys Lett 2001;347:493.
[19] Nakatsuji H. Acta Chim Acad Sci Hung 1992;129:719.
[20] Nakatsuji H. Computational chemistry—review of current trends. vol. 2. Singapore: World Scientific; 1997. p. 62–124.
[21] Nakatsuji H. Chem Phys 1983;75:425.
[22] Nakatsuji H, Hasegawa J, Hada M. J Chem Phys 1996;104:2321.
[23] Nakatsuji H, Hasegawa J, Ohkawa K. Chem Phys Lett 1998;296:499.
[24] Nakatsuji H, Kitao O, Yonezawa T. J Chem Phys 1985;83:723.
[25] Wan J, Nakatsuji H. Chem Phys 2004;302:125.
[26] Wan J, Hada M, Ehara M, Nakatsuji H. J Chem Phys 2001;114:842.
[27] Frisch MJ, Trucks GW, Schlegel HB, Scuseria GE, Robb MA, Cheeseman JR, et al. Gaussian03, Inc., Wallingford CT; 2004.
[28] Nakatsuji H, Ehara M, Palmer MH, Guest MF. J Chem Phys 1992;97:2561.
[29] Ditchfield R, Hehre WJ, Pople JA. J Chem Phys 1971;56:724.
[30] Becke AD. J Chem Phys 1993;98:5648.
[31] Huzinaga S. J Chem Phys 1965;42:1293.
[32] Dunning TH. J Chem Phys 1970;53:2823.

CURRICULUM VITAE

NAME	:	Miss Potjaman Poolmee		
BIRTH DATE	:	Febuary 16, 1973		
BIRTH PLACE	:	Saraburi, THAILAND		
NATIONALITY	:	Thai		
EDUCATION	:	**YEAR**	**INSTITUTION**	**DEGREE/DIPLOMA**
	:	1994	Chiang Mai Univ.	B.Sc. (Chemistry)
	:	1997	Chiang Mai Univ.	M.Sc. (Chemistry)
	:	2005	Kasetsart Univ.	Ph.D. (Chemistry)

SCHOLARSHIPS : Kasetsart University (2002-2005)

: Postgraduate Education and Research Program in Petroleum and Petrochemical Technology (MUA-ADB) (2002-2005)

: Grant for Creative Scientific Research from the Ministry of Education, Science and Culture, and Sport of Japan (Oct.-Nov. 2004)

PRESENTATIONS :

Poolmee, P., S. Suramitr, K. Sriwichitkamol and S. Hannongbua. **Conformational Analysis and Electronic Property of Fluorene-Thiophene Copolymer.** 29th Congress on Science and Technology of Thailand (STT 2003), Khon Kaen University, Khon Kaen, Thailand, October 20-22, 2003.

Poolmee, P. and S. Hannongbua. **Theoretical Investigation on Electronic Property of Fluorene-Thiophene.** 1st Asia Pacific Conference on Theoretical & Computational Chemistry, Institute of Molecular Science, Okazaki, Japan, May 12-15, 2004

Poolmee, P and S. Hannongbua. **Structural and Electronic Properties of Fluorene-Thiophene Copolymer.** 8th Annual National Symposium on Computational Science and Engineering, Suranaree University of Technology, Nakhon Ratchasima, Thailand, July 21-23, 2004.

Poolmee, P., M. Ehara, S. Hannongbua and H. Nakatsuji. **SAC-CI Investigation on Electronic Structure of Fluorene-Thiophene Oligomer**. 2nd Asia Pacific Conference on Theoretical & Computational Chemistry, Chulalongkorn University, Thailand, May 2-5, 2005.

Poolmee, P. S. Suramitr, R. Chidthong and S. Hannongbua. **Theoretical Investigation on Blue-light Emitting Conducting Polymer.** 11th Asia Chemical Congress, Korea University, Seoul, South Korea, August 24-26, 2005.

PUBLICATIONS :

1. Poolmee, P., Hannongbua, S., Theoretical Investigation on Energy Gap of Fluorene-Thiophene Copolymer *J. Theor. Comp. Chem*, **2004,** 3, 481.

2. Poolmee, P., Hannongbua, S., Ehara, M., Nakatsuji, H., SAC-CI Theoretical Investigaiton on Electronic Structure of Fluorene-Thiophene Oligomers *Polymer*, **2005,** 46, 6474.